Detection and Coding Techniques for Fourth Generation Air-Interfaces based on Multicarrier Modulation

by

Akram Jamal Awad

Submitted in accordance with the requirements for the degree of
Doctor of Philosophy

The University of Leeds
School of Electronic and Electrical Engineering

September, 2007

The candidate confirms that the work submitted is his/her own and that appropriate credit has been given where reference has been made to the work of others.

To my loving parents …

Acknowledgements

In the name of Allah, the Most Beneficent, the Most Merciful.

I wish to express my gratitude to my supervisor Prof. Timothy O'Farrell for his guidance and invaluable advice, for sharing his insight, for our numerous discussions and for reviewing the manuscript.

I am thankful to all of my colleagues in the Institute for Integrated Information Systems and the School of Electronic and Electrical Engineering for the enjoyable atmosphere and for their help, with particular mention to: Asr, Jamal, Anna and Juan Carlos.

I wish to thank my good friends Imad, Fahad and Waleed for the beautiful time we shared together.

I am eternally grateful for the endless love, encouragement and support that I received from my lovely sisters: Areej, Aseel and Atheer and the best brother ever: Ahmed.

Finally, I would like to express my deepest gratitude to my parents for their relentless support, priceless guidance, continuous prayers and boundless love.

Abstract

This thesis investigates a number of multiple-access, multiuser detection (MUD) and channel coding methods for the downlink of 4G wireless systems based on multicarrier modulation. Two joint Orthogonal Frequency Division Multiplexing (OFDM) and Code Division Multiple Access (CDMA) schemes have been characterised and compared in respect of their performance in different environments and configurations. The first scheme is Multicarrier Direct Sequence CDMA (MC-DS-CDMA), based on time domain spreading. The second is Multicarrier CDMA (MC-CDMA), based on frequency domain spreading. The results demonstrate that, though MC-CDMA benefits from frequency diversity even in the absence of channel coding and antenna diversity, MC-DS-CDMA performs better than MC-CDMA with channel coding and antenna diversity.

MC-CDMA becomes subject to MAI enhancement in frequency selective fading channels. To reduce the effects of the MAI and exploit the available frequency diversity, MC-CDMA requires MUD. However, the optimal Maximum Likelihood (ML) detector is prohibitively complex. A novel near-ML MUD algorithm based on the Chase algorithm has been proposed in this thesis. The proposed algorithm offers significant improvement to the performance of MC-CDMA using much less complexity compared to ML-MUD. A gain of 1dB to 4dB over the non-MUD

performance was achieved depending on the spreading factor and the number of error patterns.

Finally, a novel symbol-level Chase-based decoding algorithm has been proposed for non-binary Block Turbo Codes (BTC) with application to OFDM. The conventional bit-level decoding algorithm requires the components of a non-binary code to be represented by binary bits, which is inconsistent with the use of non-binary codes; whereas the proposed symbol-level decoding algorithm does not require such a binary representation. The superiority of the new decoding algorithm has been confirmed through simulation results. Moreover, the bit-level decoding algorithm works only with Grey coded constellations. The new symbol-level algorithm is not limited by this condition. This enables any mapping constellation to be used with BTC, especially those which enhance power efficiency and reduce peak-to-average-power-ratio effects.

Contents

Figures

Tables

Acronyms

3G	Third Generation
4G	Fourth Generation
AMC	Adaptive Modulation and Coding
AWGN	Additive White Gaussian Noise
BER	Bit Error Rate
BPSK	Binary Phase Shift Keying
BTC	Block Turbo Code
CDMA	Code Division Multiple Access
CR	Code Rate
CSI	Channel State Information
CTC	Convolutional Turbo Code
DAB	Digital Audio Broadcasting
DFT	Discrete Fourier Transform
DVB-M	Mobile Digital Video Broadcasting
DVB-T	Terrestrial Digital Video Broadcasting
EGC	Equal Gain Combining
FDM	Frequency Division Multiplexing
FD-MC-CDMA	Frequency Division MC-CDMA

FFT	Fast Fourier Transform
GF	Galois Field
GMD	Generalised Minimum Distance
GSM	Global System for Mobile Communications
HYPERLAN	High Performance Radio LAN
ICI	Inter-Channel Interference
IFFT	Inverse Fast Fourier Transform
IID	Independent Identical Distribution
IP	Internet Protocol
ISDB-T	Terrestrial Integrated Services Digital Broadcasting
ISI	Inter-Symbol Interference
IST	Information Society Technological
LAN	Local Area Network
LDPC	Low-Density Parity Check
LLR	Log Likelihood Ratio
LML	Local Maximum Likelihood
LTE	Long-Term Evolution
MAI	Multiple-Access Interference
MAN	Metropolitan Area Network
MBWA	Mobile Broadband Wireless Access
MC-CDMA	Multi-Carrier CDMA
MC-DS-CDMA	Multi-Carrier Direct-Sequence CDMA
MCI	Multicode Interference
MIMO	Multiple-Input Multiple-Output

MISO	Multiple-Input Single-Output
ML	Maximum Likelihood
MLD	Maximum Likelihood Detection
MLSE	Maximum likelihood Sequence Estimation
MRC	Maximal Ratio Combining
MT-CDMA	Multi-tone CMDA
MUD	Multi User Detection
OFCDM	Orthogonal Frequency and Code Division Multiplexing
OFDM	Orthogonal Frequency Division Multiplexing
OFDMA	Orthogonal Frequency Division Multiple Access
ORC	Orthogonal Ratio Combining
PAN	Personal Area Network
PAPR	Peak to Average Power Ratio
PER	Packet Error Rate
PHY	Physical Layer
PN	Pseudo Noise
PWTP	Pre-Whitening Tree Pruning
QAM	Quadrature Amplitude Modulation
QPSK	Quadrature Phase Shift Keying
RRNS	Redundant Residue Number System
RS	Reed-Solomon
S/P	Serial to Parallel
SC-CDMA	Single Carrier CDMA
SEW	Sliding Encoding Window

SFH	Slow Frequency Hopping
SIMO	Single-Input Multiple-Output
SISO	Single-Input Single-Output
SMS	Short Message Service
SNIR	Signal-to-Noise-and-Interference Ratio
SNR	Signal-to-Noise Ratio
SOFDMA	Scalable Orthogonal Frequency Division Multiple Access
SSTS	Steered Space-Time Spreading
STBC	Space-Time Block Coding
SUD	Single User Detection
SVD	Singular Value Decomposition
TCM	Trellis Coded Modulation
TF	Time-Frequency
TPC	Turbo Products Code
UMTS	Universal Mobile Telephone System
UTRAN	Universal Terrestrial Radio Access Network
XDSL	Digital Subscriber Line

Symbols

$\{\ \}$	Set of values or codewords
$[\ ]$	Matrix or vector
$[\ ]^{\mathrm{T}}$	Non-conjugate transpose of a matrix or vector
α	Weighting factor to reduce dependency on early decoding iterations
β	Weighting factor used in the case of lack of alternative competing codewords in the BTC decoder
ρ	Covariance factor
$b_{k,i}(t)$	Transmitted data symbol of user k at time t
B	Matrix of transmitted symbols within one MC-DS-CDMA or MC-CDMA symbol
$c_k(t)$	Spreading sequence chip of user k at time t
C^0	Nearest codeword to the received signal
C^l	l-th codeword
C_{mux}	Number of multiplexed users
D	Decision of the Chase algorithm
$D_{\exp}$	Distance between paths in the CIR model
E	Transmitted codeword
H_g	Diagonal frequency domain channel matrix at the g-th antenna
$\ln$	The natural logarithm
L	Load factor

M	Euclidean distance matrix
N	AWGN matrix
N_c	Number of OFDM subcarriers
p	Number of low-confidence positions in a the received signal
R_g	Received signal at the g-th receive antenna
R_t	Ratio between delay spread and symbol duration
$s_k(t)$	Transmitted signal of user k at time t
SF	Spreading factor
SF_f	Spreading factor in the frequency domain
SF_t	Spreading factor in the time domain
T_c	Chip duration without guard interval
T_c'	Chip duration with guard interval
T_g	Guard interval duration
T_{rms}	Rms delay spread duration
T_s	OFDM symbol duration
w	Extrinsic information within the BTC decoder
X_l	Transmitted signal on the l-th subcarriers subgroup
Y	Set of error patterns

Chapter 1
Introduction

Since its inception about 20 years ago, mobile communication systems have taken large strides towards bringing the "Mobile World" vision into reality. Starting from only one service, voice transmission and reception, the applications of these systems are now widely ranging from the short message service (SMS), which was first introduced as part of the second generation standard GSM (Global System for Mobile Communications), to the mobile video conferencing service, one of the many features promised by third generation (3G) systems: UMTS (Universal Mobile Telephone system) and CDMA2000.

The maximum data rate of almost 2 Mbps offered by 3G systems is a huge jump compared to the few tens of kbps provided to GSM. Nevertheless, even the 2 Mbps rate is very low, especially for the downlink, considering the increasing demand on

high-data-rate services. This is the main force driving research on the next generation of mobile communication systems, or what is known as the Fourth Generation (4G).

1.1   Motivation

Several technologies have been comprehensively investigated in order to determine their suitability for the 4G system needs. In regard to the physical layer (PHY), the main specifications to fulfil are undoubtedly a robust and spectrally efficient use of radio resources, while featuring reasonable implementation complexity and low power consumption [1]. To achieve this, orthogonal frequency division multiplexing (OFDM) has been the modulation scheme preferred by most of the 4G PHY studies conducted. High spectral efficiency, robustness to frequency selective fading, inter-symbol Interference (ISI) mitigation and simple implementation are among some of the features that make OFDM such an attractive scheme.

Furthermore, significant research activities have been taking place looking for ways to combine OFDM with different multiple access techniques; many of which consider different variants based on Code Division Multiple Access (CDMA). When the spreading is applied physically in the frequency domain this is called Multi-Carrier CDMA (MC-CDMA). Spreading in the time domain, on the other hand, yields Multi-Carrier Direct-Sequence CDMA (MC-DS-CDMA).

Researchers advocating MC-CDMA usually support their stand by the fact that it is more capable of exploiting the frequency domain diversity inherited from OFDM. On the contrary, advocates of MC-DS-CDMA consider the avoidance of Multiple-Access Interference (MAI) caused by frequency selective fading a major advantage of MC-

DS-CDMA over MC-CDMA. Nevertheless, no major effort has been spent in conducting a fair and thorough comparison between time domain and frequency domain spreading, except for a few papers that focus on certain imperfections or non-linearities of the system (these papers are reviewed in Chapter 2).

It is established that ML-based Mutliuser Detection (MUD) is the optimal detection method for CDMA in general [4]. Some research has been conducted in the past on ways of reducing the complexity of the MC-CDMA's ML-MUD and proposing sub-optimal solutions [55]. The Chase algorithm [3] was originally proposed as a suboptimal near-ML algorithm for the decoding of linear block codes. In this context, utilising the features of the Chase algorithm to achieve the complexity reduction of the MC-CDMA's MUD is a natural next step.

In what may at first sound a totally different topic, Block Turbo Codes (BTC), introduced by Pyndiah [2] were of interest to us in our research. Pyndiah's proposal of BTC was based on the use of Product Codes. One of the advantages of these codes is the ability to construct powerful error correcting codes that have large minimum hamming distances using simpler linear block codes. Another advantage is their very good performance even with high code rates. A number of researchers have investigated the concept of BTC with different types of inner codes. Reed-Solomon (RS) codes were tested in a Turbo Product Code (TPC) arrangement as a special class of non-Binary BCH codes. There are still, however, several important questions to be answered in respect of the performance of RS-TPC over multicarrier channels.

Furthermore, the BTC decoding algorithm proposed by Pyndiah and inspired by the Chase algorithm uses a binary representation of the block codes. The same algorithm was equally applied in the literature for both binary and non-binary codes. Though RS

codes represented the application of a non-binary code in BTC research, and as these codes are a class of BCH codes, the straightforward approach to decode is first to demap them into binary codewords and apply Pyndiah's binary decoding algorithm to these soft bits. Although this method sounds logical it does not exploit the non-binary q-ary nature of RS codes, not to mention that other non-binary codes may not demap to a useful binary representation. Additionally, the conventional BTC decoding algorithm assumes the employment of Grey-coded mapping in higher-order modulation schemes, which is not always a valid assumption.

The motivation behind using the Chase algorithm was to develop an algorithm that almost achieves Maximum Likelihood Detection (MLD). Though MLD is optimal, it is also prohibitively complex to implement while the Chase algorithm offers lower complexity. This was achieved by searching for the best codeword estimate across the most probable candidates only instead of searching the whole code space. These candidates are generated by erasing the least reliable symbols of the received word and replacing them with all the possible alternatives.

1.2   Original Contributions of the Thesis

- In this thesis, both MC-CDMA and MC-DS-CDMA were individually investigated to obtain a thorough characterisation of their performances. This included studying and analysing the systems' performances in both single-cell and multi-cell environments. The effects of employing MIMO and Turbo codes were also included in the investigations. No similar detailed investigation of both schemes can be found in the literature.

- MC-CDMA was also investigated with different Single-User Detection (SUD) methods, using relative delay spread and symbol duration values instead of their absolute ones. This allows a deeper understanding of the MC-CDMA's trade-off between MAI and frequency diversity in any system setup.

- The use of consistent parameters for both MC-CDMA and MC-DS-CDMA made it possible to conduct a comparative study of both schemes. The key conclusion of the study was 'adaptation', and the comparative study teaches to adapt the signal for either frequency or time domain spreading based on the channel conditions and link requirements. Although this study is the first to put both MC-DS-CDMA and MC-CDMA under this thorough and fair comparison, no claim can be made that this work provides a complete understanding of the relative behaviour of the two schemes running as candidates for the air interface of 4G wireless communications systems. Nonetheless, the outcomes of this study go a long way to answering these questions.

- A novel near-ML MUD algorithm was designed for MC-CDMA utilising the Chase algorithm to significantly reduce the complexities of ML detection. The soft-input soft-output nature of the proposed algorithm, along with its simplicity, makes it attractive for future research aiming at integrating this algorithm within joint solutions that include the demapper and/or channel decoder of the system's receiver.

- Finally, a novel symbol-level iterative algorithm was developed for the decoding of non-binary BTC based on the original binary BTC decoding algorithm. Unlike the conventional algorithm, the new approach uses neither a binary representation of the block code nor Grey coding of high-order

mapping constellations. This new class of processing can be further developed to simplify the detection, demapping and decoding of non binary symbols with enhanced bit error rate performance.

1.3   Thesis Layout

The remainder of this chapter describes the layout of this thesis, which is organised into seven chapters.

Chapter 2 reviews the literature covered as part of our research. The chapter starts with a brief discussion of the research trends toward 4G wireless communications systems, giving an insight into recent standardisation efforts by IEEE and 3GPP working groups to specify the requirements and technologies of a new evolutionary generation of wireless and mobile systems. This builds the case for OFDM which is then presented as a concept, reviewing its main strengths and challenges before moving to the core interest of this thesis: OFDM-CDMA based schemes. Research conducted on both MC-CDMA and MC-DS-CMDA as representatives of these schemes is perused with special focus on works done to compare both schemes. The research conducted on near-ML MUD for MC-CDMA is reviewed later in the chapter. And finally, the Chase algorithm is introduced with a summary of research conducted on comparing its performance with other algorithms, modifying the original algorithm, or employing it in different applications. The spotlight here was on the application of the Chase algorithm in BTC iterative decoding.

In Chapter 3 MC-DS-CDMA is introduced highlighting its main advantages and disadvantages. The MC-DS-CDMA system is then described followed by computer

simulation results and analysis of the system's performance in both single and multi-cell environments.

On the other hand, Chapter 4 deals with MC-CDMA which is studied in a similar manner to MC-DS-CDMA in Chapter 3. After describing the system structure, a simulation-based investigation is conducted to study the performance of MC-CDMA with different SUD methods. Later on, the performance of MC-CDMA is simulated and analysed for both single and multi-cell environments.

Chapter 5 combines both MC-DS-CDMA and MC-CDMA in one comparative study. After analytically comparing both system's merits and demerits, simulation results of both MC-DS-CDMA and MC-CDMA are presented and analysed emphasising the differences in their performance trends and establishing where the potential of every scheme actually lies.

In Chapter 6 the Chase algorithm is first advocated to be a proper approach to solve the complexity burden of ML MUD for MC-CDMA. The new Chase-assisted simplified MUD algorithm is then described. This is followed by computer simulation results and a discussion of these results.

Non-binary BTC decoding is the body of investigation in Chapter 7. After introducing the concept of BTC and TPC the conventional bit-level Chase-based decoding algorithm is described with application to non-binary codes. This is followed by the description of our novel symbol-based decoding algorithm. Simulation results start with comparing RS-based BTC with CTC as a proof of concept for OFDM systems. The comparison of bit and symbol-level decoding of RS-BTC appears later with simulation results and their analysis.

Finally, in Chapter 8, the main conclusions and contributions of the thesis are highlighted, certain limitations of the work are identified, and areas for possible further work are suggested.

Chapter 2
Literature Review

There has been a continuous debate since the first 3G mobile communication system was deployed about what the next generation system will look like. Although it is still early to describe the 4G system elaborately, its major characteristics can be predicted from the different visions used to describe it. These visions have been always driven by the question: Why do we need a 4G system? From the viewpoint of operators and users, the explosive growth of demand for multimedia services has the potential to saturate 3G systems. Not only are the number of subscribers expected to increase rapidly, but also the data rates required by new high data rate content services which are expected to find popular markets in the near future. Examples of these services are video conferencing, high-speed internet access, public database access, information distribution services and Personal Area Network (PAN) remote control systems. Taking the above into consideration, it seems that it is

a necessity to develop a new system with a much wider bandwidth interface that would be able to satisfy the users' needs. From a commercial point of view, the large costs of developing and installing 3G equipment has led to high service process compared with GSM thereby creating a condition that 4G might be more economical. From another more technical viewpoint, the wide range of access networks currently in service should merge to a point where all these networks can be accessed seamlessly through one terminal. Moreover, with the expansion of internet applications and users everywhere, it is timely to utilise the Internet Protocol (IP) which provides a pervasive means of interconnecting users.
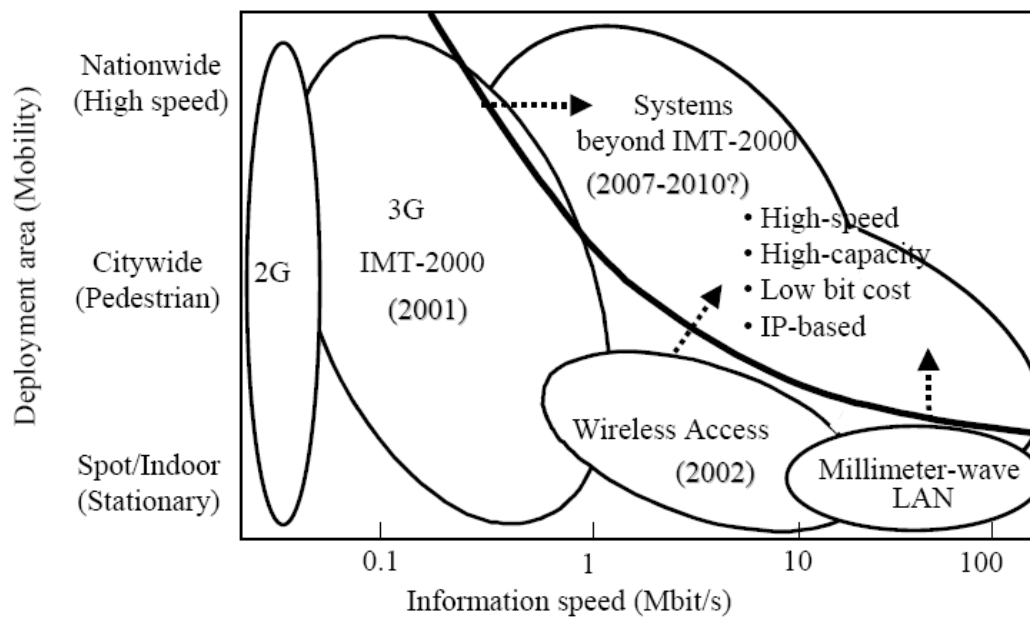
Figure 3.1   Capability of Wireless Systems

Bearing the above in mind, one can state that a main aim of 4G systems is to achieve a much higher data rate with the capability to work reliably in high-speed mobility conditions. This is described in Figure (2.1) [93]. The new system is expected to have the best of all the systems currently in service, starting from 3G systems, which offer reasonable data rates at high speeds to wireless LANs (Local Area Networks) with

data rates of tens of Mbps serving stationary or low-mobility users. The main features

of 4G that have been agreed upon by most of the literature can be summarised as:

- High-speed data transmission rate (20 Mbps to 1 Gbps)

- Larger capacity (at least 10 times greater than 3G)

- Seamless connectivity to other access networks and technologies, including cellular mobile radio systems (e.g. GSM and UMTS), short-range connectivity networks (e.g. Bluetooth), WLAN (e.g. IEEE802.11a/g/n and HIPERLAN/2), broadcasting systems (e.g. DAB, DVB-T and DVB-M) and XDSL networks.

- Low bit cost compared to the extremely expensive costs of 3G systems.

- Adaptability: where services are adapted according to the user preferences, terminal capabilities and channel conditions.

Extensive research is currently ongoing in different parts of the world which aims at

fulfilling the requirements of the new 4G system. In terms of the physical layer, the

strongest candidate technologies proposed for the system's architecture are:

- Orthogonal Frequency Division Multiplexing (OFDM)

- Multiple-Input Multiple-Output Antennas (MIMO)

- Turbo Codes

- Adaptive Modulation and Code Rating

Some "Beyond 3G" standards are already established such as WiMAX. Although

none of them claim to be a 4G standard, there is no doubt that they are indicative of

the next generation of wireless communications systems and help to define the

requirements of the 4G systems based on the market trends. WiMAX [5], or

IEEE802.16, is probably the most widely recognised standard among the new set of

standards currently available. WiMAX will enable the delivery of last mile wireless broadband access as an alternative to cable and DSL. Although WiMAX was first introduced as a fixed Wireless Metropolitan Area Network (Wireless MAN), a later version of the standard, IEEE802.16e, adds a capability for full-mobility support. However, the focus of WiMAX remains to be optimised for fixed and very-low – speed mobility. In addition to offering mobility, IEEE802.16e's improvements over the fixed WiMAX version (IEEE802.16d) included the introduction of Scalable Orthogonal Frequency Division Multiple Access (SOFDMA) as opposed to the OFDM version with 256 subcarriers in IEEE802.16d. This allows WiMAX to overcome the differences in RF spectrum allocations around the world. Furthermore, IEEE802.16e also supports Multiple Input Multiple Output (MIMO) as well as turbo codes and Low-Density Parity Check (LDPC) codes. IEEE802.16m, represents the vision of WiMAX development toward the next generation mobile network [6].

The 3GPP Long-Term Evolution (LTE) for the Universal Terrestrial Radio Access Network (UTRAN) is another effort to standardise the technologies that will allow 3G to maintain its future competitiveness. In terms of the data rate requirements of the LTE, these were defined in [7] as a 100Mb/s peak data rate within a 20-MHz download spectrum allocation. LTE will be optimised for a low mobile speed from 0 to 15 km/h, while higher mobile speeds between 15 and 120 km/h should be supported with high performance.

Although UTRAN-LTE is yet to be finalised as a standard, it has been already agreed that the new system will use some form of OFDM on the downlink. The use of MIMO techniques was also agreed and, re-using the expertise from the UTRAN, the same channel coding type (Turbo Codes) has been agreed for the LTE [8].

A third effort to push the wireless communications systems beyond their current capabilities is that of the IEEE Mobile Broadband Wireless Access (MBWA) working group, or IEEE802.20. A key difference between IEEE802.20 and the other two schemes introduced above, IEEE802.16e and UTRAN LTE, is that the former will be optimised for full mobility up to vehicular speeds of 250 km/h. To achieve this, the targeted spectrum for the system has been restricted to below 3.5 GHz. An example of high-speed mobility optimisation is given in [9] by requiring the spectral efficiency of the system to drop by no more than 25% when moving from a 3 km/h speed to 120 km/h speed (given 2.0 b/s/Hz/sector and 1.5 b/s/Hz/sector as minimum spectral efficiencies for both speeds, respectively). The IEEE802.20 working group was temporarily suspended in June 2006 before it was resumed in September 2006, putting the group behind its scheduled deadlines. Therefore, IEEE802.20 remains open to alternative technology proposals compared to IEEE80.16 and UTRAN-LTE as its technology selection process is still in progress.

In respect of the downlink physical layer of the next generation system, and bearing in mind the evolution of current or near-future systems such as WiMAX and 3GPP LTE, forecasts are becoming more confident that OFDM is going to be a very strong candidate for the modulation, multiplexing and multiple access in the 4G systems.

2.1   OFDM

The concept of using parallel data transmission and Frequency Division Multiplexing (FDM) was first published in the mid 1960s. Some early development can be traced back to the 1950s [10]. In a classical parallel data transmission system, the total carrier's frequency band is divided into N non-overlapping subcarriers and each subcarrier is modulated by one symbol. Conventional FDM avoids spectral

overlapping between subcarriers in order to eliminate Inter-Channel Interference (ICI). However, this leads to an inefficient use of the available spectrum.

OFDM, in contrast, achieves high spectral efficiency by overlapping subcarriers as illustrated in figure (2.2). However, the choice of the subcarrier spacing to be $f_c = 1/T_s$, where T_s is the active symbol period, ensures that all subcarriers are orthogonal and do not interfere with each other [11].
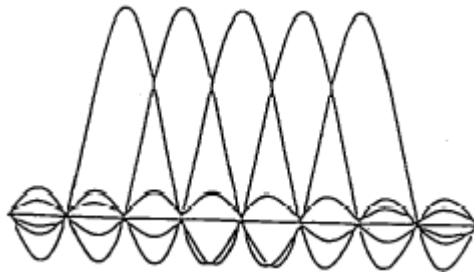
Figure 3.2   Overlapping OFDM subcarriers spectrum [11]

One feature of OFDM is its ability to ameliorate ISI by inserting a guard interval between consecutive OFDM symbols in the time domain. When this interval is longer than the delay spread in a multipath channel, OFDM is not affected by the occurrence of ISI. ICI can also be avoided in a multipath channel by filling the guard interval with a cyclic extension, or cyclic prefix, from the signal itself. This ensures that every subcarrier will constitute full cycles during any T_s-long window of time as in figure (2.3) [10].
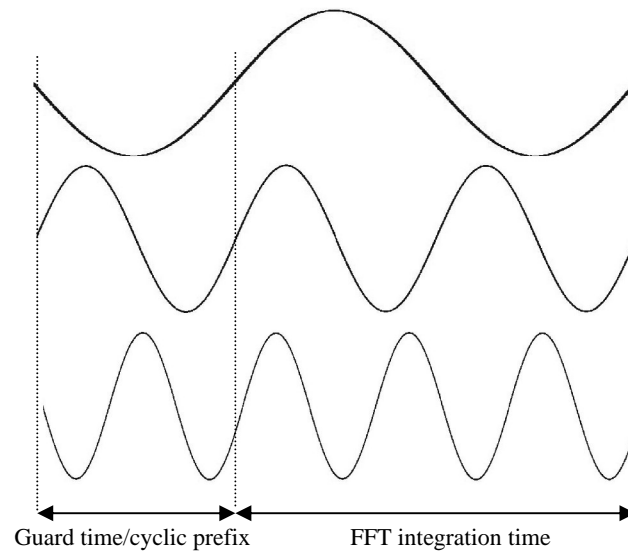
Guard time/cyclic prefix   FFT integration time
Figure 3.3   OFDM symbol with cyclic prefix [10]

Since the total bandwidth of the wide-band carrier is split into a number of narrow-band subcarriers, the frequency selective fading of the channel is shifted into a flat-fading characteristic per subcarrier if the subcarrier's bandwidth is narrower than the coherence bandwidth over which the channel can be considered correlated. This results in simplifying the equalisation process into a one-tap equaliser per subcarrier. Moreover, because the overall channel exhibits frequency selective fading, not all data symbols being transmitted in parallel will be erased. With the proper use of error correcting codes and bit interleaving, the data transmitted on the severely faded subcarriers can be recovered from the surviving data. From a time-domain perspective, increasing the number of subcarriers within a given bandwidth will lead to the subcarriers becoming narrower and the symbol period longer. Increasing the symbol duration beyond a certain point would expose the signal to fast fading where the symbol suffers from envelope variations during the period T_s. The trade-off between the bandwidth and duration of a subcarrier's symbol is explained in figure (2.4).
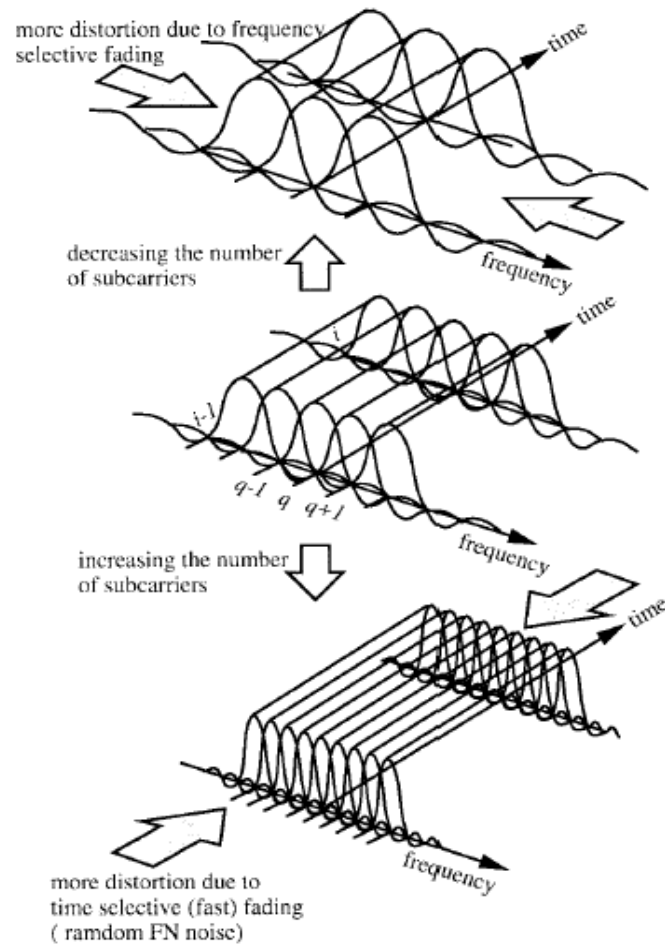
Figure 3.4   Trade-off between subcarrier's bandwidth and symbol length [10]

In [12], Weinstein and Ebert applied the Discrete Fourier Transform (DFT) to parallel data transmission systems as part of the modulation and demodulation processes. In addition to eliminating the banks of subcarrier oscillators and coherent demodulators required by FDM, a digital implementation could be built around special-purpose hardware performing the Fast Fourier Transform (FFT) and Inverse FFT (IFFT). Recent advances in VLSI technology make high-speed large-scale FFT chips commercially affordable [13]. A general OFDM system block diagram is depicted in figure (2.5).
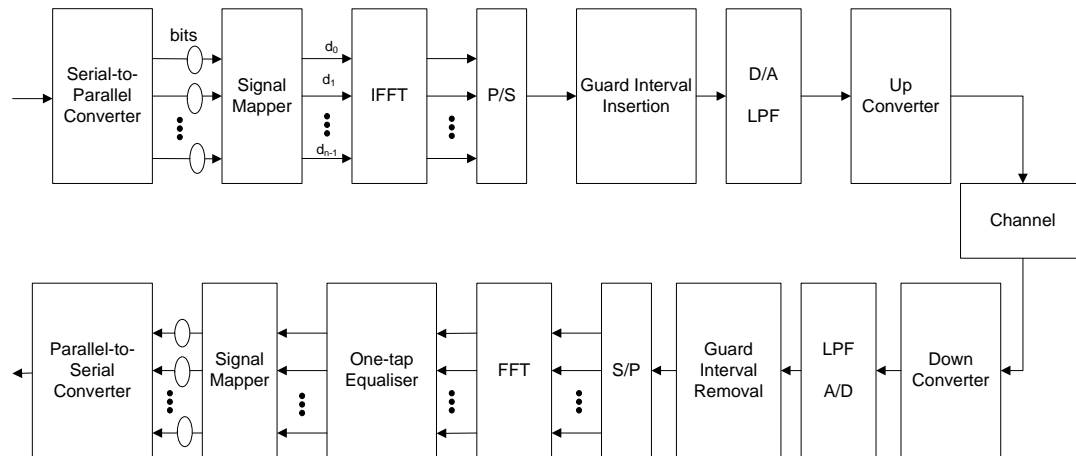
Figure 3.5   FFT-based OFDM System

Hence, the advantages of OFDM can be summarised as follows:

- The effect of ISI is prevented by the insertion of guard intervals.

- ICI is avoided by a cyclic prefix

- The flat fading per subcarrier simplifies the equalisation process to a one-tap equaliser.

- High spectral efficiency through subcarrier overlapping.

- Simple implementation using IFFT/FFT.

Due to these advantages and features, OFDM has been applied to a wide range of systems in both digital broadcasting and communications. It has already been employed in the European DAB (Digital Audio Broadcasting), European DVB-T (Terrestrial Digital Video Broadcasting) and the Japanese ISDB-T (Terrestrial Integrated Services Digital Broadcasting). OFDM has been used also in the wireless LAN standards IEEE802.11a, g and n, as well as HIPERLAN/2 and MMAC [14]. Coded OFDM is currently one of the strongest candidates for the physical layer

architecture of 4G mobile communication systems. This has been affirmed by the use of OFDM in WiMAX and 3GPP LTE.

It is worth mentioning that with all the strengths of OFDM, it still has some drawbacks which are under investigation. These are [10]:

- Sensitivity to frequency offset and phase noise.

- Large Peak to Average Power Ratio (PAPR), which tends to reduce the power efficiency of the RF amplifier.

There are several methods of providing multiple access in multicarrier systems. Traditionally, Orthogonal Frequency Division Multiple Access (OFDMA) has been utilised, where users are assigned one or more subcarriers for transmitting data. Several introduced variants of OFDM employ Code Division Multiple Access (CDMA) to provide multiple access. These technologies are likely candidates for 4G systems because of their multiple access benefits over OFDM [15]. The next section reviews different OFDM-CDMA schemes with focus on research done for the downlink of 4G systems.

2.2   OFDM-CDMA Based Schemes

Much research has been done on the combination of OFDM with multiple access techniques based on CDMA. Combining CDMA with OFDM yields several schemes: when the spreading takes place in the frequency domain MC-CDMA is obtained, when it takes place in the time domain MC-DS-CDMA is obtained. Spreading may also be applied in both the time and frequency domains.

2.2.1 MC-CDMA

The MC-CDMA transmitter spreads the original signal using a given spreading code in the frequency domain. More specifically, a fraction of the symbol corresponding to a chip of the spreading code is transmitted on a distinct subcarrier. For multi-carrier transmission, it is essential to have frequency non-selective fading over each subcarrier. Therefore, if the original symbol rate is high enough to become subject to frequency selective fading, the signal needs first to be serial-to-parallel (S/P) converted before being spread over the frequency domain. The basic transmitter structure of MC-CDMA is similar to that of a normal OFDM scheme except that in MC-CDMA the same symbol is transmitted in parallel through many subcarriers whereas the OFDM scheme transmits different symbols on every subcarrier [10].

Whether the chips corresponding to one symbol should be placed on adjacent subcarriers or not has been discussed in a number of papers [16][17]. Spreading the symbol on spaced subcarriers was called chip or carrier interleaving to differentiate it from bit interleaving applied at the output of the channel encoder. Chip interleaving ensures that chips of one symbol are transmitted over independent identically-distributed subcarriers, which increases diversity. On the other hand, it destroys spreading sequence orthogonality –if any- leading to a high level of Multiple Access Interference (MAI) in a multi-code transmission configuration. On the contrary, when only bit interleaving is applied and if the total bandwidth occupied by one symbol's chips is narrower than the coherence bandwidth of the channel, the channel frequency response becomes flat over that bandwidth and thus no MAI occurs. However, there would be no diversity gain either. From the above it can be seen that there is a trade-off between diversity and MAI. Carrier interleaving maximises the exploitation of

frequency domain diversity at the expense of MAI, while bit interleaving maintains MAI at a low level at the expense of frequency diversity [1].

Extensive research has focused on the development of MC-CDMA and the evaluation of its suitability for the downlink Physical Layer of the Next Generation wireless systems. The motive for those research efforts is that MC-CDMA inherits all the advantages of OFDM, including the avoidance of ISI and ICI, while exploiting the frequency diversity available in multipath channels. By spreading users' signals over a number of subcarriers equal to the length of the spreading sequences, all users can share the whole spectrum. This is similar to Single Carrier CDMA (SC-CDMA) except that the equalisation, combining and detection process is much easier when each subcarrier in MC-CDMA assumes flat fading.

In addition to the traditional MC-CDMA, a number of modified versions have been proposed in the literature to improve the overall system performance or to overcome a particular problem. For instance, Tayoon [18] introduced a Multi-Code MC-CDMA which gives the system the flexibility to transmit various data rates for different users while still benefiting from frequency diversity. In another effort, Frequency Division MC-CDMA (FD-MC-CDMA) was suggested by Wu in [19] with the aim of reducing MAI among the spreading codes in use by dividing the available spectrum into a number of subsets of subcarriers while slightly increasing the system complexity. In [20], by properly choosing subsets of Walsh-Hadamard codes, a MAI-free MC-CDMA is claimed to be achieved. Though, the proposed setup is inefficient as it assumes serving only a fraction of the cell's capacity if the reception is to be maintained MAI-free. The size and number of the spreading sequence subsets as well as their reuse factor depend on the delay spread of the channel, which makes it

impractical for real system implementation. Furthermore, Auffray, Tao and Deng studied the performance of MC-CDMA combined with different versions of MIMO, applying multiple Antennas at the transmitter, receiver, or both to exploit diversity or increase spatial efficiency [21-23]. A large part of the research on MC-CDMA focused on Multiuser detection and interference cancellation techniques. These are discussed later in this chapter.

In addition to individual researches suggesting MC-CDMA explicitly or implicitly as being the best candidate for the next generation wireless communication system's downlink, a number of collaborative initiatives focused on investigating MC-CDMA for future systems have been undertaken. *MATRICE* was one of those initiatives in Europe. As part of the IST (Information Society Technological) fifth framework programme (5th FWP), *MATRICE* aimed at defining and validating concepts based on MC-CDMA technology for the provision of the broadband component of future mobile communication systems [24]. As a complement to *MATRICE*, the *4More* project of the 6th FWP has focused on developing an innovative architecture suitable for the advanced signal processing techniques involved in MC-CDMA [25].

In this context, Chapter 4 is concerned with the characterisation of MC-CDMA and the evaluation of its performance in variant configurations and environments. The study parameters are set up in a manner that would allow us to compare the performance of MC-CDMA with other OFDM-CMDA schemes later in this thesis.

2.2.2   MC-DS-CDMA

In MC-DS-CDMA, the transmitted data stream is S/P converted and then each of the parallel streams is spread using a given spreading code in the time domain so that the resulting spectrum of each subcarrier can satisfy the orthogonality condition with a minimum frequency separation [26]. In [27] MC-DS-CDMA was proposed where each of the S/P converted streams is repeated on multiple subcarriers after the spreading is applied to each stream. It was suggested that the identical streams are interleaved across the total channel bandwidth [28].

MC-DS-CDMA has gained a lot of interest in research on new solutions for future systems. This is true for both the uplink and the downlink interfaces. In terms of the downlink, the performance of MC-DS-CDMA was investigated by Yang in [29]. The effects of two major problems facing MC-DS-CDMA, frequency offset and phase jitter, were studied by Steendam in [30][31].

The fact that MC-DS-CDMA does not suffer from MAI in frequency selective fading channels has resulted in more attention being given to systems architectures based on the combination of MC-DS-CDMA and MIMO to allow the recovery of symbols severely faded on one subcarrier channel as long as those symbols are received on better-quality channels on alternative antennas. In [32], Cai proposed a MC-DS-CDMA scheme employing Space-Time Block Coding (STBC) as well as Slow Frequency Hopping (SFH) allowing the system to combat fading while giving every user the chance to efficiently utilise all the system's frequency resources. The spreading of the MC-DS-CDMA was extended in [33] to become a Space-Time spread MC-DS-CDMA, offering a significant improvement to the overall system performance when the user density is relatively low. Hu [34] proposed a MC-DS-

CDMA scheme in which both smart antennas and steered space-time spreading are employed, minimising the downlink interference caused in co-channel mobiles, while achieving frequency, time and spatial diversity.

MC-DS-CDMA was also considered in some larger-scale projects. The TRUST project of the IST's 5th FWP, for example, researched re-configurable radio systems, with a focus on MC-DS-CDMA as the core physical layer technique [35].

In a manner similar to MC-CDMA, this thesis has characterised the performance and highlighted the features of MC-DS-CDMA for a number of system performance simulations in single cell and multi cell environments using the same parameters applied to the MC-CDMA study, in an effort to compare fairly both systems.

2.2.3   Time-Frequency (TF)-Spread CDMA-OFDM

In addition to research conducted on MC-CDMA and MC-DS-CDMA, some researchers have proposed systems based on two-dimensional spreading of CDMA-OFDM symbols in both the time and frequency domains. The first mention of this concept can be traced back to 1999 when Matsutani [36] proposed MC-DS-CDMA with frequency domain spreading, in which every transmitted symbol is spread in the frequency domain over a number of subcarriers before the actual time-domain spreading is applied. The motivation behind this was revealed to be the exploitation of the potential frequency diversity without the need to expand the overall signal's bandwidth. Later, two significant research projects emerged: one on Generalised MC-DS-CDMA by Hanzo's research group at Southampton University, and the other on

Orthogonal Frequency and Code Division Multiplexing (OFCDM) by the NTT DoCoMo research team in Japan.

Time-Frequency (TF)-spread MD-DS-CDMA was first discussed in a monograph co-authored by Hanzo et al. [26]. It was compared with both SC-CDMA and MC-CDMA. The book concluded that MC-DS-CDMA offers the system more degrees of freedom. In [37] TF-spread MC-DS-CDMA was investigated with the aid of Space-Time spreading and Transmit diversity. Yang intimated that the system is capable of mitigating a number of issues including frequency selectivity and PAR. It was also suggested that the new system could support a higher number of users without any tradeoffs imposed on the achievable diversity order. However, the paper concluded that "the best broadband MC-DS-CDMA system should only use transmit diversity and no frequency diversity at all" i.e. suggesting that higher transmit diversity (deploying more transmit antennas) would perform better than frequency-domain spreading for the same degree of diversity. This conclusion does not consider complexity and cost of using several transmit antennas in comparison with the employment of frequency domain spreading.

TF-spread MC-DS-CDMA was further enhanced in [34] by replacing the transmit antennas with antenna arrays each with a number of antenna elements, providing the system with Steered Space-Time Spreading (SSTS). This allowed the system to minimise the downlink interference inflicted upon-co-channel mobiles, while achieving frequency, time and spatial diversity. Furthermore, user grouping was employed to reduce the effects of multiuser interference. Later in the literature [38], a new differential space-time modulation scheme was proposed for the TF-spread MC-DS-CDMA, allowing the system to run even in fast-fading channels without any need

to estimate the channel. Although the scheme was 3 dB worse than non-differential space-time spreading it offered a solution to the total loss of information challenge when the channel fading is fast enough to make channel estimation impossible or inefficient. Finally in [39], the scheme proposed earlier in [34] was reintroduced with the application of Singular Value Decomposition (SVD) pre-processing, transferring the processing complexity from the receiver to the transmitter with the assumption of full knowledge of the downlink CIRs and replacing the complex mutliuser detector at the receiver with low complexity matched-filter detection.

OFCDM, on the other hand, was initially used by the NTT DoCoMo research team to describe the conventional MC-CDMA architecture (Spreading in the frequency domain). Although the first proposal of OFCDM as a two-dimensional spreading scheme was made in [40] in the year 2002, two reports originally written in Japanese by the same team and published in 2000 and 2001 investigated the possibility of extending OFCDM to include time-domain spreading [41] [42]. The proposed scheme employed Variable Spreading Factor codes allowing the system to support different data rates simultaneously. Furthermore, the scheme prioritises time-domain spreading over frequency-domain spreading. The given justification was that, in a frequency selective fading channel, time-domain spreading is superior to frequency-domain spreading in general to maintain orthogonality among the code-multiplexed channels, which is important to the application of Adaptive Modulation and Coding (AMC) employing multi-level modulation to achieve a higher data rate. However the performance results presented in the paper were limited to the time-domain only spread scheme i.e. the conventional MC-DS-CDMA.

In [43] OFCDM's performance was compared with that of OFDM in multi-cell environments. While the results focused on Time-domain spread OFCDM, some results were depicted for the performance of two-dimensional spread OFCDM. The paper concluded that while OFCDM's capacity was 1.5 fold greater than that of OFDM in a three-cell frequency re-use plan, they both demonstrate similar performances and offer almost identical capacity when a single cell frequency is applied.

In later efforts, research focused on improving different aspects of the OFCDM system's performance. This included proposing a hybrid Multicode Interference (MCI) cancellation and MMSE detection scheme to enhance the overall performance [44]. Another enhancement was the novel code assignment scheme put forward in [45] to mitigate MCI. The scheme is based on giving OVSF codes with large distance the priority to be assigned to users as these will have smaller interferences among them.

More recently, OFCDM has been picked up by other researchers who proposed different enhancements to the system's architecture. For instance, Caldwell [45] developed an adaptive subcarrier allocation algorithm to improve the overall BER performance for all spreading configurations. The algorithm assigns users to subcarrier groups that provide favourable fading characteristics, while simultaneously reducing the amount of interference imposed on other users. Furthermore, an adaptive modulation algorithm combined with adaptive subcarrier allocation was proposed for OFCDM in [56]. The algorithm used fixed thresholds to switch between modulation levels depending upon the estimated SINR for each group of subcarriers, offering an

increase in the throughput of 47% and 63% over BPSK for a target BER of 1% and 10%, respectively.

2.3   Comparison between Time-domain and Frequency-domain spreading

While both MC-CDMA and MC-DS-CDMA drew considerable attention from researchers who used either of them in proposals for the Physical Layer of the next generation wireless and mobile communications systems, very few have actually put both of them under fair comparison to enable the selection of one scheme over the other.

The first comparison of MC-CDMA and MC-DS-CDMA was published by Prasad in 1996 [48], which included MC-CDMA, MC-DS-CDMA, Multi-tone CMDA (MT-CDMA) as well as SC-CDMA. The overview of the systems included general description of their architecture along with a few basic simulation results of their performances. The author came to a conservative conclusion that MC-CDMA with MMSE MUD is the most promising scheme, while advocating the need for a more thorough study and analysis.

In a similar effort, Matsutani [36] compared the performance of MC-DS-CDMA with and without frequency-domain spreading, as well as the performance of the two-dimensional spread scheme with conventional MC-CDMA and SC-CDMA with RAKE reception. Results suggested that two-dimensional spread MC-DS-CDMA is effective when the system is heavily loaded compared to other schemes. However, the two-dimensional scheme was favoured in the simulations by allowing it to use Maximum likelihood Sequence Estimation (MLSE), a prohibitively complex process,

as a detection method to overcome the inter-code interference while using MMSE detection for MC-CDMA.

In [49], a basic comparative study concluded that MC-DS-CDMA has better performance compared to MC-CDMA. The study however was limited to one channel model and one user load profile.

Although Liang's overview [50] did not include any performance results for either MC-CDMA or MC-DS-CDMA, it provided an insight into the main differences between the two systems along with SC-CDMA. This covered the flexibility, complexity and limitations of all three systems. The trend of the work clearly favoured MC-DS-CDMA over the other two systems by listing its advantages and suggesting countermeasures to overcome the weaknesses of MC-DS-CDMA through careful selection of the system parameters. This favouring, however, was well reasoned in theory by stating that MC-DS-CDMA is more capable of supporting ubiquitous communications in diverse environments by avoiding or mitigating the problems imposed by different dispersive fading channels associated with these environments. It was also pointed out that MC-DS-CDMA has the advantage of ensuring independent fading across subcarriers, mitigating the requirements of high-chip-rate signal processing, as well as maintaining orthogonality between spreading codes, or at least not worsening the inter-code interference. Moreover, by fixing the maximum achievable frequency diversity to a constant value when communicating over a variety of fading channels, MC-DS-CDMA allows the safe employment of transmit diversity under the assumption of constant frequency diversity order. The assumptions and analysis in [50] need to be verified through both mathematical analysis and computer simulations.

The work reported in [16] gives a fair comparison of frequency domain and time domain spreading. The paper presented simulation results of the effect of frequency and time domain spreading factors on the performance of the system in both heavily and lightly loaded scenarios. The study was conducted using both QPSK and 16QAM signal sets with the aid of Turbo encoding and receive antenna diversity. Contrary to other comparative studies where BER or PER were used as evaluation criteria, simulation results in [16] were depicted against the required received Es/No per antenna to achieve an average PER of 10^{-2}. This approach made it impossible to follow the performance trends of either schemes (e.g. to identify any critical improvements of performance at some value of Es/No or irreducible error floors beyond some value of BER or PER).

Furthermore, a comparative study between OFDM, MC-CDMA and MC-DS-CDMA in [51] concluded that MC-CDMA would outperform the other two schemes under all conditions. Although the paper mentioned that the comparison was conducted for both fast and slow fading channels, many system parameters were omitted and it was unclear whether the compared systems were supported by any channel coding and/or antenna diversity. Simulation results were also limited to the case of a fully loaded system.

In addition to the comparative studies above, some research concentrated on comparing the performance of MC-CDMA and MC-DS-CDMA when affected by non-linearities. For instance, Hathi studied the effect of PAR and Power Amplifier non-linaerities on the performance of both MC-CMA and MC-DS-CDMA, in [52] and [53], respectively. In [52], the performances of both systems were investigated with different code allocation schemes resulting in varying levels of PAR. The study

concluded that while MC-CDMA's performance significantly changes when using different code allocation schemes at light-load conditions, all schemes were observed having similar performances when moving to the fully-loaded system scenario. On the other hand, MC-DS-CDMA exhibited consistent performance no matter what code-allocation method was used. Finally, in [54] Steendam conducted a comparison of the effect of subcarrier frequency offsets on both MC-CDMA and MC-DS-CDMA. The study results established that both schemes are equally degraded when they share the same frequency offset to carrier spacing ratio.

It is clear from the above that decisions to adopt either MC-CDMA or MC-DS-CDMA as platforms for the next-generation wireless and mobile communications systems were not based on thorough and fair comparisons between the two schemes. Thus a main motivation of this thesis is to use the individual characterisation results of both MC-DS-CDMA and MC-CDMA in chapters three and four to compare both multiple access schemes in different environments and configurations, seeking better understanding of the relative performances of MC-DS-CDMA and MC-CDMA before making critical decisions about the deployment of either of them in 4G systems.

This thesis investigates multiple access, MUD and channel coding techniques for Multicarrier systems. Multiple access methods were discussed in this section. The rest of this chapter is devoted to MUD and channel coding techniques.

2.4   Near-ML MUD for MC-CDMA

A major feature of MC-CDMA is its ability to exploit the inherent frequency diversity of OFDM in frequency selective channels while still dealing with the frequency selectivity manifested as flat fading per subcarrier. Nevertheless, designing MC-CDMA to achieve the most from frequency diversity yields a new problem: increased inter-code interference across the different codes in use. Therefore, substantial research related to MC-CDMA with focus on minimising or eliminating the inter-code interference or MAI in order to improve the MC-CDMA's system performance has been carried out.

Research in this space can be categorised into:

- Equalisation

- Multi User Detection (MUD), and

- Interference Cancellation (parallel or successive)

It is almost impossible to review all the research conducted on any of the categories mentioned above. Therefore our review will be limited to cover the part most relevant to our contribution and that is Sub-Optimal MUD for MC-CDMA.

Optimal MUD involves performing a ML search in which the distances between the received word and each of the possible codeword combinations are calculated to decide on the one closest to the received signal. ML-MUD is a prohibitively complex process even for a small number of sequences, and its complexity increases exponentially with either the increase of number of sequences or the sequence length. Sub-optimal methods have been proposed in the literature to reduce the number of required searches in the code space. In [55] pre-whitening tree pruning (PWTP) was

proposed as a near-ML MUD method for MC-CDMA based on the tree search algorithm. Although this method reduces the complexity of ML detection, it is still complex in itself and quite costly for hardware implementation as it requires memorising all surviving paths in the search tree and requires sorting all node metrics at every level of the tree.

Rugini [56], on the other hand, reduced the number of searches for the best estimate in a ML-MUD by applying Local ML (LML). In LML the search is limited to the neighbourhood of the initial codeword estimate i.e. to all codewords within a certain Hamming distance from that codeword. This approach significantly reduces the complexity of the ML decoder. Simulation results however did not mention how close LML's performance is compared to the optimal ML MUD.

In 1972, David Chase proposed his new class of algorithms to decode linear block codes using channel state information [3]. His algorithm gained exceptional interest from researchers interested in achieving sub-optimal performance not only for linear block codes, but also for other applications which share the Maximum Likelihood (ML) algorithm performance as their optimal performance benchmark (the Chase algorithm is reviewed in more detail in the next section).

We found it a natural next step to utilise the concept of the Chase algorithm, to further reduce the complexity of the MC-CDMA's MUD. This is the body of investigation in Chapter (6).

In addition to exploiting the features of the Chase algorithm in MUD simplification, we studied the Chase algorithm within its original context as a means of decoding block codes. The following section reviews the research conducted on the Chase

algorithm, focusing on work related to Block Turbo Codes (BTC) with application to Multicarrier systems.

2.5   Chase Algorithm and Block Turbo Codes

As mentioned earlier, the Chase algorithm was originally proposed to achieve a near-optimal decoding of linear block codes. While the optimal ML approach to decode linear block codes involves a search for the codeword with the minimum distance from the received word across all codewords in the code, the idea of the Chase algorithm is based on reducing the number of searched codewords. This is done by considering only those codewords within some distance from the received word that might have resulted from corrupting the least reliable positions in the received word, which are identified using the channel state information.

Research on the Chase algorithm can be categorised into three themes [2, 58-84]:

- Comparing the performance of the Chase algorithm with other soft decision decoding algorithms [58-61,

- Modifying the original algorithm to achieve better performance or complexity reduction [70-84], and

- Employing the Chase algorithm for different applications and uses within the communication system architecture [2, 62-69].

Before we go through the review of research conducted on the Chase algorithm, it is worth noting that while Chase required a $\lfloor (d-1)/2 \rfloor$ binary error- correcting decoder for decoding a binary linear block code of minimum distance d, Tendolkar asserted

[57] that it is possible to use a binary decoder that can correct less than $\lfloor (d-1)/2 \rfloor$ hard errors, concluding that the Chase algorithm was just one particular case of a more generalised class of algorithms.

In terms of comparing the performance of the Chase algorithm with other algorithms, Nilsson put both the Chase algorithm and the Generalised Minimum Distance (GMD) algorithm under comparison [58]. In both systems a set of tentative codewords is generated by several decoding attempts. The main difference, however, is that GMD erases the least reliable positions in the received sequence and decodes the resultant sequence by an error-erasure decoder. The Chase algorithm inverts the least reliable bits to their complements and uses an error-only decoder to decode the modified sequences. The results of comparison indicated that even the weakest version of the Chase Algorithm -called Chase-3 Algorithm- was more powerful than the GMD algorithm. Furthermore, Kaneko compared the performance of the Chase Algorithm with that of the Tanaka-Kakigahara algorithm and his own developed algorithm [59]. The study pointed out that while there were marginal differences between the performances of the three algorithms, the Chase Algorithm was the only one to maintain a constant complexity level when the SNR value was varied, while the other two schemes' complexities notably change with SNR. Nevertheless, this work did not apply the optimal version of the Chase algorithm but rather a simplified version proposed also by Chase and given the name Chase-2 algorithm, making the assertion of the conclusion given in [59] that their algorithm's performance was better than the Chase -2 algorithm to the optimal Chase algorithm doubtful.

It was argued in a number of publications [60, 61] that the Chase algorithm does not suffer from the weaknesses of Sphere Decoding. Although Sphere decoding, like the

Chase algorithm, is a suboptimal ML decoding method which aims at simplifying the complexity of the ML search, its complexity is unstable and becomes prohibitive at low SNR. Besides, a sphere decoder does not have a simple algorithm to choose the radius of the searched sphere.

It was not until Pyndiah's proposal to employ the Chase algorithm in the decoder of the Block Turbo Codes (BTC) in [2] that the Chase algorithm captured substantial attention in the soft-decision processing research arena or, more precisely, for iterative soft-input-soft-output processing. Pyndiah used the Chase algorithm as the core of his scheme to iteratively decode the row and column codewords composing a Product Code. Pyndiah's decoding scheme allowed the performance to reach the asymptotic coding gain of the optimal ML decoding in AWGN channels but with a substantially less complex receiver. In [62], he extended his earlier work to higher-order modulation schemes, specifically to 16QAM and 64QAM. It was concluded from the simulation results with BCH codes of different lengths that for BTC coded QAM modulations all signal-to-noise ratios were within 2.9 dB of their respective Shannon's limit. The comparison with 64-state Trellis Coded Modulation (TCM) yielded the conclusion that BTC coded QAM is always superior to 64-state TCM. Furthermore, when compared with Convolutional Turbo Coded (CTC) QAM, BTC offered better performance for spectral efficiencies higher than 4 bits/s/Hz. CTC, however, offered better performance when using codes of rate less than 0.75. Pyndiah argued, however, that this advantage of CTC over BTC would almost vanish when comparing their hardware performances.

Pyndiah's team continued to focus their research on BTC afterwards. In [63], the BTC was applied to Product codes using Reed Solomon (RS) codes as a representative of

BCH codes with non-binary elements. Simulation results emphasised the superiority of Chase-algorithm based decoding to other algorithms proposed for the iterative decoding of RS codes. Simulation results indicated that the BER performance in both AWGN and Rayleigh fading channels have curves with identical slopes that are 6 dBs apart. However, the iterative decoding algorithm appeared to be less efficient for RS codes compared to binary BCH codes, and the given reason was the fact that RS codes are q-ary codes. In later work [64], Zhou used single-error correcting RS codes instead of the extended RS codes used in [63] resulting in a significant rise of the code-rate efficiency and the reduction of the very large number of error patterns required by low-rate RS codes during the Chase-algorithm based decoding. In addition to achieving reliable transmission at less than 1 dB from the Shannon model, single-error-correcting RS codes had the advantage of exhibiting smaller block sizes in comparison with BCH-BTC, giving RS-BTC the advantage of smaller memory size requirements and a shorter encoding/decoding delay.

The first attempt by Pyndiah and his team to modify the originally proposed BTC scheme proposed in [2] was made in [65] when two previously estimated and fixed parameters, called α and β, were changed to follow formulas which take into account a number of factors including the number of decoding steps and the ratio of the variance of the channel noise to the variance of the extrinsic information. Simulations confirmed that this amendment to the original algorithm was beneficial, as for short codes the performance improved by 2 dB compared with the case of predetermined parameters, and for long codes the number of decoding steps was reduced by 1 or 2 steps to achieve similar performance.

Pyndiah's team also looked at the possibility of including BTC in Space-Time systems. In [66], a previous work by Stefanov [67] to use CTC as Space-Time codes was extended to BTC. Investigation suggested that, while BTC can achieve as good performance as that of CTC, it achieves higher spectral efficiency with less number of iterations. However, BTC suffers from prohibitively complex Log Likelihood Ratio (LLR) computations before soft-input soft-output decoding to the extent that the author admitted the need for future research focusing on reducing the processing complexity even if that was at the cost of some performance degradation.

In addition to the application of BTC and Chase-based iterative decoding to BCH and RS codes, other researchers applied the concept to other types of codes. Liew, for instance, used the Chase-Pyndiah algorithm to iterate the decoding process of Redundant Residue Number System (RRNS) codes [68]. These codes exhibit identical distance properties to RS codes; and, because of their non-binary nature, they are attractive codes when error burst correction is required, especially in the context of M-ary systems. Computer simulation indicated that the coding gain of RRNS' performance is in excess of 1 dB. Furthermore, in [69] Hirst proposed a BTC scheme in which generalised Low Density Parity Check (LDPC) codes are iteratively decoded using the Chase Algorithm. Chase-based iterative decoding was stated to be efficient enough to bring the LDPC's performance as close as 0.75 dB to the Shannon's limit with relatively low decoding costs.

As mentioned earlier, there is a significant amount of research on the Chase algorithm focused on modifying the algorithm to enhance its performance or reduce its complexity. This is explicitly true when the Chase algorithm was investigated as part of an iterative decoding scheme. One example is the Fast Chase Algorithm introduced

in [70] with application to turbo decoding. The proposed algorithm made use of the Forced Erasure algorithm to reorder the Chase-Algorithm's decodings to reduce the inherent computational redundancy, making the system less complex and much faster with no degradation in performance.

In the same context, Lu proposed a simplification to the original iterative decoding applied to extended Hamming codes [71]. In fact it is the use of the algebraic structure of the extended Hamming codes and the number of algebraically detected errors in the received word that made possible their proposal to reduce the complexity for the same performance of the original algorithm, or to enhance the system's performance while maintaining the same complexity level. Similarly, Chen [72] chose to simplify the iterative decoding of extended Hamming codes utilising the same features of the codes, adding to them the ability to reduce the memory requirements of the iterative decoding algorithm.

In [73], [74] and [75], three different methods were developed to allow significant reduction of the error patterns generated by the Chase algorithm during the decoding process while still achieving the same performance as the original algorithm. Vicente's approach [73] was to replace the fixed number of error patterns used by the Chase algorithm with a dynamically updated set of patterns based upon a brief analysis of the received reliability information. This was claimed to be able to achieve asymptotically optimal performance using only one fourth of the error patterns originally needed by the simplest Chase-3 algorithm. Arico [74] dropped the dynamic error pattern option and pointed out that, by carefully selecting the set of error patterns, the number of error patterns can be reduced below the requirements of the simplest Chase 3 algorithm while getting a similar or better performance. Simulation

results demonstrated that the proposed modification with 2 error patterns outperformed the original Chase-3 algorithm with 3 error patterns for a BCH(15,7,5) code in AWGN channel. Weber extended the work in [74] by reducing the size of the error-pattern set by deliberately removing some error patterns while preserving the bounded-distance decoding property [75].

In a more recent work [76], Geller believed that it is unnecessary to memorise the competing codewords resulting from encoding the different error patterns of the Chase algorithm. He also suggested that other functionalities of the originally proposed BTC decoder can be safely omitted without affecting the system's performance. This resulted in appreciable system complexity reduction or performance enhancement if the reduced complexity on the procedure was balanced with a higher number of error patterns.

Both Tang [77] and Liu [78] proposed threshold-based simplifications of the original Chase-Pyndiah BTC decoding algorithm. These modifications consider only least reliable positions of the received signal that do not go beyond a certain threshold level of reliability, resulting in generating a smaller number of error patterns and reducing the overall complexity of the decoder while speeding up the decoding process. Nevertheless, it is inconsistent that while in [77] the threshold-based approach was advocated to outperform the Chase-2 algorithm for a varying level of complexity ranging from a high complexity realisation of Tang's algorithm at lower values of *Eb/No* to lower complexity beyond *Eb/No=2.5*, Liu's results indicated that the original Chase-2 algorithm always performs better than the threshold-based simplified algorithm at the cost of extra complexity.

Likewise, Mahran used the reliability threshold as a measure to adapt the number of the least reliable received symbols to be considered for erasure and therefore used in generating the error patterns. Mahran reported in [79] and [80] that, by optimising the reliability threshold, significant reductions in complexity can be achieved for the same performance of the Chase-2 algorithm. Simulations showed that complexity reduction can be as high as 60% for BCH codes at BER=10^{-5}.

In additions to solutions aiming at simplifying the original Chase-based BTC decoding algorithm, some researchers directed their research toward the enhancement of the system's performance. For instance, Le [81] proposed a modification to the original Chase-Pyndiah algorithm that replaces the calculation of soft outputs using the scaling factor α and the estimated reliability value β by a direct calculation of the soft output utilising the distance property of a decision codeword by first evaluating the confidence value of the decoded codeword followed by the generation of the soft output. This was demonstrated via computer simulation to improve the system's performance while still reducing the processing complexity.

Lalam's focus [82], on the other hand, was to tackle the problem of lacking codeword diversity that would allow the decoded codeword to compete with other possible alternatives in the Chase algorithm. This is particularly a weakness of BTCs with high code rates as well as non-binary BTCs. In [82] the proposed solution was to apply a Sliding Encoding Window (SEW) concept that made it possible to generate a list of codewords close to the decoded codeword, which means more reliable soft outputs can be calculated at the output of the Chase algorithm compared to the case when the lack of competing codewords is always translated to strong confidence in the initially

decoded codeword. Lalam observed that the performance gain can be as high as 1.5 dB in Guassian channels for the cost of minor additional complexity.

Argon and Zhang [83] developed schemes that would speed up the Product-Code-based BTC decoding process by decoding in parallel the rows and columns of the Product Code. In [83], simulations demonstrated that the decoding latency can be reduced to half that of the conventional serial decoder. Slight performance degradation was observed in addition to the extra memory and hardware requirements. Zhang's proposal in [84] claimed to achieve the same performance of the original Chase-Pyndiah algorithm while still consuming shorter time and memory compared to Argon's method. Furthermore, while Argon's proposal was limited to two parallel processes at once (one row and one column), Zhang's can be applied to any number of simultaneous decodings.

Block Turbo codes based on the Chase-Pyndiah decoding algorithm were also investigated in association with other technologies [85-88]. OFDM was one technology that was studied along with BTC in a number of papers. Torabi [85] applied the concept of BTC to OFDM using the parameters of the IEEE 802.11a WLAN standard. BTC-OFDM offered 1 dB gain over Single-carrier BTC in Rayleigh fading channels. Besides, the employment of a BTC reduced the length of the required OFCM cyclic prefix by eliminating the residual ICI and ISI, thereby enhancing the system's efficiency. The investigation, however, did not compare the performance of BTC with CTC for an OFDM system.

A BTC was also used in [86] combined with antenna diversity. Two approaches to implement the joint scheme were studied: the first was a BTC-only system i.e. with no Space-Time coding (this was denoted as BTC-Diversity); the second was for a system

using a BTC concatenated with a STBC with rate one (and this is called BTC-STBC). Computer simulations established that BTC-STBC is superior to BTC-Diversity in a flat Rayleigh fading single carrier channel with a gain of up to 8.5dB in quasi-static channels.

A natural next step was Du's work [87] studying the performance of STBC-OFDM with a concatenated BTC. The proposed scheme's performance was compared with a CTC-based scheme in four typical channel models with different delay profiles. BTC outperformed CTC in almost every channel, with a SNR gain ranging from 0.5 to 3.8 dB depending on the channel model. An investigation by He [88] examined the coupling of STBC-OFDM with BTC using the standard IMT2000 reference channel models and 2x2 antenna diversity. Nevertheless, the system's performance was not compared with any benchmark performance.

In the context of BTC, we first investigated the performance of Reed-Solomon BTC applied to OFDM in AWGN and Rayleigh fading channels using the conventional Chase-based decoding algorithm proposed by Pyndiah. This was also compared with the performance of CTC for the same channel.

Decoding non-binary block turbo codes using the same technique applied to binary block codes i.e. by demapping the codeword to its binary components was the mainstream approach to the problem. On at least one occasion in the literature, the q-ary nature of RS codes was blamed for the lower efficiency of applying iterative decoding compared to binary BCH codes. It will be demonstrated in Chapter 6 that the original Pyndiah's BTC decoding algorithm sets at least two implicit conditions for the algorithm to function. One condition is the use of codes with binary elements of the code space, while the second condition is the mapping of symbols on the

constellation using Grey coding with respect to the binary components of every symbol. This is unambiguously the case when using higher order mapping schemes e.g. 16QAM.

The work in this thesis, in regards to BTC, has focused on a modified BTC decoding algorithm that can remove the constraints of binary codes and Grey coding. This was realised by using symbol-level processing rather than bit-level processing. Besides the new degrees of freedom offered by the new algorithm, it allows the simplification of the non-binary BTC decoding process without degrading the system's performance. An OFDM system was used to validate our findings through computer simulations.

2.6   Conclusions

It is apparent from the literature that multicarrier modulation is the strongest candidate to support the requirements of the 4G air interfaces. In terms of the multiple access, joint OFDM-CDMA schemes inherit the strengths of both OFDM and CDMA. Therefore, many publications have advocated either MC-DS-CDMA (time domain spreading) or MC-CDMA (frequency domain spreading) as being the best approach for the multiple access of a multicarrier system. Very few, however, supported their argument with a fair comparison of both schemes.

The first part of our study is, therefore, concerned with providing better understanding of how the performances of MC-DS-CDMA and MC-CDMA compare to each other. Although both systems have been individually studied in detail in the literature, we will have to first investigate them again with unified system parameters. This way a fair comparison of the performance of both schemes can be carried out. MC-DS-

CDMA and MC-CDMA are individually characterised and evaluated in Chapters 3 and 4, respectively. The comparison of the two systems is covered in Chapter 5 of this thesis.

Although MC-CDMA benefits from frequency diversity in a frequency selective fading channel, the drawback is excessive MAI between users. This is the main disadvantage of MC-CDMA compared to MC-DS-CMDA which is ideally MAI-free. There are various methods to minimise MAI with ML-MUD being the optimal yet most expensive method. A number of solutions have been proposed in the literature to reduce the complexity of ML detection while still achieving suboptimal performance. The Chase algorithm [3] is one near-ML method which gained noticeable interest as a means of decoding linear block codes.

We believe that the application of the Chase algorithm to the MUD of MC-CDMA should achieve a performance close to the optimal ML-MUD with a fraction of its complexity. This is the body of investigation in Chapter 6 of the thesis.

Finally, when looking in depth at the Chase-based BTC decoding algorithm, originally proposed by Pyndiah [2], it was noticed that the algorithm assumes a binary structure of the inner codes of a BTC. Consequently, even a non-binary code, such as RS codes, has to be represented by binary components prior to decoding. The algorithm also assumes Grey mapping of the BTC components.

Our hypothesis is that by finding a BTC decoding algorithm that can process the non-binary code elements as symbols, rather than bits, these codes are expected to perform better. This is because the bit-level processing in the original decoding algorithm is not consistent with a non-binary code. Besides, by developing such an algorithm the

system is automatically freed from the Grey mapping condition, which opens the door to any mapping constellation to be used with BTC, especially ones which enhance power efficiency and PAPR effects.

Chapter 3

MC-DS-CDMA: Characterisation and Performance Analysis

Multicarrier Direct-Sequence CDMA (MC-DS-CDMA) has been proposed by a number of researchers in the literature as a candidate for the multiple access of the next generation wireless communications schemes. However, apart from Hanzo's effort in [26] as well as that of Abeta et al in [89], no research has ever been conducted to fairly and thoroughly compare MC-DS-CDMA with other multiple-access schemes. In this chapter MC-DS-CDMA is first introduced in section 3.1 featuring its main advantages and disadvantages. In section 3.2 the system is described with focus on the signal processing at the transmitter and receiver sides of the system. In section 3.3 the channel and system parameters used in the computer simulations are described for both the single-cell and multi-cell environments. The

simulation results are presented and discussed in section 3.4, and the chapter is finally

concluded in section 3.5.

3.1   MC-DS-CDMA

In MC-DS-CDMA, the transmitted data stream is S/P converted and then each of the

parallel streams is spread using a given spreading sequence in the time domain. Each

user uses a unique spreading sequence. The spreading sequences belonging to

different users are summed and each set of summed spread sequences modulates a

conventional OFDM subcarrier i.e. all users use all subcarriers. To clarify any

ambiguity, when we say that the spreading is applied in the time domain we mean that

the chips of a spreading code are multiplied by duplications of a transmitted symbol in

the time domain. Whether this results in consuming more resources in the time or

frequency domain depends on the system configuration and parameterisation. The

building of a MC-DS-CDMA signal is portrayed in figure (3.1)
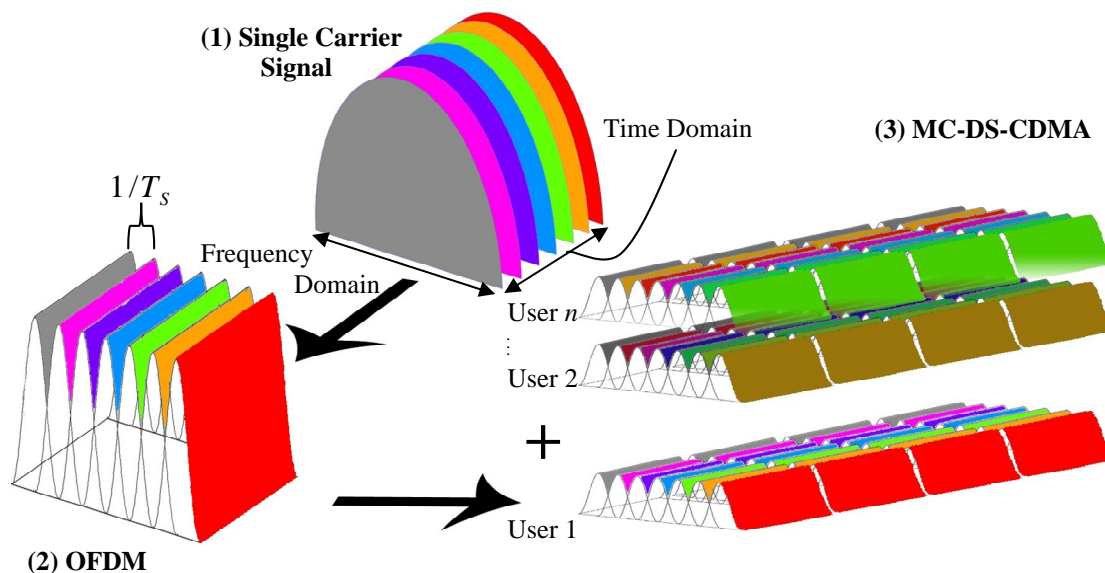
Figure 3.1   Signal Representation of MC-DS-CDMA

MC-DS-CDMA can be viewed as a natural extension to OFDM which makes use of CDMA as a multiple access scheme. Using CDMA in this context gives the system the flexibility of hosting as many users as the spreading code pool can provide. Unlike FDMA where particular users may suffer from loss of information due to severe fading at the subcarriers allocated to them, all users in a MC-DS-CDMA system have access to all subcarriers. The availability of the whole bandwidth per user makes MC-DS-CDMA inherit the strengths of a CDMA system which including the immunity against intentional jamming.

An extra advantage of time-domain spreading is that, given flat fading per subcarrier, the MAI is not affected by frequency selective fading. In other words, if the codes in use are orthogonal, such as Walsh-Hadamard codes, there should be no MAI interference among users when each subcarrier experiences flat fading. This simplifies the detection process to the conventional single-user detector and provides each user with a single-user loaded system performance even when the system is fully loaded i.e. all available spreading codes are in use. Combining the spreading code chips using MRC by weighting the signal by its Signal-to-Noise Ratio (SNR) can be safely conducted as all chips are affected with the same channel fading and hence using SNR weighting cannot destroy the orthogonality among the spreading codes.

It is worth noticing that maintaining the orthogonality among users is conditional on having the spread signal length to be shorter than the coherence time of the channel. If the Doppler frequency of the channel is high enough to cause a fast-fading channel and reduce the coherence time to become shorter than the spread signal time, MC-DS-CDMA loses its advantage of avoiding MAI.

On the other hand, MC-DS-CDMA with time-domain spreading lacks the chance of exploiting two dimensions of diversity: frequency and multipath diversity. Because each symbol is placed and spread over a single subcarrier it can simply be lost if that subcarrier faces severe fading and it is left then to the power of the channel code to recover the lost symbols. Furthermore, because the chip length of the spreading code in MC-DS-CDMA is equal to the original OFDM symbol before spreading, the channel paths are more likely expected to "fit" within the length of a single chip and hence it becomes impossible for the system to use a RAKE receiver to differentiate between these channel paths unless the delay spread of the channel is very large. Exploiting as many diversity dimensions as possible becomes more crucial in multi-cell environments as multi-cell interference becomes the bottleneck of the system's performance.

Although time-domain spreading gives the system the flexibility to increase the number of simultaneously served users by using longer codes in the time domain without the need to re-dimension the signal in the frequency domain, it is limited to the fact that the signal period in the time domain needs to be much less than the coherence time so that the pilot-to-data ratio remains within acceptable levels. Otherwise, assuming that the signal is just within the coherence time, each symbol will need to be followed by a pilot symbol to update the channel estimation, reducing the channel efficiency of the system and making it more sensitive to Doppler and synchronisation errors.

3.2   System Description

Figure (3.2) illustrates the MC-DS-CDMA downlink's transmitter and receiver structures. After channel coding, bit interleaving is applied to the encoded bits. A block interleaver is used where encoded bits in one symbol are uniformly permuted across all bit positions in the constellation. The interleaving scheme (similar to the IEEE802.11 specification) is defined by two permutations. The first permutation ensures that adjacent bits are modulated onto nonadjacent subcarriers and the second permutation ensures that adjacent bits are mapped alternatively onto less and more significant bits of the constellation. This will randomise the bits, so that error events due to deep fades are maximally de-correlated. If the interleaver has sufficient depth the fading processes that affect successive symbols belonging to the same codeword will be uncorrelated. After constellation Gray mapping, N_c symbols are serial-to-parallel (S/P) converted. The new symbol duration after conversion is $T_c = T_s \times N_c$, where T_s is the original symbol period before S/P conversion and N_c is the number of subcarriers. Each symbol is then duplicated into SF_t serial copies, where SF_t is the spreading factor in the time domain, and each of these copies is multiplied by one of the SF_t chips of the spreading code assigned for the user.
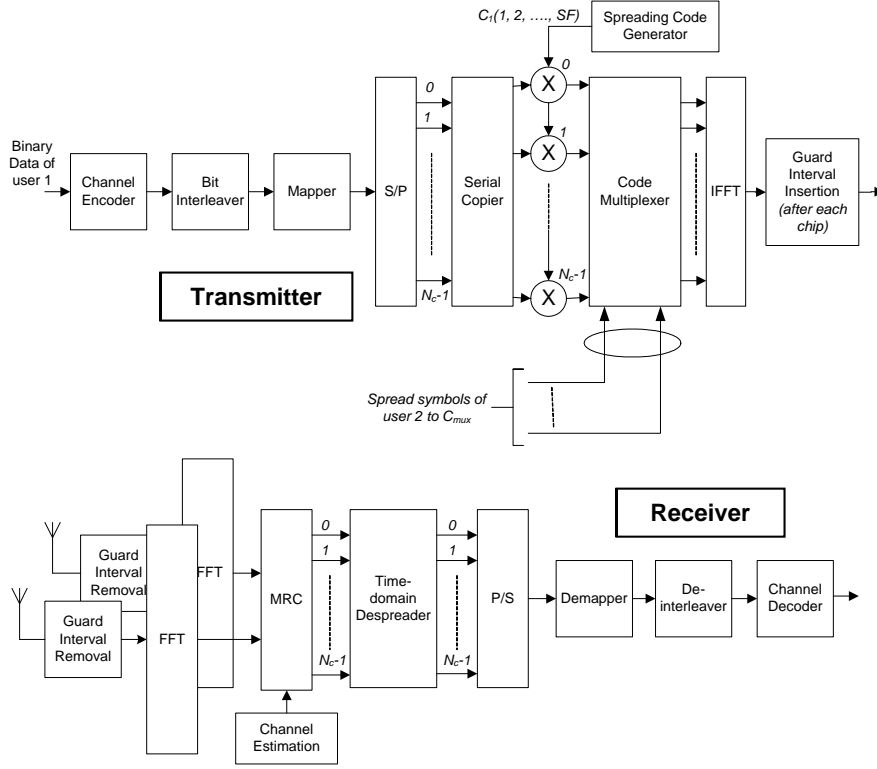
Figure 3.2   MC-DS-CDMA system model

After multiplexing the symbols of C_{mux} users, the resultant N_c parallel sequences are converted into an MC-DS-CDMA frame using the Inverse Fast Fourier Transform (IFFT) and followed by the insertion of the guard interval of period T_g after every chip. The chip duration is now equal to T_c and the new symbol duration becomes $T = T_c' \times SF$, where $T_c' = T_c + T_g$. The output is then transmitted over the corresponding N_c subcarriers. The transmitted signal of user k can be formulated in the time domain as;

$$s_k(t) = \sum_{i=1}^{N_c} b_{k,i}(t)c_k(t)e^{(2\pi f_i t)} , \qquad (3.1)$$

where N_c is the number of subcarriers, $b_k(t)$ is the transmitted data symbol of user k at time t, and $c_k(t)$ is the spreading code chip's form at time t.

The receiver is provided with g antennas ($g \geq 1$) where the transmitted signal is subjected to an independent Rayleigh fading multipath channel H_g between the transmit antenna and each of the receive antennas. The subcarrier bandwidth in MC-DS-CDMA is narrow enough to ensure that every subcarrier is affected by flat fading even in the worse delay conditions. Thus at the receiver, the received signal at the $g-th$ receive antenna can be expressed as:

$$R_g = C^T B H_g + N ,\qquad (3.2)$$

where C is a $C_{mux} \times SF$ matrix containing the spread codes in use:

$$C = \begin{bmatrix} c_1[1] & \cdots & \cdots & \cdots & c_1[SF_t] \\ \vdots & \ddots & & & \vdots \\ \vdots & & \ddots & & \vdots \\ \vdots & & & \ddots & \vdots \\ c_{c_{mux}}[1] & \cdots & \cdots & \cdots & c_{c_{mux}}[SF_t] \end{bmatrix}.\qquad (3.3)$$

B is the $C_{mux} \times N_c$ matrix of the data symbols corresponding to all active users and transmitted in one MC-DS-CDMA frame, and it is given by:

$$B = \begin{bmatrix} b_{1,1} & \cdots & \cdots & \cdots & b_{1,N_c} \\ \vdots & \ddots & & & \vdots \\ \vdots & & \ddots & & \vdots \\ \vdots & & & \ddots & \vdots \\ b_{c_{mux},1} & \cdots & \cdots & \cdots & b_{c_{mux},N_c} \end{bmatrix},\qquad (3.4)$$

where $b_{n,k}$ is the symbol corresponding to the $n-th$ user and $k-th$ subcarrier. The term X^T denotes the non-conjugate transpose function. H_g is the diagonal channel matrix for the signal received at antenna g given by:

$$H_g = \begin{bmatrix} h_g(1) & 0 & \cdots & \cdots & 0 \\ 0 & h_g(2) & 0 & & \vdots \\ \vdots & & \ddots & & \vdots \\ \vdots & & & \ddots & \vdots \\ 0 & \cdots & \cdots & \cdots & h_g(N_c) \end{bmatrix}, \tag{3.5}$$

and N is the $SF_t \times N_c$ Additive White Gaussian Noise (AWGN) matrix with zero mean and double-sided power spectral density of $N_0/2$.

If more than one receive antenna are considered the signals from all receive antennas are first maximally-ratio combined (MRC) exploiting the spatial diversity available to form one signal. As the channel is assumed to be fixed over at least one symbol period T, there will be no MAI amongst users when orthogonal spreading codes such as Walsh-Hadamard codes are used; therefore despreading and combining do not need any further equalisation or weighting. The resultant can then be sent to the modulation demapper from which soft output values are fed to the deinterleaver and passed to the channel decoder to get an estimation of the transmitted bits.

3.3   System Configuration

The channel model in use is similar to that suggested in [40]. As depicted in figure (3.3), it is a 24-path independent identically distributed (IID) Rayleigh-faded channel with an exponential decay profile of the paths' average power levels. The paths are placed at equal distances of D_{exp} samples. L in the figure refers to the number of the delayed path. In this chapter's simulation results, a fixed delay of 0.3 µsec was used. The guard interval is set so that it is always longer than the dispersion of the channel.
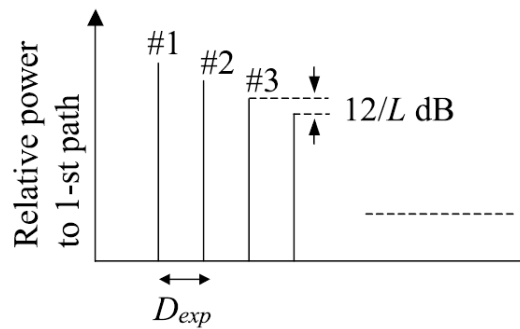
Figure 3.3   Exponentially decaying CIR model [40]

In the multi-cell environment, the mobile station is assumed to have synchronised inter-cell interference from one neighbour cell with an identical total power level making the signal to interference ratio S/I equal to zero dB. This setup is sketched in figure (3.4). The signals from different cells are separated with Pseudo Noise (PN) scrambling codes assigned to cells.
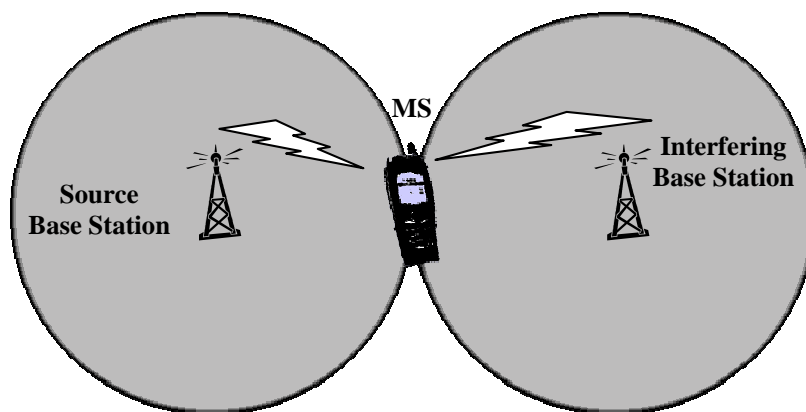
Figure 3.4   Zero Inter-Cell Interference Setup

The main parameters of the system under investigation are summarised in table (3.1). When a parameter is used as a variable in any experiment this will be clearly defined within the experimental description.

Table 3.1   MC-DS-CDMA simulation system parameters

	MC-DS-CDMA
Bandwidth	100.5 MHz
Subcarrier Spacing	500 KHz
Guard Interval	0.500 μSec.
Number of Subcarriers (Nc)	200
Packet size	3200 Data bits
Spreading Code	Walsh-Hadamard
Scrambling Code	Pseudo Random
Spreading Factor	SF =16
Modulation	QPSK, 16QAM
Coding/Decoding (if applicable)	Turbo coding (CR=1/3-1/2, K=4) generator polynomials g0=13 and g1=15 (in octal) Max-Log-MAP decoding (6 iterations)
Interleaving	Block Bit Interleaving
User Detection	SUD
Channel Impulse Response (CIR)	As shown in figure (3.3)

3.4   Simulation results and analysis

3.4.1   Single-cell environment

3.4.1.1 Effect of Modulation and Coding Rate

Figure (3.5) present the BER and PER performance simulation results for MC-DS-CDMA in a single-cell Rayleigh fading environment with three different modulation and FEC combinations. The combinations are QPSK with a code rate CR=1/3, QPSK with CR=1/2 and 16QAM with CR=1/2. It is noticed from the results that MC-DS-CDMA is capable of maintaining a monotonically improving performance as E_b / N_0 increases. This is expected to be the result of the maintained orthogonality between the spreading codes, iterative decoding of the turbo code and the application of the two receive antennas. The depicted results show an SNR penalty of 1 dB to increase the code rate from 1/3 to 1/2 and a further loss of about 2.5 dB when moving from QPSK to the higher modulation order of 16QAM. The following experiments

investigate further MC-DS-CDMA with the aim of explaining where this scheme derives most of its performance gain from.

3.4.1.2 Effect of Iterative Decoding

The gain of using FEC and iterative decoding is studied in this subsection. The BER and PER performances of uncoded and encoded MC-DS-CDMA are depicted in Figure (3.6). The depicted results do not utilise any multiple antennas at either the transmitter or the receiver. It can be clearly noticed that although applying FEC by itself (without iterations) offers a significant improvement to the system, it is incapable of removing the error floor for both BER and PER. Such behaviour is expected recalling that MC-DS-CDMA does not use any diversity dimension other than FEC to recover symbols that are lost on severely faded subcarriers. Hence, the performance depends on the power of FEC to recover the lost information using the surviving symbols. This explains the dramatic improvement of the system's performance when strengthening the Turbo codes with an increased number of iterations (2 and 6 iterations). The figures show, however, that there would only be a 2dB improvement when going from 2 to 6 iterations. This observation suggests that the performance gain of the turbo decoder becomes small after 2 iterations.
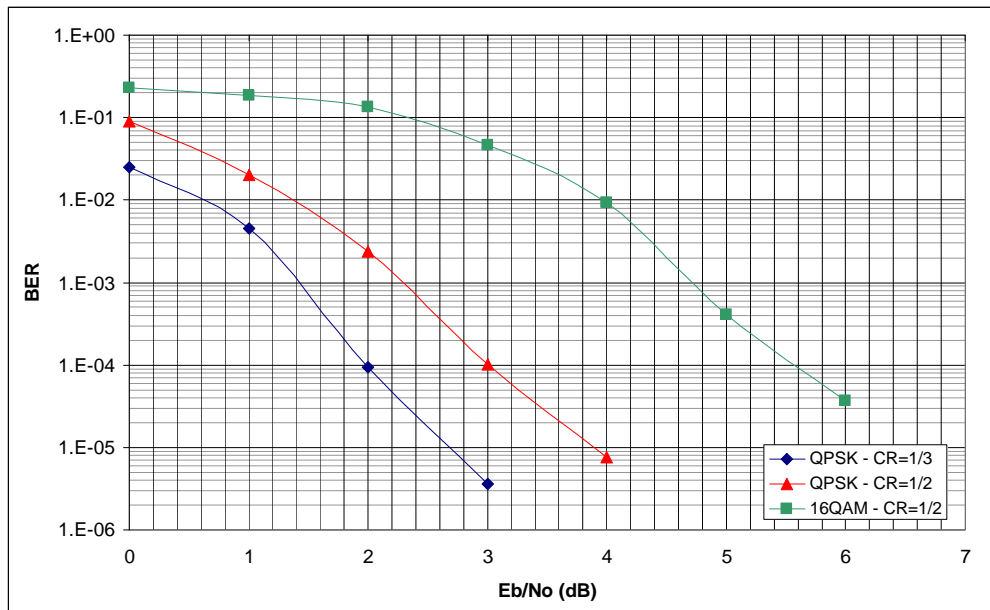
(a)
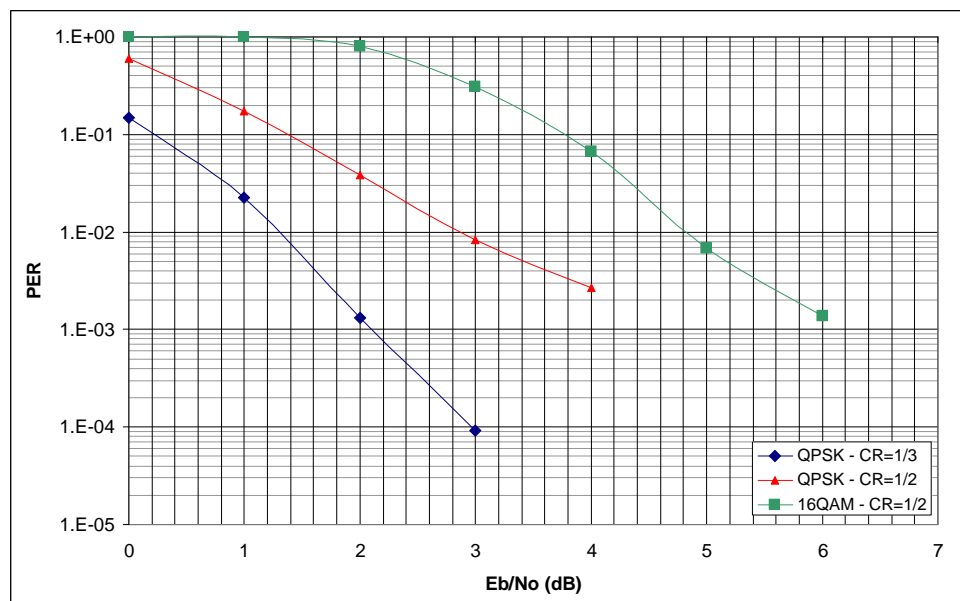
(b)

Figure 3.5   BER and PER Performance of MC-DS-CDMA with three configurations: a. QPSK and CR=1/3, b. QPSK and CR=1/2 and c. 16QAM and CR=1/2 [Rest of parameters as in table (3.1)]

(a)

(b)

Figure 3.6   BER and PER Performance of MC-DS-CDMA with iterative decoding [Rest of parameters as in table (3.1)]

3.4.1.3 Effect of MIMO

The performance of uncoded and encoded MC-DS-CDMA aided by Single-Input-Multiple-Output (SIMO) antennas is depicted in figure (3.7). In this case, two antennas are assumed at the receiver side whose signals are MRC combined and used as one signal afterwards. The application of SIMO impressively gives MC-DS-CDMA a gain of almost 10dB. This can be understood 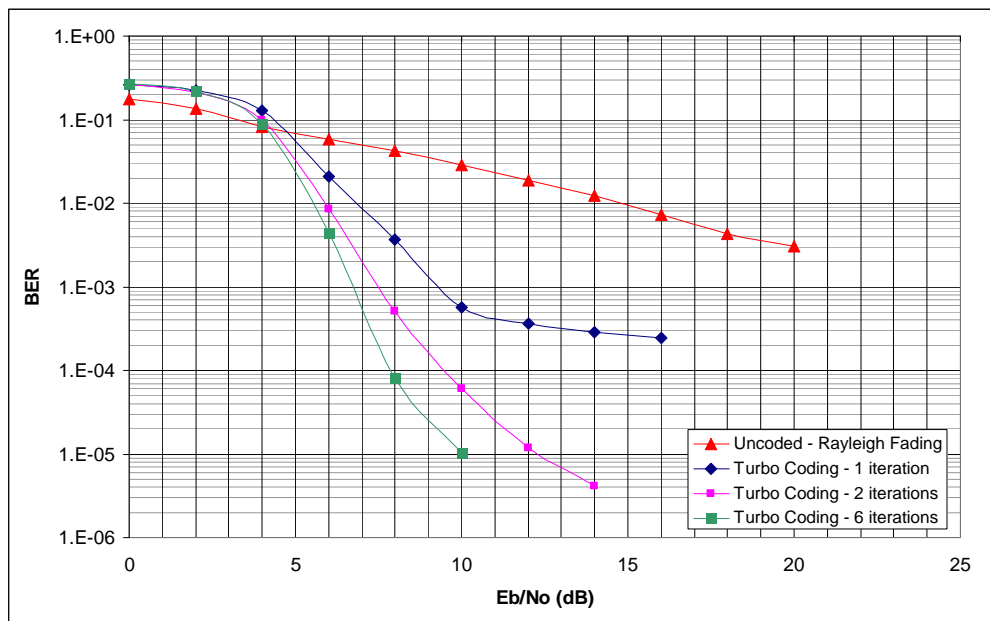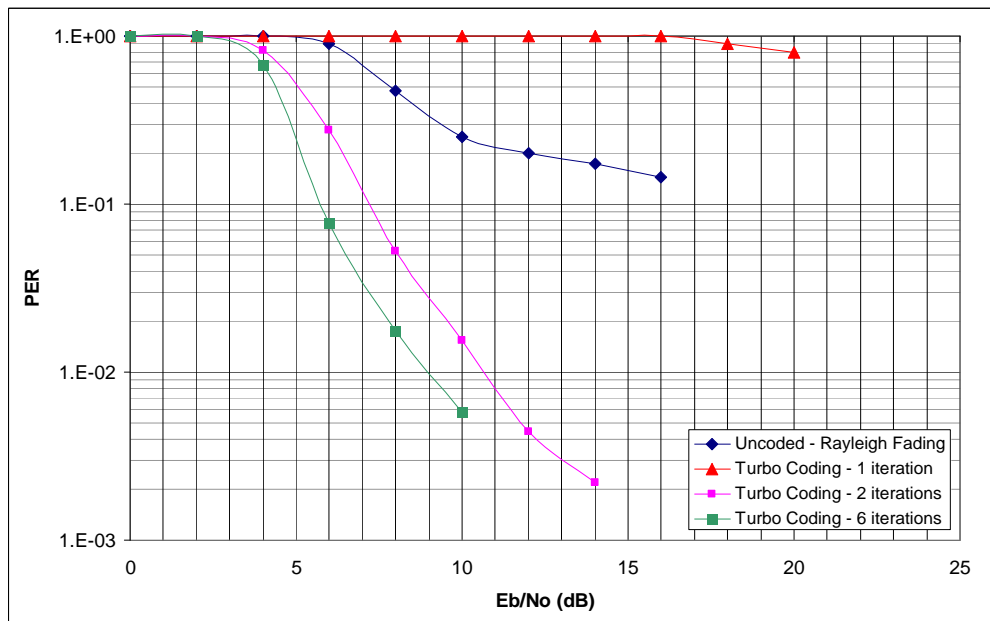as giving each subcarrier a second chance of not being fully lost at the second antenna if it is heavily faded at the first antenna, assuming that the channel characteristics of the two antennas are fully uncorrelated. The biggest improvement, however, comes from assisting the multiple antennas with a FEC block. The dramatic enhancement is interpreted conversely by saying that FEC works better when fewer initial errors are present. By applying SIMO the number of received errors significantly decreases, which leaves the FEC with few errors at faded subcarriers to recover.

It is relevant to compare MC-DS-CDMA when FEC, SIMO or both are used. This should give an insight into the relative gains achieved from both methods and would help indicate which method MC-DS-CDMA benefits from more. Figure (3.8) depicts the performance of MC-DS-CDMA with 1x2 SIMO with and without FEC and when using SISO aided by iterative FEC. While both SIMO and FEC offer significant enhancement to the system performance, it is clear that iterative FEC outperforms SIMO when they are both applied individually. However, when SIMO is aided with a non-iterative FEC it improves on fully-powered iterative FEC with 6 iterations. This has been already explained in that MC-DS-CDMA's weakness is its susceptibility to severely faded subcarriers where some symbols are lost. While iterative FEC tries to overcome the consequences of this problem by using the surviving symbols to estimate the lost ones, MIMO works on solving the actual problem, fading, by

offering the receiver two replicas of the same symbols delivered on two independent channels.
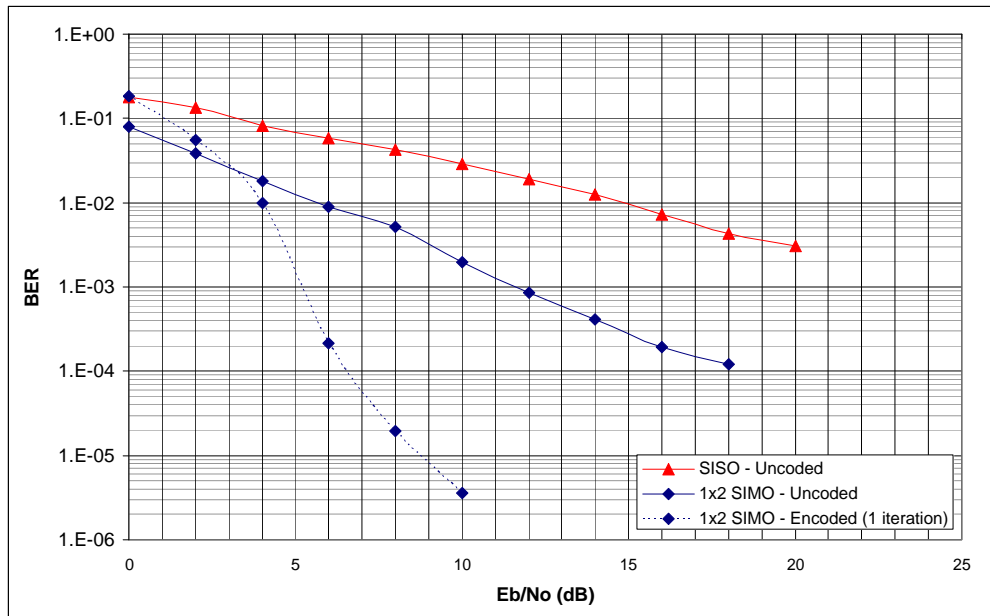
(a)
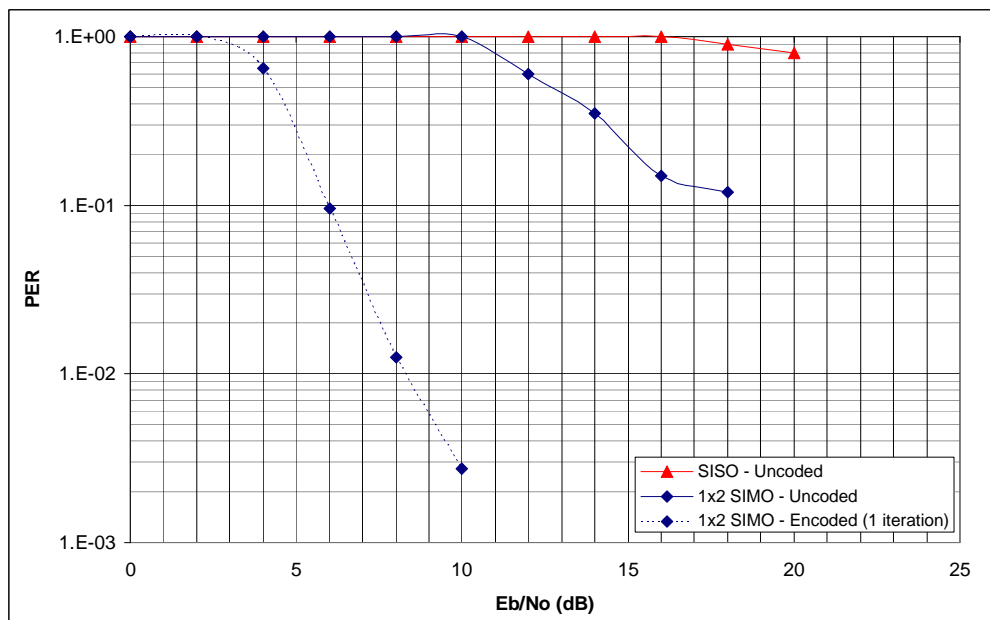
(b)

Figure 3.7   BER and PER Performance of MC-DS-CDMA with SIMO [Rest of parameters as in table (3.1)]
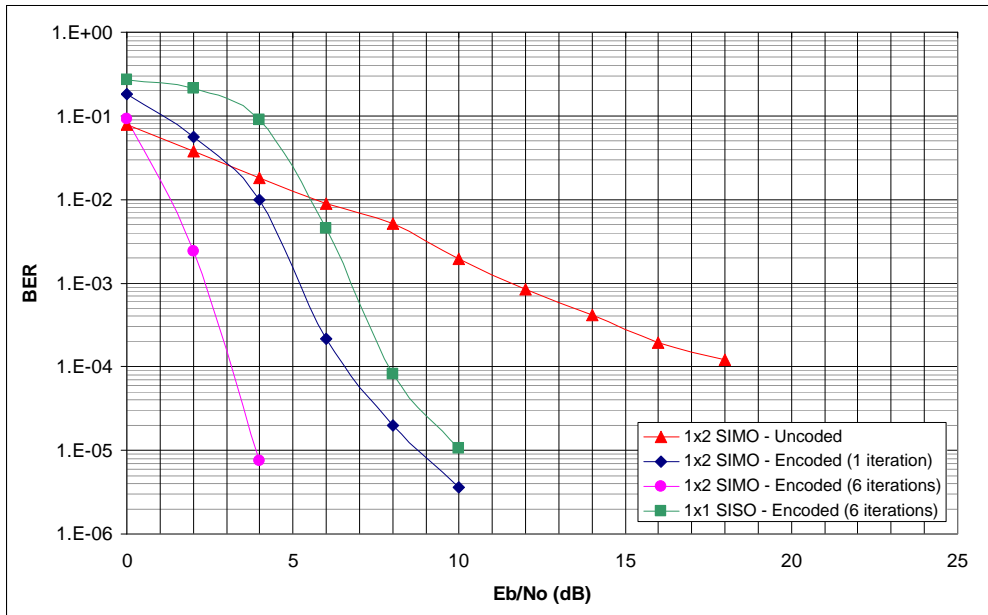
(a)
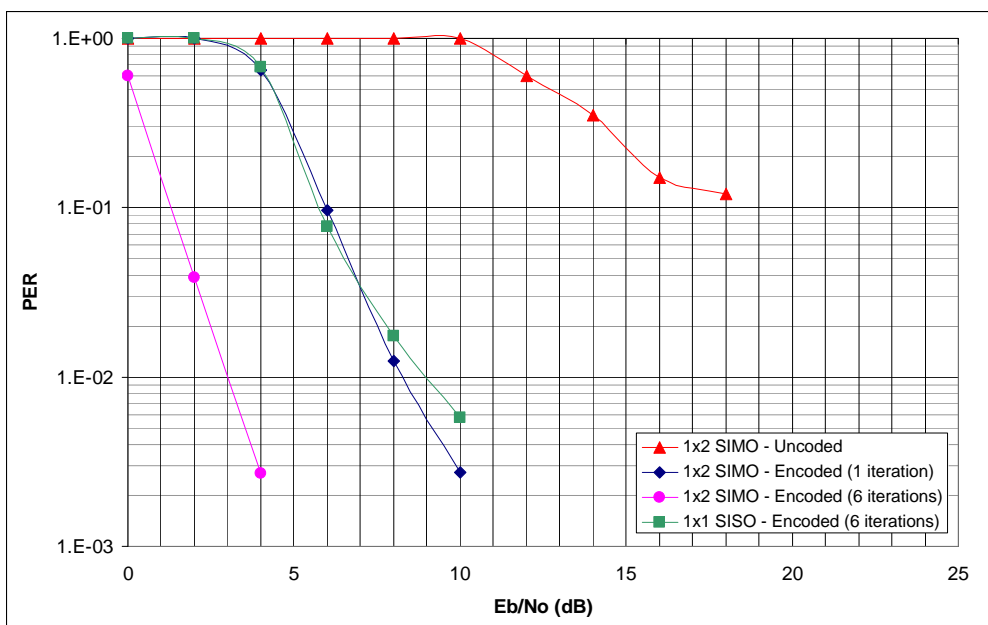
(b)

Figure 3.8 BER and PER Performance of MC-DS-CDMA with iterative decoding and SIMO [Rest of parameters as in table (3.1)]

Finally In this section, the performance of Multiple-Input-Single-Output (MISO) antennas setup is compared with that of SIMO in figure (3.9). Bearing in mind that with MISO the power of the signal transmitted from each transmit antenna is half that of the signal transmitted from the single transmit antenna in a SIMO configuration, the 2-3dB loss when moving from SIMO to MISO is justified. It is also worth noticing that, within the range of the BER and PER being looked at, SIMO does not suffer from the error floor which limits MISO's performance.
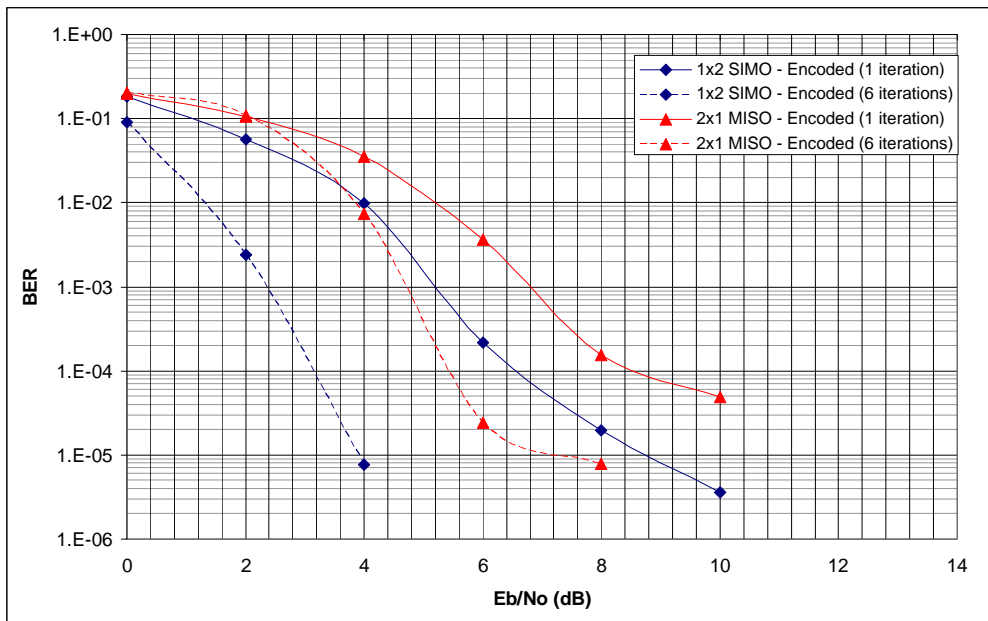
(a)
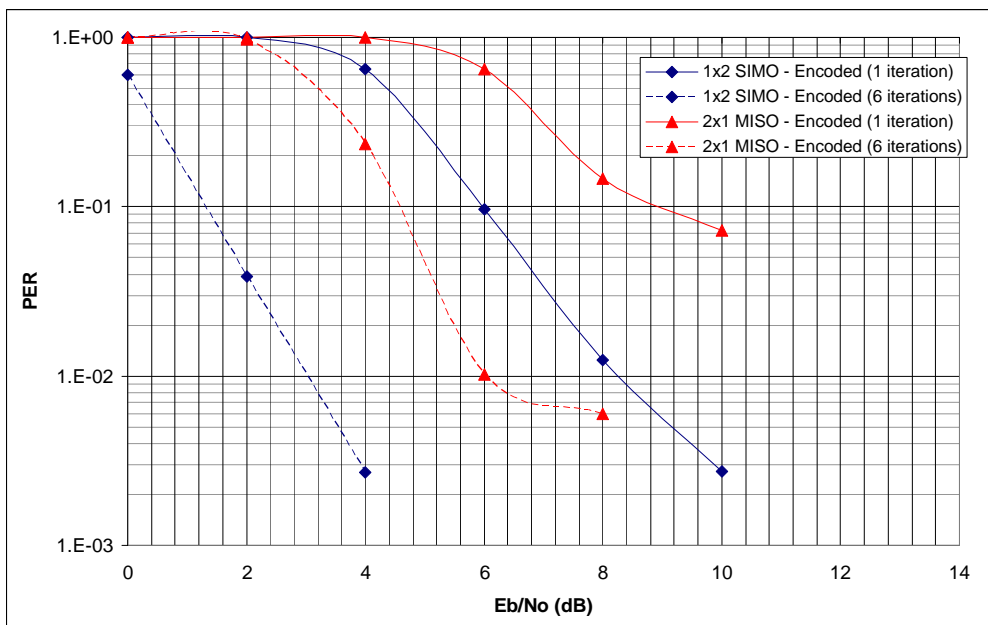
(b)

Figure 3.9   BER and PER Performance of MC-DS-MDMA with SIMO and MISO [Rest of parameters as in table (3.1)]

3.4.2   Multi-cell environment

The following simulation results and analysis deal with the performance of MC-DS-CDMA in a multi-cell environment. 4G networks are expected to perform seamlessly under all conditions. Therefore a 4G system will undoubtedly deal with issues related to inter-cell interference as well as handover and switching between cells. Although we do not look deeply into the multicell environment performance, our aim through this part of the study is to evaluate the performance of MC-DS-CDMA via basic multicell simulations in order to have an insight of its performance in such environments when the time comes to compare MC-DS-CDMA with MC-CDMA later in this thesis.

The parameters used are the ones summarised in table (3.1). Continuing with the assumption that the spreading codes used in each cell are orthogonal, in a multi-cell environment MC-DS-CDMA only suffers from inter-cell interference from other cells sharing the same frequency band.

Figure (3.10) presents the BER and PER performances of MC-DS-CDMA in a multi-cell environment with different coding rate and modulation order combinations. The depicted figures show a gradual improvement of performance when moving toward lower code rates and modulation orders. With the exception of the case when QPSK and Code Rate CR=1/3 are used, fully loaded MC-DS-CDMA cannot function when the inter-cell interference is high. All combinations follow a trend of having a wide gap between the single-user and full-load performances, with the combination of QPSK and CR=1/2 appearing to suffer the worst degradation when moving toward the fully loaded case. This raises the question of what inter-cell interference level can MC-DS-CDMA tolerate?
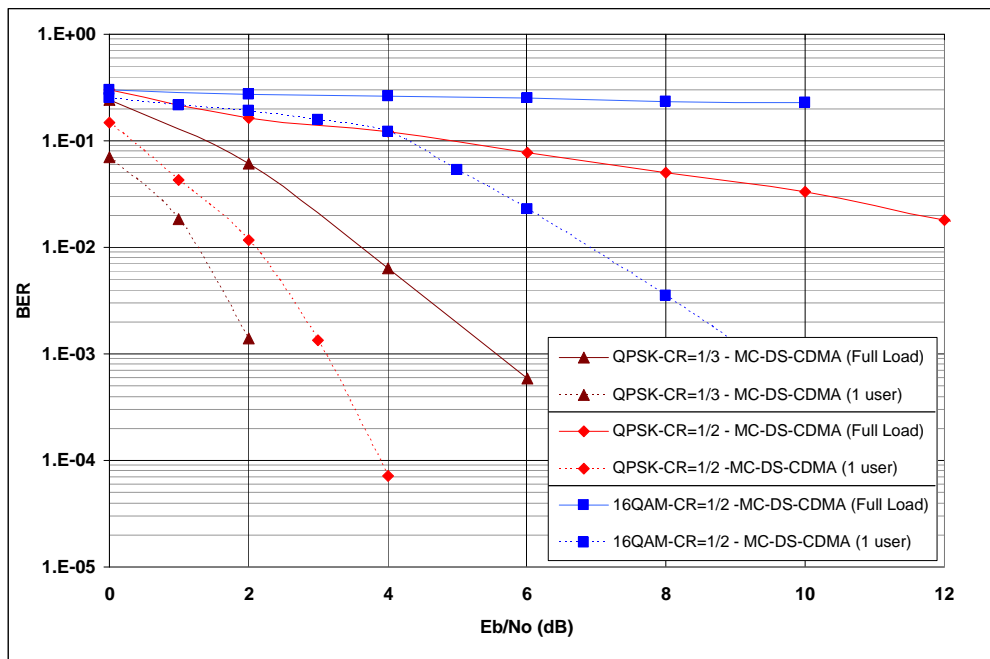
(a)
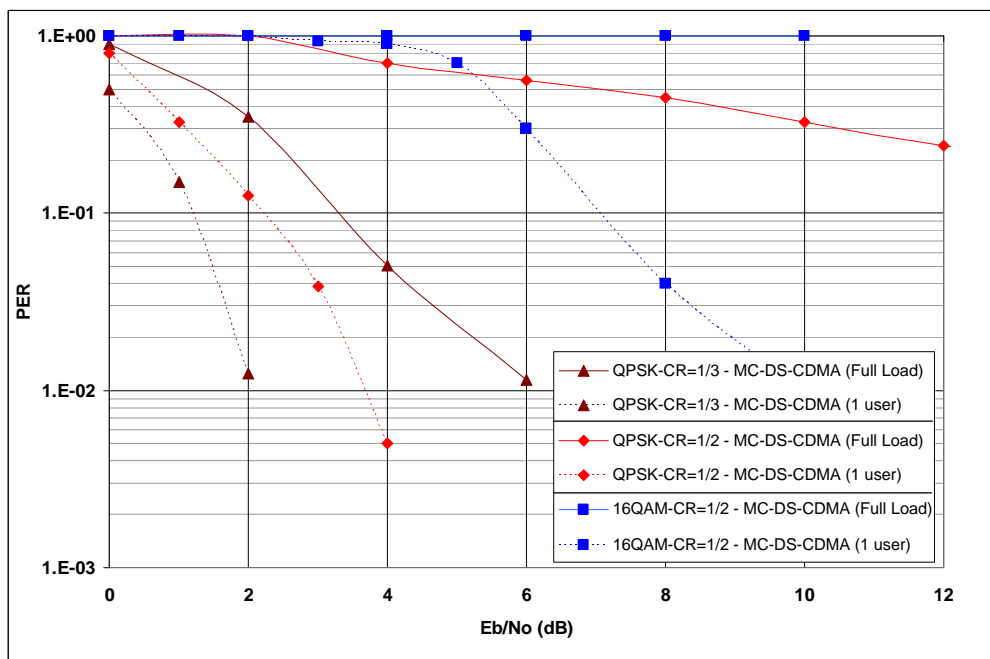
(b)

**Figure 3.10   BER and PER Performance of MC-DS-MDMA in multicell environment (*S/I* = 0)
[Rest of parameters as in table (3.1)]**

To answer this question, the performance of MC-DS-CDMA is depicted in figure (3.11) with varying loading factors L ranging from $L = 0.0625$ to $L = 1$ with QPSK as a modulation scheme and Turbo coding of CR=1/2. The primary observation from the graphs is the gradual smooth improvement of performance when moving from the full load case toward the low-load one. This suggests that MC-DS-CDMA does not suffer from a sudden collapse of performance at some level of inter-cell interference, making it a good candidate when performance can be traded off with the system's user intensity. Moreover, for a target BER=10^{-3} and PER=10^{-2} MC-DS-CDMA can achieve an efficiency of 50% ($L = 0.5$) at the worst case scenario of $S / I = 0$.
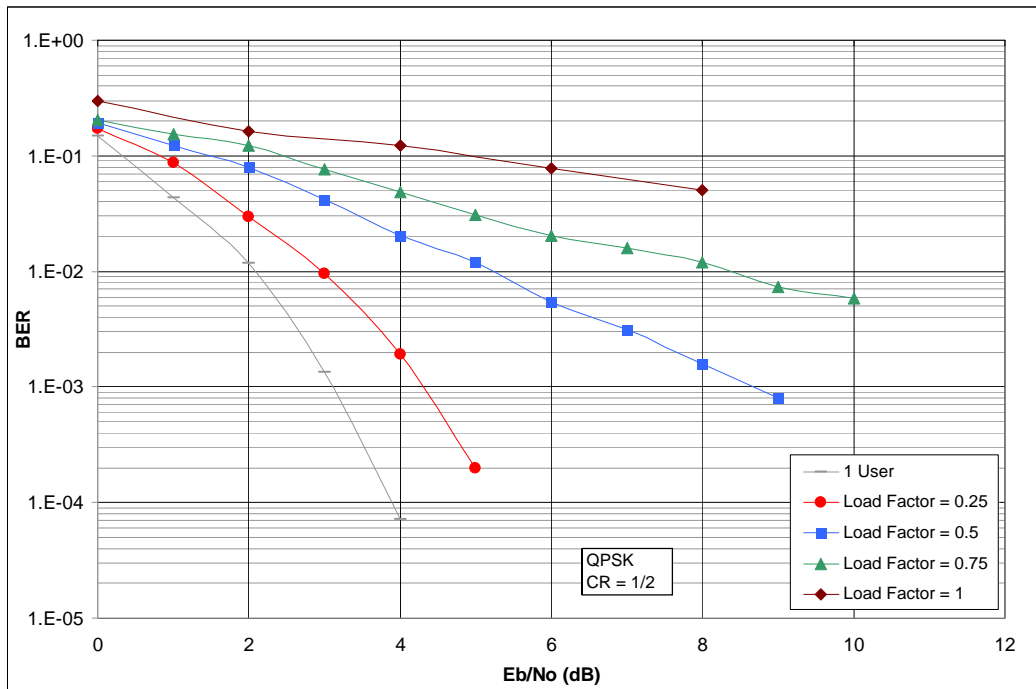
(a)
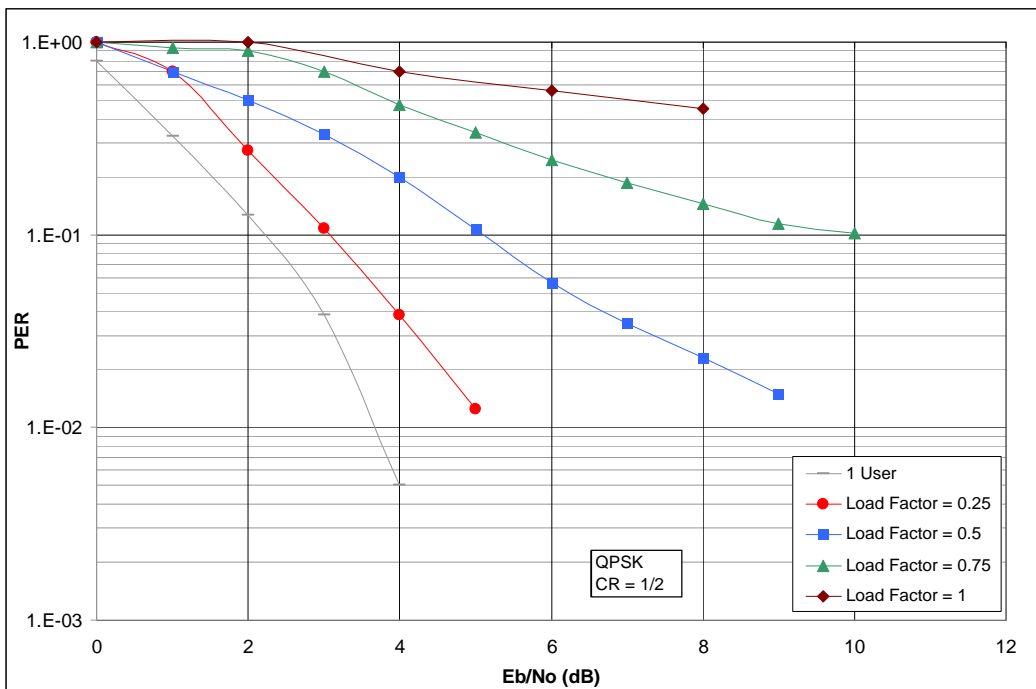
(b)

Figure 3.11   BER and PER Performance of MC-DS-MDMA in multi-cell environment with the loading factor L as a variable ($S/I = 0$) [Rest of parameters as in table (3.1)]

3.5   Conclusions

In this chapter MC-DS-CDMA, the first of two joint OFDM-CDMA schemes to be studied, was considered. The scheme was thoroughly described featuring its main advantages and disadvantages. Its performance in both single-cell and multi-cell environments was investigated using computer simulations with analysis of their results. The main results of the MC-DS-CDMA system's performance are summarised in table 3.2 for the QPSK-modulated system with code rate CR=1/2 in a single cell environment.

While MC-DS-CDMA does not suffer from MAI in a single cell environment (assuming no fast fading), it lacks diversity in both the frequency and time domains. This is perceived as a weak performance attribute when MC-DS-CDMA is not supported by any additional diversity. When the issue of diversity is resolved by employing two receive antennas, the system's performance gains over 8dBs of SNR enhancement over an uncoded system as shown in figure (3.7).

Although channel coding significantly improves the performance of SISO-antenna MC-DS-CDMA, it reaches an error floor which decreases with increasing number of decoding iterations (figure (3.6)). When channel coding is applied to a SIMO-assisted MC-DS-CDMA system, the BER performance is enhanced by a further 6dBs for one decoding iteration. This enhancement increases with more decoding iterations (5dB more improvement was observed in figure (3.8) after 6 decoding iterations).

When the total transmitted power is fixed, the performance of MC-DS-CDMA with MISO antennas is always inferior to SIMO antennas as demonstrated in figure (3.9). The gap between the two performances becomes wider with more decoding iterations. Also because MC-DS-CDMA does not suffer from MAI, it maintains the same

performance for any number of users in an ideal regime where neither ISI nor ICI exists.

The performance of MC-DS-CDMA was also investigated in a multi-cell environment for the same modulation-FEC combinations applied earlier to single cell simulations, as well as with multiple antennas. The results showed that the performance of MC-DS-CDMA gradually degrades with increasing inter-cell interference (assuming balanced loading across adjacent cells). This makes MC-DS-CDMA a good candidate when linear trade-off between the performance and number of users is sought or accepted.

MC-DS-CDMA with QPSK and CR=1/3 can achieve BER=10^{-3} and PER=10^{-2} even at the edge of two fully loaded cells (S / I =0). With CR=1/2 the system's efficiency decreases to 50%. Finally, studying different modulation/coding combinations revealed areas of overlapping performances of these combinations as figure (3.11) illustrates. For example, a single user QPSK system with CR=1/2 can perform better than a fully loaded QPSK system with CR=1/3. There is potential for further research to investigate the possibility of achieving a similar or higher efficiency by switching to higher modulation orders beyond certain loading factors.

In Chapter 4, the second scheme called MC-CDMA will be characterised in a similar way to that applied in this chapter before they are both compared later in Chapter 5.

Table 3.2   Required *Eb/No* for target BER=10^{-4} and target PER=10^{-2} in a MC-DS-CDMA system [Single-cell environment with QPSK and *CR*=1/2]

	BER = 10^{-4}	PER = 10^{-2}
1x1 SISO + 6 iterations	7.8 dB	9 dB
1x2 SIMO (Uncoded)	18 dB	∞
1x2 SIMO + 1 iteration	6.5 dB	8.3 dB
1x2 SIMO + 6 iterations	3 dB	2.9 dB

Chapter 4
MC-CDMA: Characterisation and Performance Analysis

In continuation of the comparative study into the different joint OFDM-CDMA candidate schemes for the next-generation wireless systems, this chapter focuses on Multicarrier CDMA (MC-CDMA), a multiple-access method which has traditionally received more attention than MC-DS-CDMA which was discussed in the previous chapter. Although MC-CDMA has been thoroughly studied in the literature [1, 10, 16-25], we found it crucial to investigate the performance of MC-CDMA for the same channel and environment conditions as MC-DS-CDMA in order to establish a fair comparison.

In the next section the main features of MC-CDMA are discussed, followed by a more detailed description of the MC-CDMA system and the channel parameters used to simulate the system. The simulation results are then shown and discussed. The last section of this chapter draws the salient conclusions from this part of the study.

4.1   MC-CDMA

In MC-CDMA the transmitter spreads a modulation symbol using a given spreading code in the frequency domain. More specifically, each chip of the spreading code is transmitted over a different subcarrier. For multi-carrier transmission, it is essential to have frequency non-selective fading over each subcarrier. Therefore, if the original symbol rate is high enough to make the signal subject to frequency-selective fading, the signal needs first to be S/P converted before being spread over the frequency domain.

Whether the chips corresponding to one symbol should be placed on adjacent subcarriers or not is an issue of investigation. Distributing a symbol over the whole available bandwidth involves chip interleaving and is distinct from bit interleaving applied at the output of the channel encoder. Chip interleaving ensures that chips of one spreading code are transmitted over independent identically-distributed subcarriers, increasing the possibility of having uncorrelated fading over the related subcarriers thereby enabling the system to exploit more frequency domain diversity. On the other hand, reducing the correlation in fading among the spreading code's chips destroys the orthogonality among the different spreading codes in use which leads to a high level of MAI in a multi-code transmission scenario. However, when no chip interleaving is applied and if the total bandwidth occupied by one spreading code is narrower than the coherence bandwidth of the channel, the channel frequency response becomes flat over that bandwidth and there should be no MAI at reception if the spreading codes themselves are orthogonal. However, in this case no diversity is gained by the receiver in the frequency domain. Thus it is a trade-off between diversity and MAI. Chip interleaving maximises the frequency domain diversity

exploitation at the expense of increasing MAI while the opposite maintains MAI at a low level at the expense of frequency diversity.

In multi-cell scenarios, MC-CDMA offers a system the capability of distributing the intercell interference over a number of subcarriers for each symbol. Whether such an advantage overcomes the intercell interference caused by MAI is another point of investigation in order to determine the performance of MC-CDMA.

MAI can be ameliorated with the aid of multi-user detection (MUD). However, good performing multi-user detectors are always of a considerably high complexity compared to the basic Single-User detector (SUD). Therefore, improving the performance of MC-CDMA in terms of detection is frequently at the cost of increasing complexity in the system. The amount of improvement in the performance of MC-CDMA when moving from the simple SUD to the more complex MUD is part of this chapter's investigation.
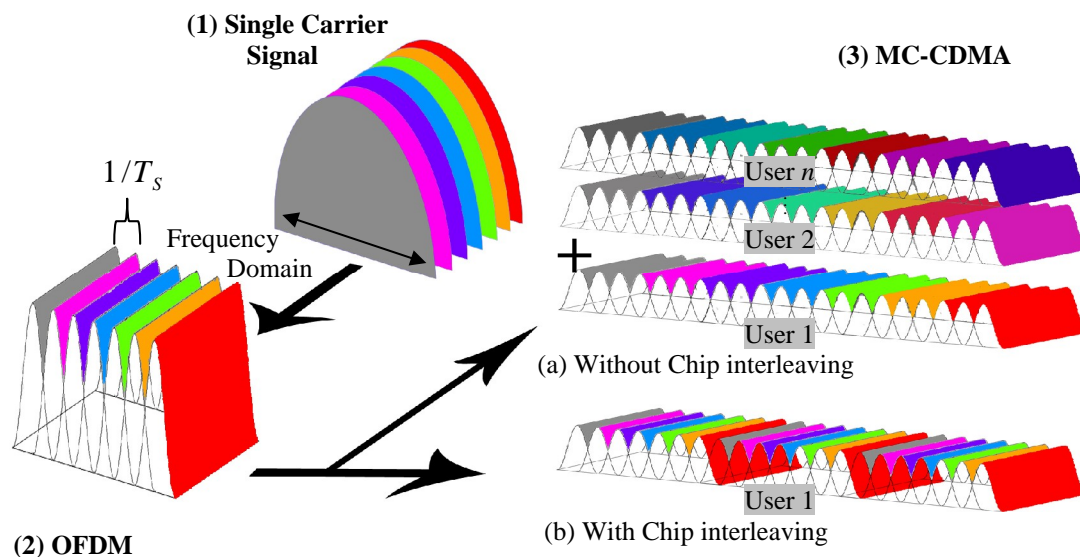
Figure 4.1   Signal Reshaping in MC-CDMA without and with chip interleaving

As wireless communications systems are often restricted in terms of the bandwidth available for them to use, then MC-CDMA is limited in terms of expansion across the frequency domain when the need arises to use longer spreading codes to accommodate more users simultaneously. One way to overcome this limitation is to increase the number of subcarriers within the same bandwidth. This becomes now a question of how flexible the system should be to adapt the number of subcarriers and the spacing between these subcarriers according to the users need. Furthermore, it needs to be bore in mind that increasing the number of subcarriers will increase the peak-to-average power ratio (PAPR), which is one of the main limitations of a multi-carrier system.

4.2   System Description

As shown in figure (4.2), in MC-CDMA N_c/SF_f data symbols are S/P converted, where SF_f is the spreading factor in the frequency domain. Each of the S/P converted symbols is copied SF_f times so that the total number of symbol copies available to modulate the subcarriers is equal to N_c. The next step is to multiply each of the spread symbol copies corresponding to one symbol, known as the relative symbols, by one chip of a given code of length SF_f assigned to the users. The copies of every symbol can be distributed using two different methods:
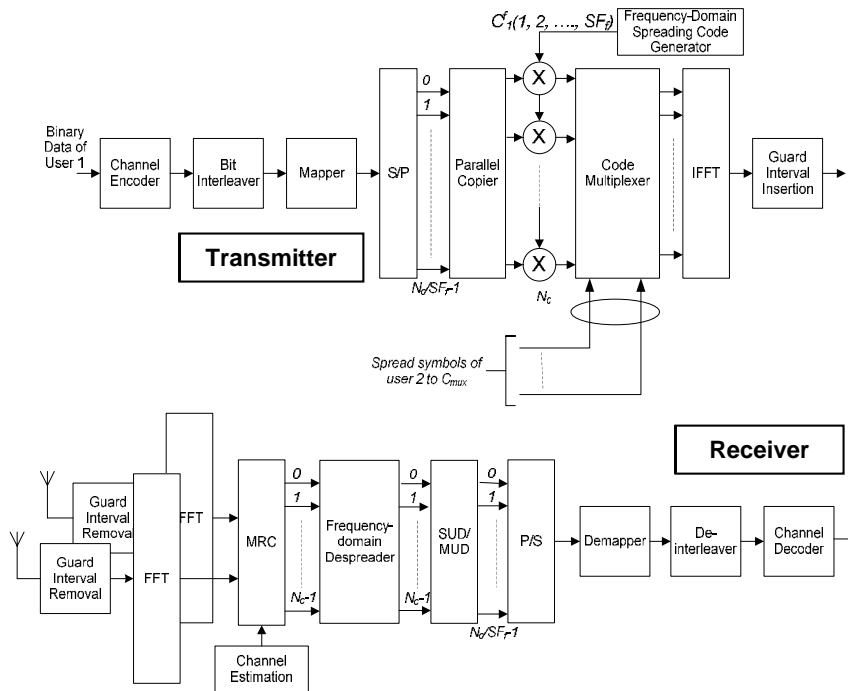
Figure 4.2   MC-CDMA system model

- Placing all relative symbols on adjacent subcarriers will result in minimising the MAI if the delay spread of the channel is short enough to cause quasi flat fading over a number of consecutive subcarriers instead of just one.

- Interleaving relative symbols across the frequency domain so that the maximum possible distance is assumed between any two relevant symbol copies. With these settings the subcarriers corresponding to one symbol are much less likely to have any correlation in their fading characteristics. Such a configuration increases the chances of exploiting the frequency diversity available in the channel.

All symbols transmitted within one OFDM symbol are multiplied with the same code; in other words, the code is used N_c / SF_f times in every frame.

After multiplying the data of all the users, the new N_c chipped symbols transmitted in parallel form one MC-CDMA frame using the IFFT, where every chip symbol is carried on one subcarrier. The transmitted signal of user k can be represented in the time domain by equation (4.1)

$$s_k(t) = \sum_{i=1}^{N_c/SF_f} \sum_{j=1}^{SF_f} b_{ki}(t)c_k^f(t)e^{(2\pi f_{ij}t)} \, , \tag{4.1}$$

where N_c/SF_f is the number of symbols transmitted in parallel per subcarrier, $b_{ki}(t)$ is the i-th transmitted data symbol of user k at time t, and $c_k^f(t)$ is the frequency-domain spreading code of user k at time t.

Similar to MC-DS-CDMA, the subcarrier bandwidth and spacing in MC-CDMA are set such that no ISI affects the subcarriers. The same assumption that all the chips on one subcarrier within a frame are faded simultaneously is also valid here. At the receiver, the received signal at antenna g ($g \geq 1$) corresponding to the l-th transmitted symbol can be represented as:

$$R_{l,g} = X_l H_{l,g} + N_{l,g} \qquad l = 1, 2, \ldots, N_c/SF_f \, , \tag{4.2}$$

where X_l is an SF_f-long vector representing the symbols spread over the l-th group of subcarriers in the frequency domain, and is given by:

$$X_l = \left[X_l(1,1) \cdots \quad \cdots \quad \cdots \quad X_l(1,SF_f) \right] \tag{4.3}$$

and

$$X_l(m,k) = \sum_{n=1}^{C_{mux}} C_n^f[k] b_{n,l} , \qquad (4.4)$$

where $b_{n,l}$ is the data symbol corresponding to user n and transmitted over the l-th

group of subcarriers. $C_n^f[k]$ is the k-th chip of the frequency domain spreading code

assigned to user n.

$H_{l,g}$ is the diagonal channel matrix for the signal received at antenna g over

subcarrier group l, and is given by:

$$H_{l,g} = \begin{bmatrix} h_{l,g}(1) & 0 & \cdots & \cdots & 0 \\ 0 & h_{l,g}(2) & 0 & & \vdots \\ \vdots & & \ddots & & \vdots \\ \vdots & & & \ddots & \vdots \\ 0 & \cdots & \cdots & \cdots & h_{l,g}(SF_f) \end{bmatrix} \qquad (4.5)$$

and $N_{l,g}$ is the SF_f-length Additive White Gaussian Noise (AWGN) vector with zero

mean and double-sided power spectral density of $N_0/2$.

If more than one receive antenna are in use, the resultants from all antennas are

maximal ratio combined. The signal is then despread in the frequency domain where

the orthogonality between codes is violated due to the frequency selective fading

across the code chips. The dispreading, detection and separation methods of the user's

signal fall into one of the following two categories:

1. Single-User Detection (SUD): This is done the same way as in the time

   domain by multiplying the signal with the user's designated frequency-domain

   code incorporating a weighting factor and then summing the resultant signals

   together. The weighting factor can take different values depending on the

combining method in use; this may be ORC, MRC, EGC… etc. Using a single-user detection technique has the advantage of simplifying the detection algorithm, and utilising the spreading and frequency diversity gain, but the MAI issue is not addresses.

2. Multi-User Detection (MUD): The MUD method used in this chapter is the general MMSE-based MUD. In this technique the despreading is first done by multiplying the signal with the frequency-domain code matrix. The next step is to detect the wanted user signal using MMSE-based MUD which balances the MAI and noise amplification processes. To obtain the MMSE weight matrix Z, the covariance matrix R is calculated as:

$$R = \begin{bmatrix} 1 & \rho_{12} & \cdots & \cdots & \rho_{1SF_f} \\ \rho_{21} & 1 & & & \rho_{2SF_f} \\ \vdots & & \ddots & & \vdots \\ \vdots & & & \ddots & \vdots \\ \rho_{SF_f 1} & \rho_{SF_f 2} & \cdots & \cdots & 1 \end{bmatrix},$$

(4.6)

where ρ_{xy} is defined in (4.7):

$$\rho_{xy} = \frac{\sum_{k=1}^{SF_f} C_x^f[k] C_y^f[k] \sum_{g=1}^{2} H_{l,g}(k)}{\sum_{k=1}^{SF_f} \sum_{g=1}^{2} H_{l,g}(k)}.$$

(4.7)

Then the signal is multiplied by the matrix Z given by:

$$Z = (R + \frac{N_0}{E_s} I)^{-1},$$

(4.8)

where I is the identity matrix of size $SF_f \times SF_f$.

After despreading in the frequency domain, the resultant can be sent to the demapper; soft outputs are deinterleaved according to the algorithm described in section (3.2) of the previous chapter, and then forwarded to the channel decoder to estimate the actual transmitted data bits.

4.3   System Configuration

The aim of this study is to characterise the performance of MC-CDMA, hence many parameters need to be varied for some experiments and fixed for others. In the first experiment relative delay spread to symbol duration values, instead of absolute values, are used to characterise the performance of MC-CDMA for different propagation channels. Whenever a fading channel is mentioned, the channel model used is based on [40] which is a 24-path Rayleigh-faded channel with an exponential decay of the paths' average power levels. The guard interval is set so that it is always longer than the delay of the channel.

In the multi-cell environment, the mobile station is assumed to have synchronised inter-cell interference from one neighbour cell with an identical total power level making the signal to interference ratio S / I equal to zero dB. The signals from different cells are separated with PN scrambling codes assigned to these cells.

The system parameters used in the experiments are summarised in table 4.1. The parameters in Table 4.1 are used unless the experiment description states otherwise.

Table 4.1   MC-CDMA simulation system parameters

	MC-CDMA
Bandwidth	101.5 MHz
Subcarrier Spacing	131.836 KHz
Guard Interval	1.674 μSec.
Number of Subcarriers (N_c)	768
Packet Size	3072 bits
Spreading Code	Walsh-Hadamard
Scrambling Code	Pseudo random
Spreading Factor	$SF_f =16$
Modulation	QPSK, 16QAM
Coding/Decoding	Turbo coding (CR=1/3-1/2, K=4) generator polynomials g_0=13 and g_1=15 (octal) Max-Log-MAP decoding (Iterations = 6)
Interleaving	Bit interleaving + Subcarrier Interleaving
User Detection	MUD (MMSE)
CIR	As in figure (3.3)

4.4   Simulation Results and Analysis

4.4.1   Single-cell environment

4.4.1.1 SUD techniques

In this experiment the relationships between three crucial parameters are characterised
and analysed. These are the frequency selectivity, loading factor *L* and combining
technique. Among many factors that define the performance of an OFDM-based
system the interaction between these three factors is unique in the sense that it defines
the initial setup and configuration of the system in terms of the number of subcarriers,
spacing between subcarriers, interleaving, detection technique …etc.

To study the frequency selectivity independently from other factors including the
delay spread and coherence bandwidth the fading channel taps on individual
subcarriers are generated based on the ratio $R_t = T_{rms} / T_s$, where R_t is the ratio
between the delay spread of the channel T_{rms} and the OFDM symbol duration T_s . A

large value for this ratio (e.g. R_t =1) means high frequency selectivity across subcarriers and therefore low correlation in the fading across subcarriers. A low value of R_t (e.g. R_t =0.01) gives a higher degree of correlated flat fading across adjacent subcarriers.

The single-user combining and detection techniques under study are Equal Gain Combining (EGC), Maximal Ratio Combining (MRC) and Orthogonal Ratio Combining (ORC). With ORC all subcarriers are weighted by a unity factor by multiplying each subcarrier by the inverse of its channel to remove the amplitude and phase variations. MRC multiplies each subcarrier with the conjugate of its channel tap resulting in the weighting of the subcarrier by its Signal to Noise Ratio (SNR) represented by the square of the channel's amplitude $|h|^2$. EGC corrects the phase rotations due to the channel leaving the signal weighted by the amplitude of the channel tap at each subcarrier $|h|$.

Figure (4.3) depicts the BER and PER performance of MC-CDMA with ORC as a combining technique. The results are shown for L =1, 0.5 and 0.0625 as well as R_t =0.01, 0.1 and 1. ORC attempts to completely equalise the channel i.e. to remove the effects of the frequency selective fading. MAI is, therefore, eliminated in the downlink. This explains the similar performances even when the load increases from 1 user to full load. However, by equalising the channel ORC is actually amplifying the noise in the presence of deep channel fades, which is the main reason behind the generally weak performance witnessed in figure (4.3). A slight improvement of ORC in highly correlated channels is also observed in the figure. In a Highly correlated channel, the noise across all subcarriers is either amplified or attenuated with small

variances across subcarriers. This adjusts the level of noise but maintains the same noise variance. The resultant noise remains white in this sense and it therefore it is treated as normal noise. On the other hand, when the channel is frequency selective the noise samples are amplified or attenuated with different equalisation factors, resulting in an increase in the noise variance and the creation of amplified noise at severely faded subcarriers which worsen the performance of MC-CDMA.
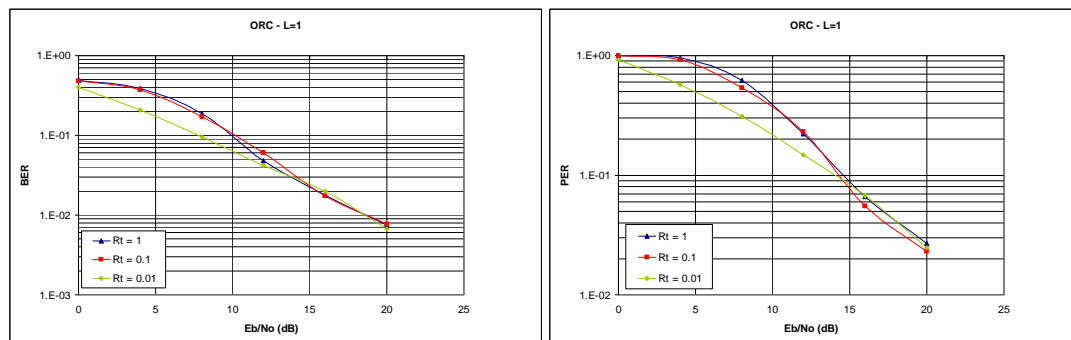
(a) Full Load (*L*=1)
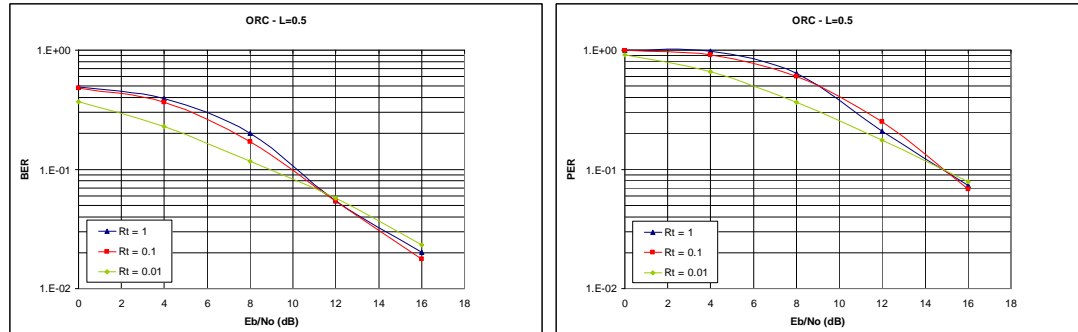
(b) *L*=0.5
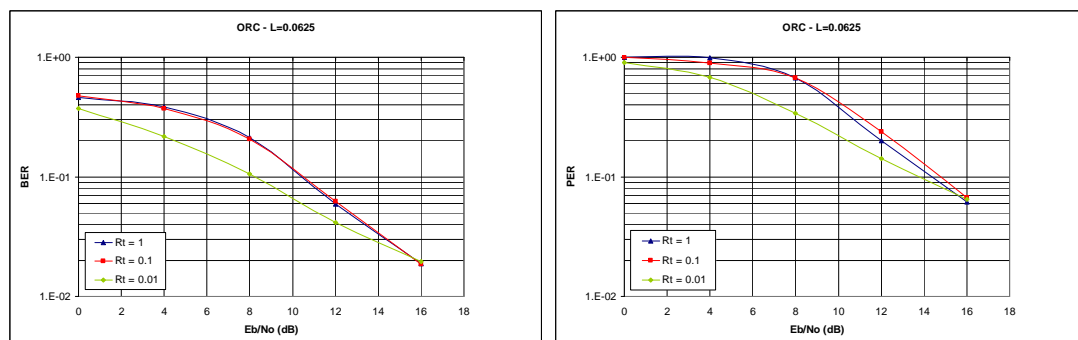
(c) 1 User (*L*=0.0625) [QPSK with *CR*=1/2]

Figure 4.3   BER and PER Performance of MC-CDMA with ORC, *L*=1, 0.5 and 0.0625, and R_t =1, 0.1 and 0.01

The performance of MC-CDMA with MRC combining is depicted in figure (4.4) for $L=1$, 0.5 and 0.0625 as well as $R_t=0.01$, 0.1 and 1. The influence of the channel parameters on the performance is more noticeable here. MRC tries to optimise the frequency diversity created by frequency selective fading among subcarriers, which results in worsening the MAI among the spreading sequences that has already been created by the breakdown of orthogonality due to frequency selectivity. The graphs show that the gain from frequency diversity is substantially less than the loss caused by MAI for the worst case load factor $L=1$.

When the MAI decreases in the case of $L=0.5$, the performance of MRC considerably improves in frequency selective channels. As figure (4.4b) shows, the frequency diversity starts to contribute more, bringing the selective fading channel performance close -and sometimes beyond- the performance in highly correlated channels. There exists, however, an error floor for the MRC performance in frequency selective channels. This is due to the remaining MAI which cannot be overcome even at high values of E_b/N_0. On the other hand, in low frequency selectivity channels the BER performance can continue to improve with E_b/N_0 despite the effect of MAI and SNR weighting.

When MAI is completely eliminated (i.e. $L=0.0625$) the performance of MC-CDMA can be dramatically enhanced with MRC by exploiting the frequency diversity available to the system. It can also be noticed that the performance improvement is monotonic with increasing frequency selectivity (unlike the case with $L=0.5$) i.e. the more frequency selectivity the system has the more frequency diversity it gains while MAI enhancement is not an issue any more.

(a) Full Load (*L*=1)

(b) *L*=0.5

(c) 1 User (*L*=0.0625)

Figure 4.4   BER and PER Performance of MC-CDMA with MRC, *L*=1, 0.5 and 0.0625, and R_t =1, 0.1 and 0.01 [QPSK with *CR*=1/2]

The performance of the EGC technique is depicted in figures (4.5) for L =1, 0.5 and

0.0625 and R_t =0.01, 0.1 and 1. Leaving the received signal as it is (except for the

phase correction) proves to be the best way of benefiting from frequency diversity.

Although SNR weighting in MRC is the optimal weighting method to represent the

signal strength, biasing the signal toward taking full advantage of frequency diversity

proved earlier to drastically degrade the system's performance. On the other hand,

being pragmatic by weighting the signal by $|h|$ instead of $|h|^2$ partially exploits the

frequency diversity available to the system without excessively increasing the MAI

among the spreading codes in use.

The performance of the three combining methods in a highly correlated channel

(R_t =0.01) is presented in figure (4.6). When the system is fully loaded (figure (4.6a)),

both MRC and ORC show similar performance. This is because limited MAI and

frequency diversity exist and, therefore, both techniques lose their advantage of either

eliminating MAI or exploiting diversity. EGC performs better than the rest because it

does not include any equalisation (except for the phase correction) and thereby, unlike

MRC and ORC, no noise enhancement occurs.

When the load is reduced to L =0.5 or L =0.0625, ORC maintains the same level of

performance. The reduction of the MAI, although small, brings the MRC performance

closer to that of EGC. That is, for values of $L \leq 0.5$ the MRC and EGC detectors can

exploit frequency diversity without MAI impairment. The performances differences

of the three combining methods are generally small however due to the channel

correlation.

(a) Full Load (*L*=1)
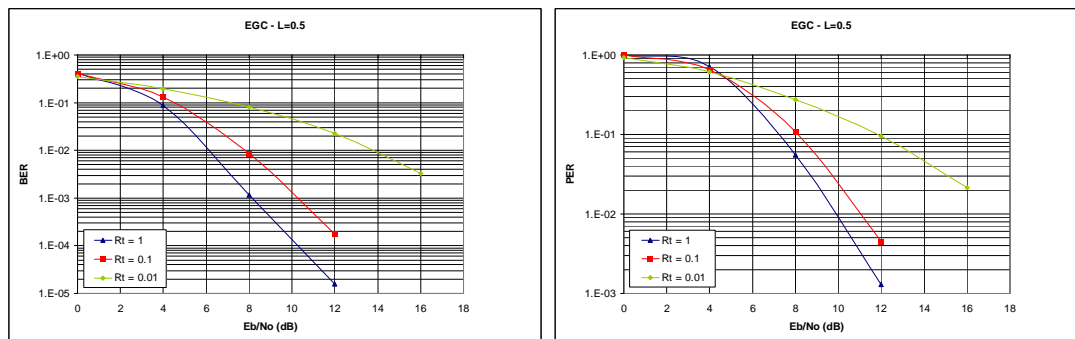
(a) *L*=0.5
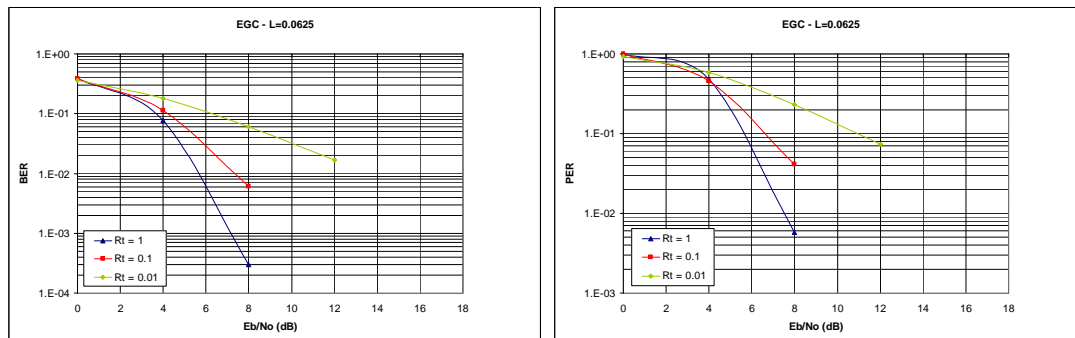
(c) 1 User (*L*=0.0625)

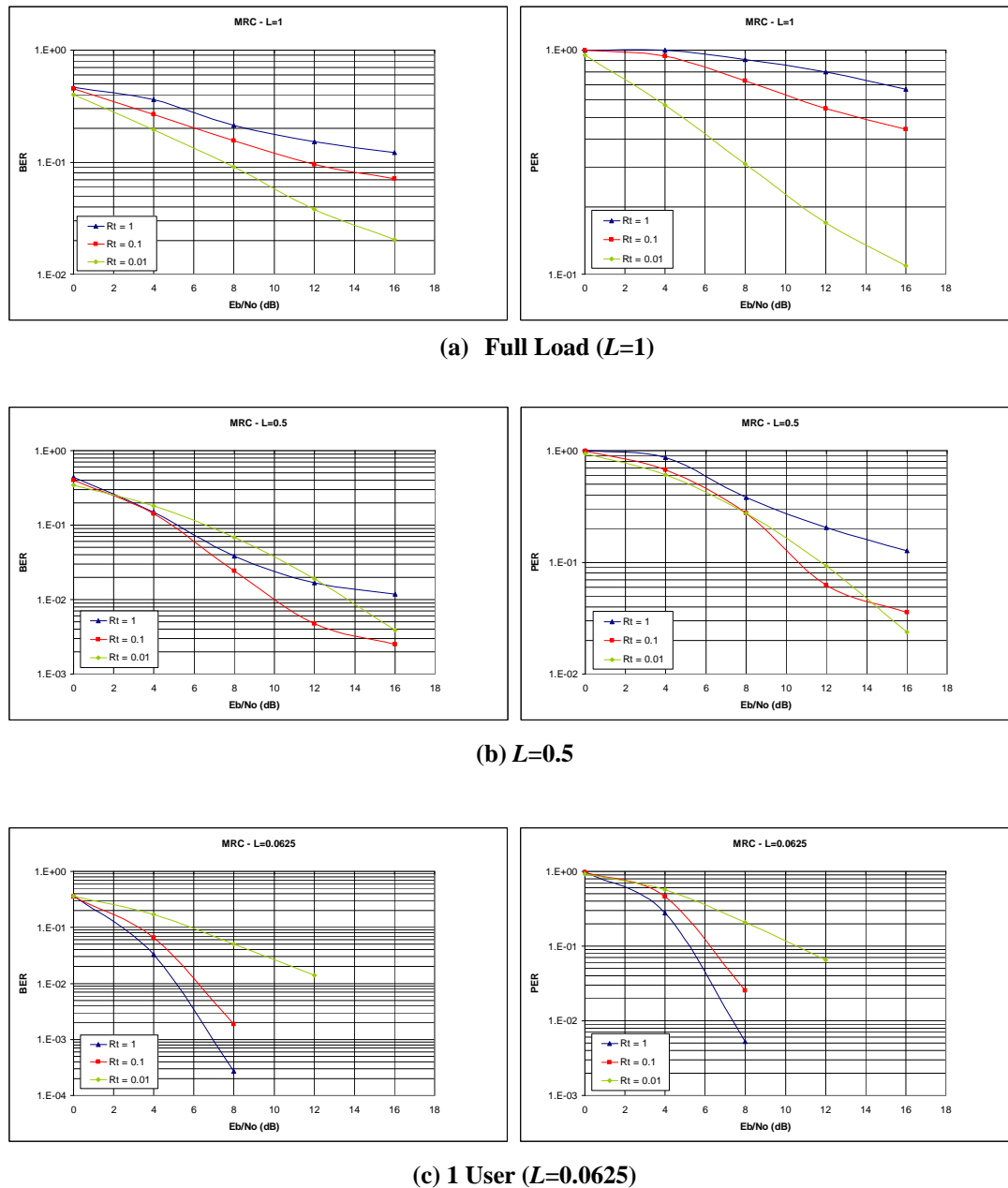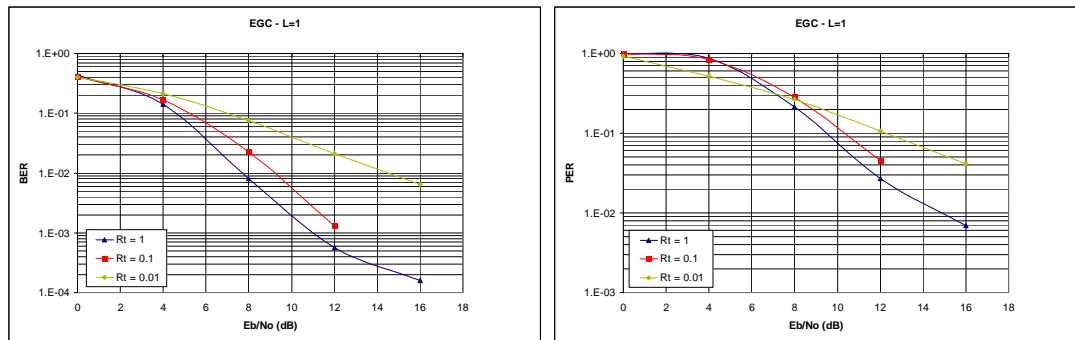**Figure 4.5   BER and PER Performance of MC-CDMA with EGC, *L*=1, 0.5 and 0.0625, and R_t =1, 0.1 and 0.01 [QPSK with *CR*=1/2]**
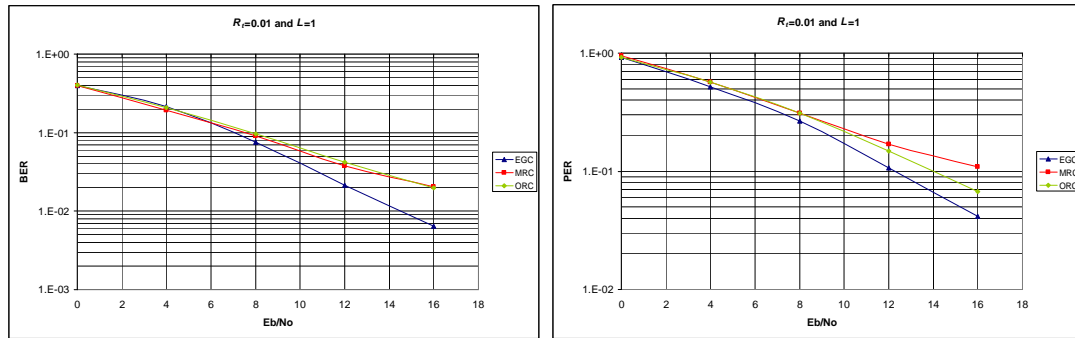
(a) $Rt = 0.01$ **and** $L = 1$
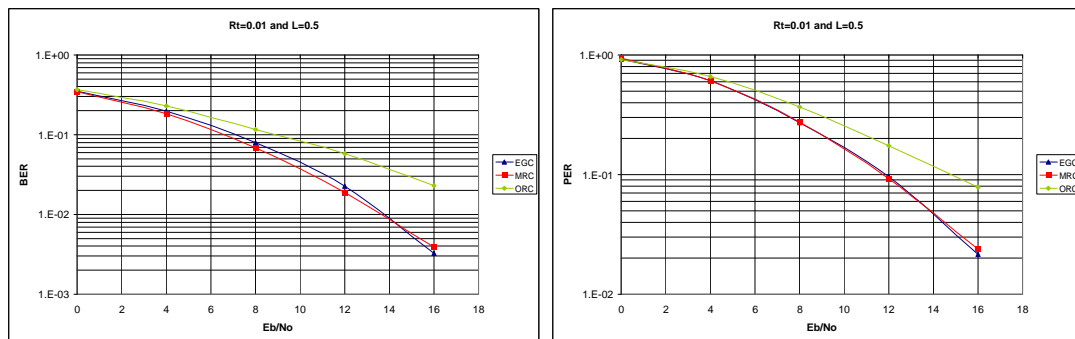
(b) $Rt = 0.01$ **and** $L = 0.5$
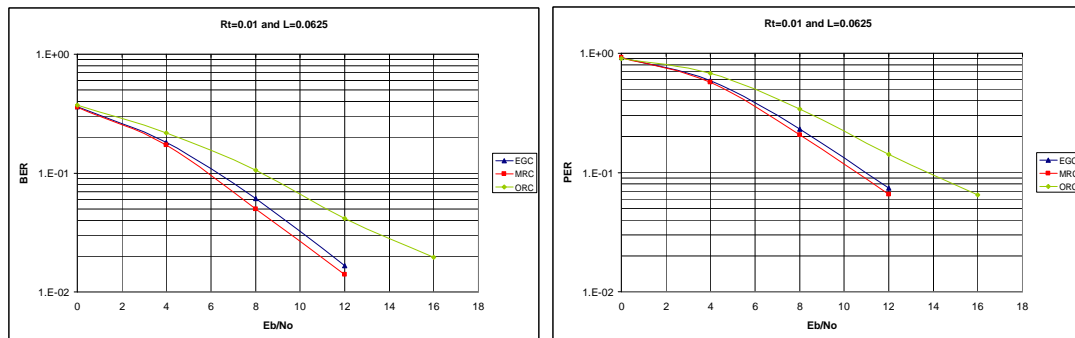
(c) $Rt = 0.01$ **and** $L = 0.0625$

Figure 4.6   BER and PER Performance of MC-CDMA with ORC, MRC and EGC, R_t =0.01, and L =1, 0.5 and 0.0625 [QPSK with *CR*=1/2]

Finally the performance results for the three combining techniques are shown in figure (4.7) for the case of high frequency selectivity (i.e. $R_t = 1$). In a fully loaded system, EGC outperforms the other two techniques due to maintaining the balance between the MAI and the frequency diversity exploitation. MRC, on the other hand, severely degrades the system performance by enhancing the MAI which is already severe due to the loss of orthogonality between sequences.

With $L = 0.5$, EGC continues to outperform the other methods. The performance of MRC, however, surpasses that of ORC. This is due to the reduction in MAI which allows better exploitation of frequency diversity. Though MRC still suffers from an error floor that limits its performance after some value of E_b / N_0.

In the case of a single user load, MRC performs slightly better than EGC due to the ability to fully exploit frequency diversity without MAI degradation. Nevertheless, EGC offers a very close performance without the need for the extra processing used in MRC.

Looking at the whole set of results, one can safely conclude that EGC is the best choice as a combining method for MC-CDMA amongst the three discussed strategies if good performance is expected under all channel correlation conditions as well as different loading factors.
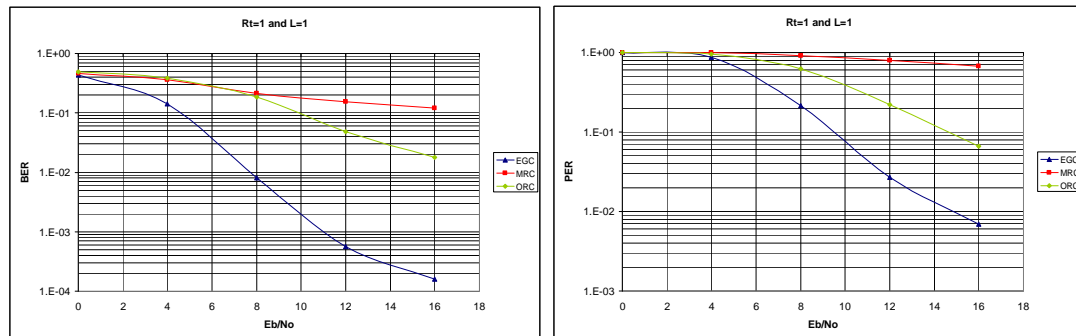
(a) $Rt = 1$ **and** $L = 1$
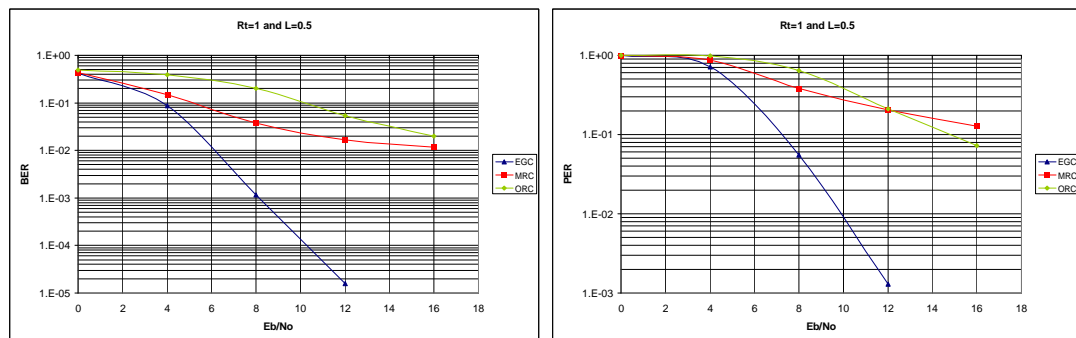
(b) $Rt = 1$ **and** $L = 0.5$
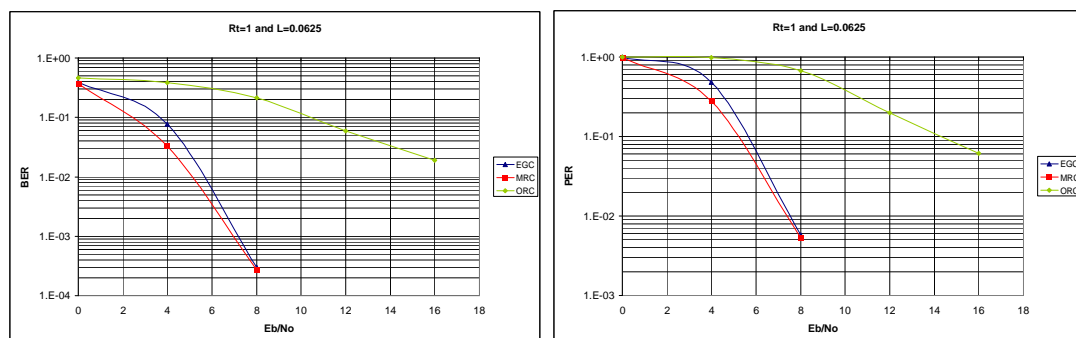
(c) $Rt = 1$ **and** $L = 0.0625$

**Figure 4.7   BER and PER Performance of MC-CDMA with ORC, MRC and EGC, R_t =1, and
L =1, 0.5 and 0.0625 [QPSK with *CR*=1/2]**

The results above are for a relative delay spread parameterisation. Such results provide useful information about the performance trends of different system configurations. A low R_t ratio means high correlation in the fading across MC-CDMA subcarriers. This can be the result of either a low delay spread multipath channel or the spreading over a number of very narrow adjacent subcarriers whose total width is commensurate to the coherence bandwidth of the channel. A high value of R_t, representing high frequency selectivity, can be due to long delay spread of the multipath channel. It can also be the result of a number of adjacent subcarrier which are wide enough to face frequency selectivity at their centre frequencies even at short delay spreads or as a result of subcarrier interleaving where the chips of every spreading sequence are placed on distant subcarriers. The latter setup forces those chips to experience independent fading even when the delay spread is not very long.

Therefore, the simulation results presented provide a tool to determine the parameters of the MC-CDMA system based on the relation between the channel statistics and the system constraints. Among the configurable parameters in the initial setup of a MC-CDMA system are the subcarrier bandwidth and accordingly the number of subcarriers within a certain channel bandwidth, as well as the chip interleaving across the total bandwidth of the channel.

After establishing the performance trends of three SUD methods for MC-CDMA, we now focus look deeper into other aspects of the MC-CDMA system. For this purpose MMSE MUD is used as a detection strategy to deal with MAI. Generally speaking, MUD offers consistently better performance compared to SUD. This is, of course, for the cost of higher complexity of the system.

The following simulations are based on the system configurations listed in table (4.1). This applies to both the single-cell and multi-cell experiments.

4.4.1.2 Effect of Modulation and Coding Rate

In this subsection the performance of MC-CDMA is studied with a number of combinations of the modulation level (QPSK) and coding rate (CR=1/2 and 1/3). The performance of MC-CDMA is depicted in figure (4.8) for three different modulation and channel coding schemes: QPSK with CR=1/3, QPSK with CR=1/2, and 16QAM with CR=1/2.
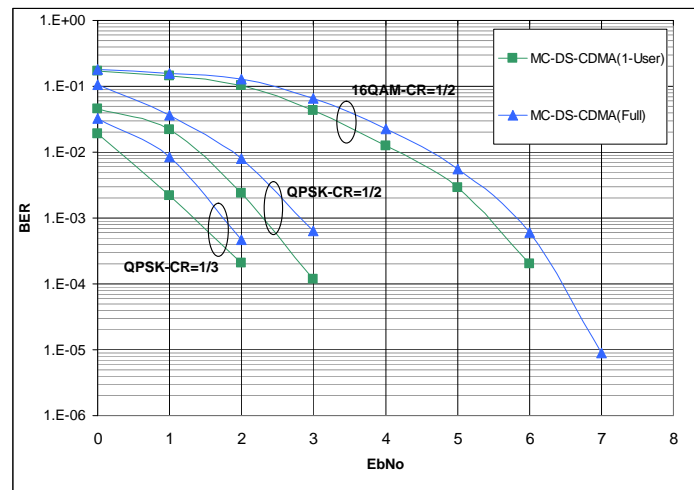
(a)
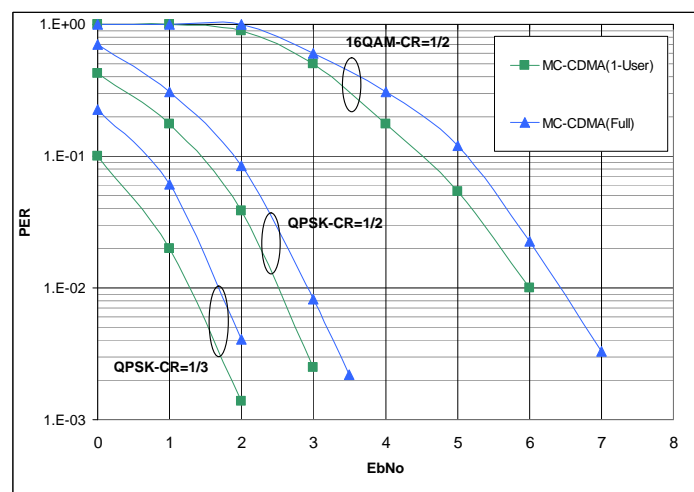
(b)

Figure 4.8   BER and PER Performance of MC-CDMA with three configurations: 1) QPSK and CR=1/3, 2) QPSK and CR=1/2 and c) 16QAM and CR=1/2 [Rest of parameters as in table (4.1)]

The results show that by applying MMSE MUD, the MC-CDMA maintains a fix SNR difference of 0.4-0.6dB between the performance for a single-user and the full-load performance. Another observation is the capability of MC-CDMA with MUD to reach a PER threshold of 10^{-2} without incurring an error floor even for high modulation orders (i.e. 16QAM) although a convolutional turbo code is used, for which the error floor is one disadvantage. The utilisation of both the frequency-domain diversity through MC-CDMA and the application of MUD help to recover the system performance when fades occur.

4.4.1.3 Effect of Iterative decoding

The performance of turbo coded MC-CDMA in a Rayleigh fading channel is depicted in figure (4.9). The coded system's performance is compared with the uncoded MC-CDMA performance in both the AWGN channel and the multipath system. By applying the turbo code with one iteration, the BER and PER performances of MC-CDMA are significantly improved. Though an error floor above 10^{-5} BER (10^{-2} PER) is observed. Increasing the number of iterations for the decoder enhances the performance beyond the uncoded AWGN performance and removes the error floor
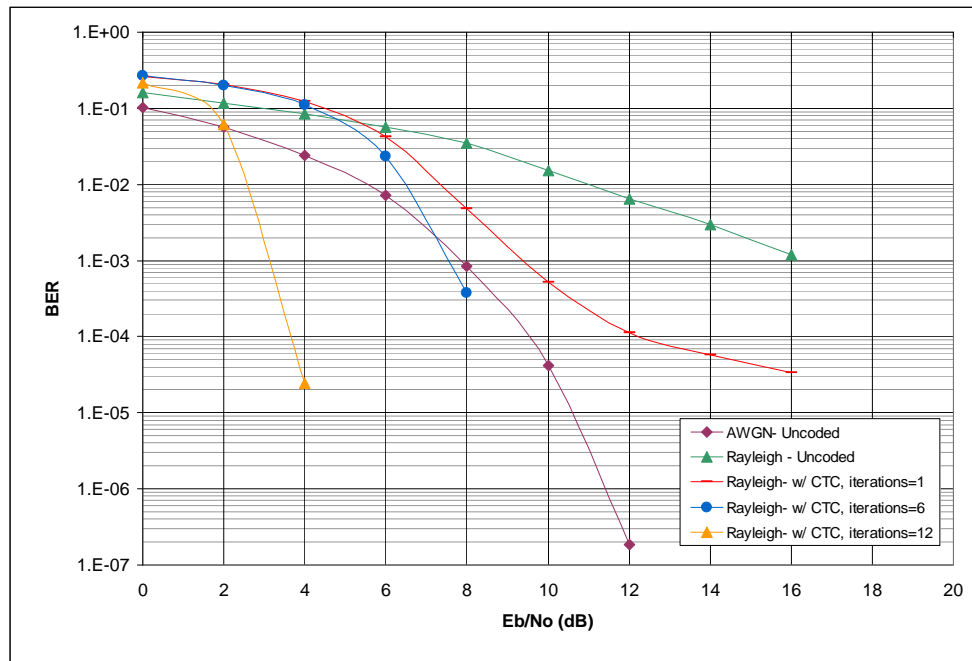
(a)
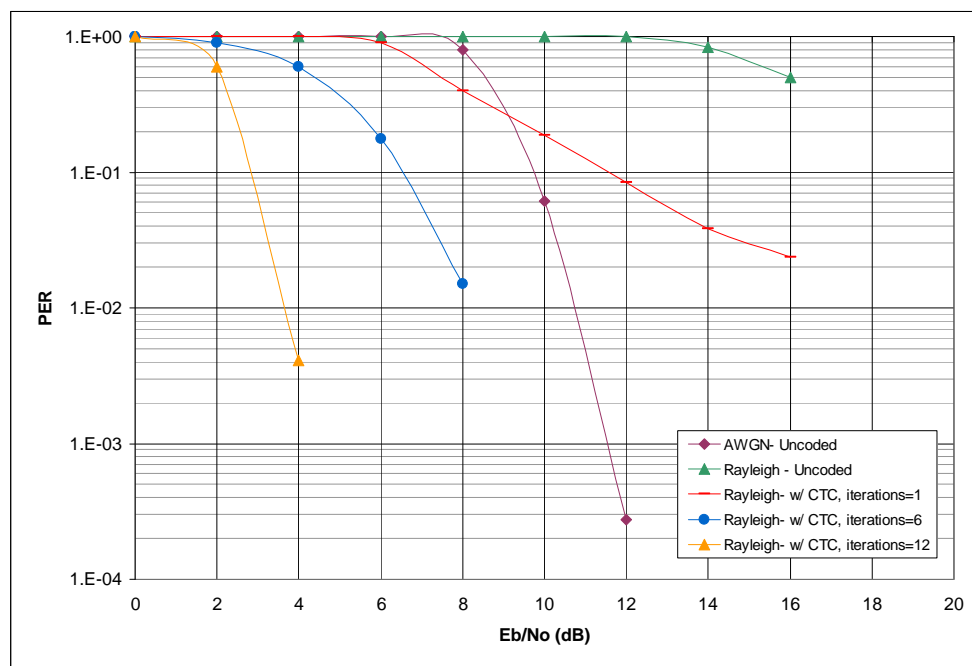
(b)

Figure 4.9   BER and PER Performance of MC-MDMA with iterative decoding [Rest of parameters as in table (4.1)]

4.4.1.4 Effect of MIMO

Figure (4.10) shows the BER and PER of MC-CDMA with different Multiple Antenna configurations. SIMO refers to the case where two or more antennas are installed at the receiver, while MISO refers to the opposite case where the transmitter uses multiple antennas. These are implemented in this study based on the basic Alamouti algorithm [90]. Simulations were conducted for both the uncoded and encoded systems so that the gain of using multiple antennas can be measured.

The results show that having multiple antennas at the receiver offers the system a significant improvement even without the assistance of FEC. It is noticed, however, that neither the multiple antennas nor the non-iterative FEC are capable of mitigating the error floor that appeared in earlier performance results. Simulation results also demonstrate that although a SIMO system is superior to a MISO system when SNR is low both systems converge to similar performance at higher SNRs. The superiority of SIMO is due to the fact that each of the MISO transmit antennas uses half of the power transmitted by the single SIMO transmit antennas to maintain the same total transmitted power.

Next, we compare the gain of using SIMO and MISO in a MC-CDMA with that of using iterative decoding. The performance of MC-CDMA with both iteratively-decoded MISO and SIMO is shown in figure (4.10) along with the performance of an iteratively decoded SISO configuration and a third setup where both multiple antennas and turbo encoding are utilised.
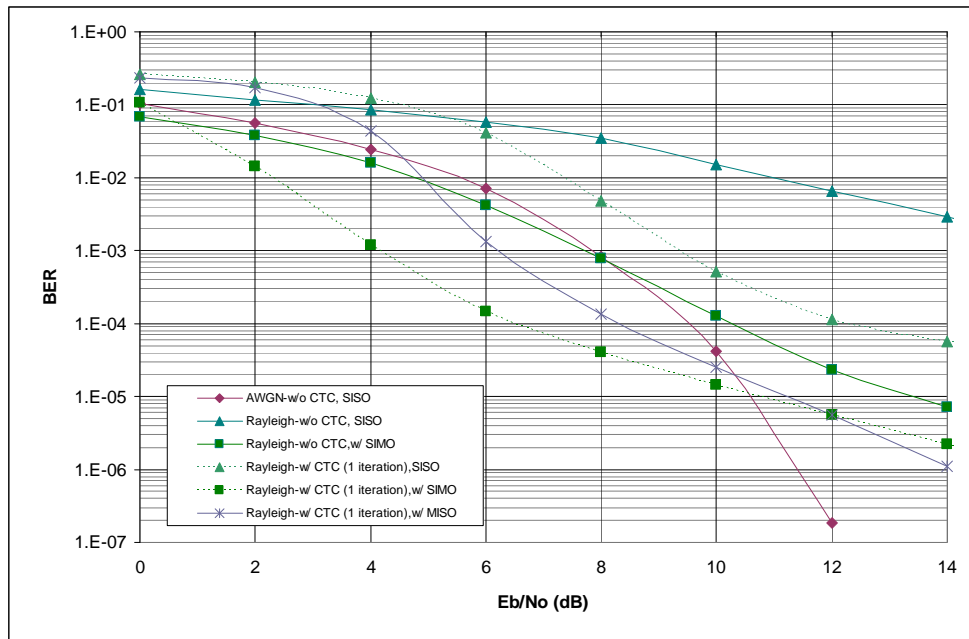
(a)
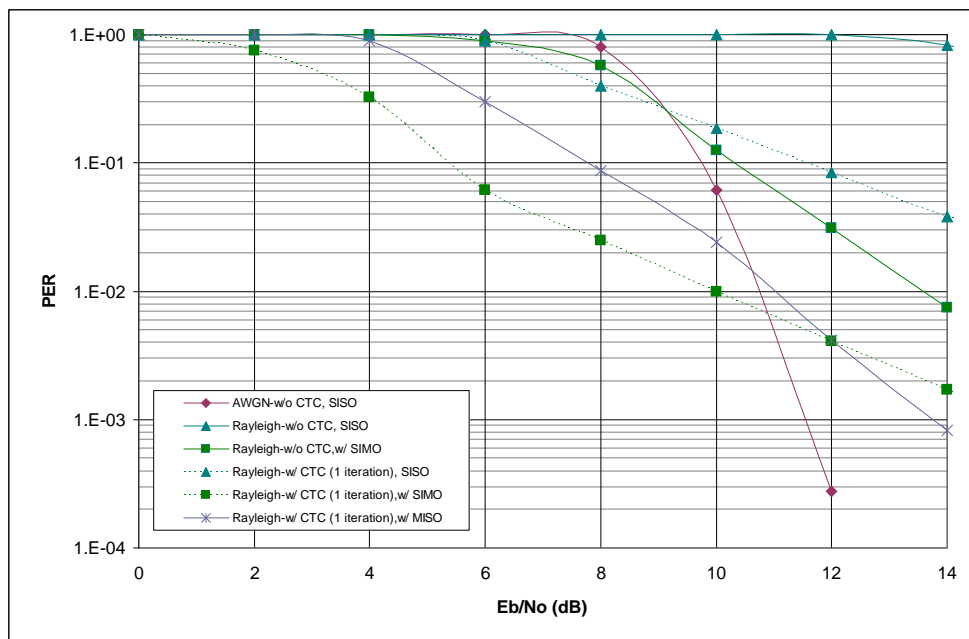
(b)

Figure 4.10   BER and PER Performance of MC-MDMA with MIMO [Rest of parameters as in table

(4.1)]
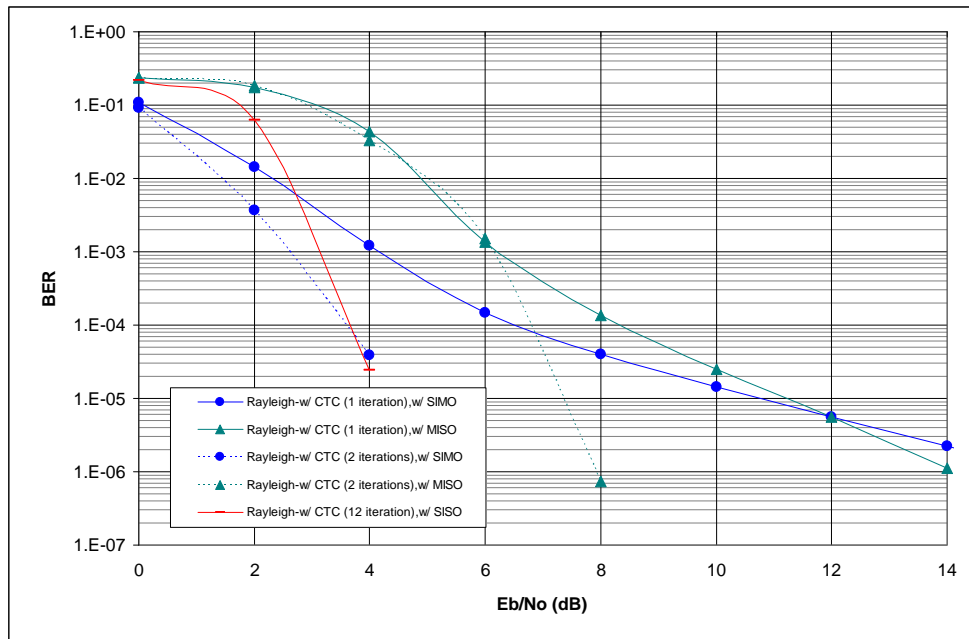
(a)
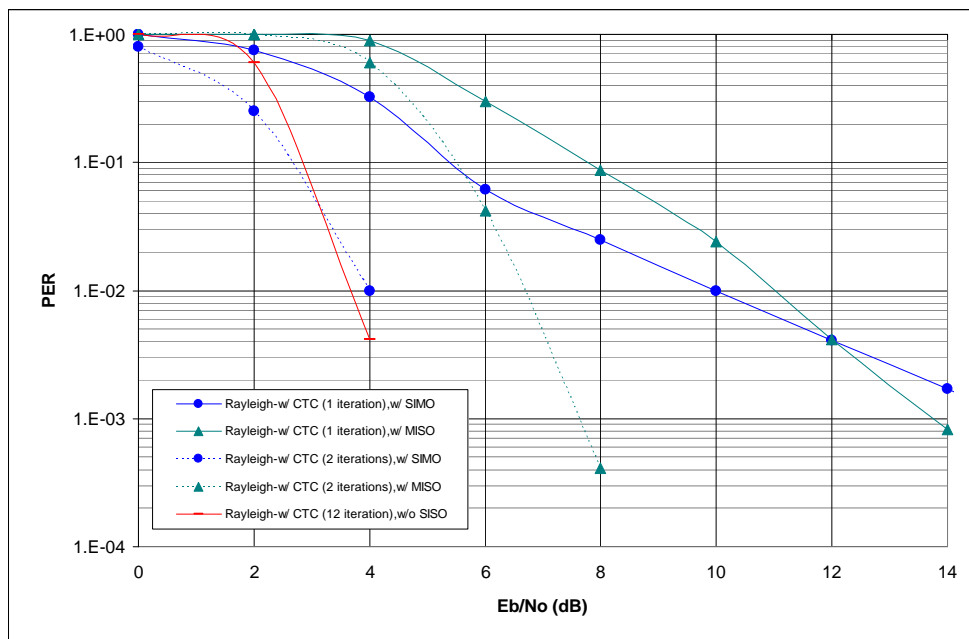
(b)

**Figure 4.11   BER and PER Performance of MC-MDMA with iterative decoding and MIMO
[Rest of parameters as in table (4.1)]**

Firstly, we notice the dramatic enhancement in the system performance when a second iteration is performed in the turbo FEC decoder processing. This enhancement removes the error floor on the BER and PER curves that appeared in figure (4.9). The latter observation may bring us to a conservative conclusion that both SIMO and MISO are making the maximum utilisation of the space diversity available to them under this setup.

It can also be seen from the depicted results that extensively iterated FEC is capable of matching the performance of SIMO system with 2 decoding iterations. This result gives a degree of freedom when it comes to the actual implementation of MC-CDMA, as the system designer can choose between increasing the system's complexity by either deploying multiple antennas (at the transmitter and/or the receiver) or running more decoding iterations based on the system requirements and constraints.

4.4.2   Multi-cell environment

The following simulation results and analysis consider the performance of MC-CDMA in a multi-cell environment. The parameters used are the ones summarised in table (4.1). In a multi-cell environment MC-CDMA suffers from inter-cell interference caused by other cells sharing the same frequency band in addition to the MAI caused by breakdown of orthogonality between the sequences of different users belonging to the same base station due to frequency selectivity.

The simulations use a multicell environment in which the target user is located at the edge of two adjacent cells that emit signals of the same strength. This scenario is explained in detail in section 3.3 of the previous chapter.

Figure (4.12) presents the BER and PER performances of MC-CDMA in a multi-cell environment with different channel coding rates and modulation orders. The figure shows that MC-CDMA with full load is severely degraded by inter-cell interference effects, except for a low modulation order (QPSK) and low coding rate (CR=1/3), where the BER and PER performances show some improvement as E_b / N_0 increases. Results also demonstrated that there is no overlapping between the different coding/modulation combinations. For example, a single user 16QAM system with code rate $R = 1/2$ performs better than a fully loaded QPSK with $R = 1/3$.

The effect of the loading factor is portrayed more clearly in figure (4.13) in the case of QPSK with code rate CR=½ and spreading factor $SF_f = 16$. Although MCCDMA performs better with low loading factors (0.0625, 0.25), it starts to degrade and approaches an error floor above BER=10^{-3} and PER=10^{-2} at load factors ≥ 0.5 and higher.
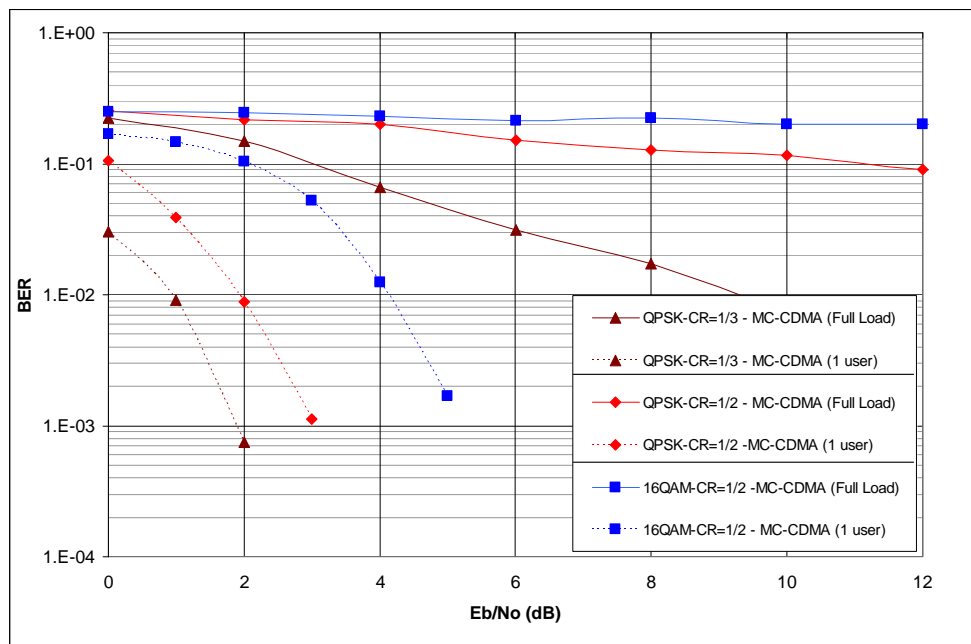
(a)
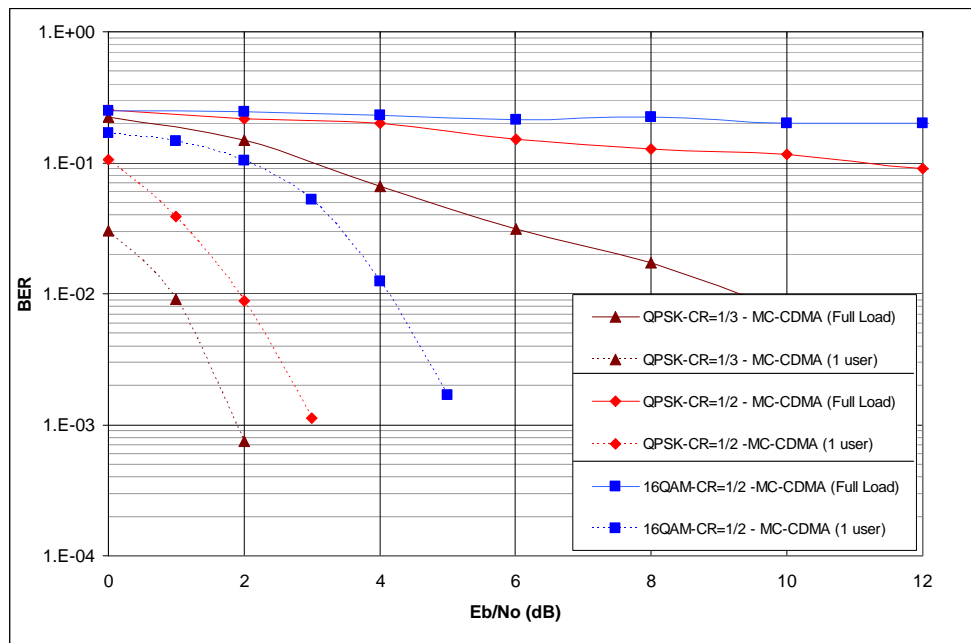
(b)

**Figure 4.12   BER and PER Performance of MC-MDMA in multicell environment (*S/I* = 0)
[Rest of parameters as in table (4.1)]**
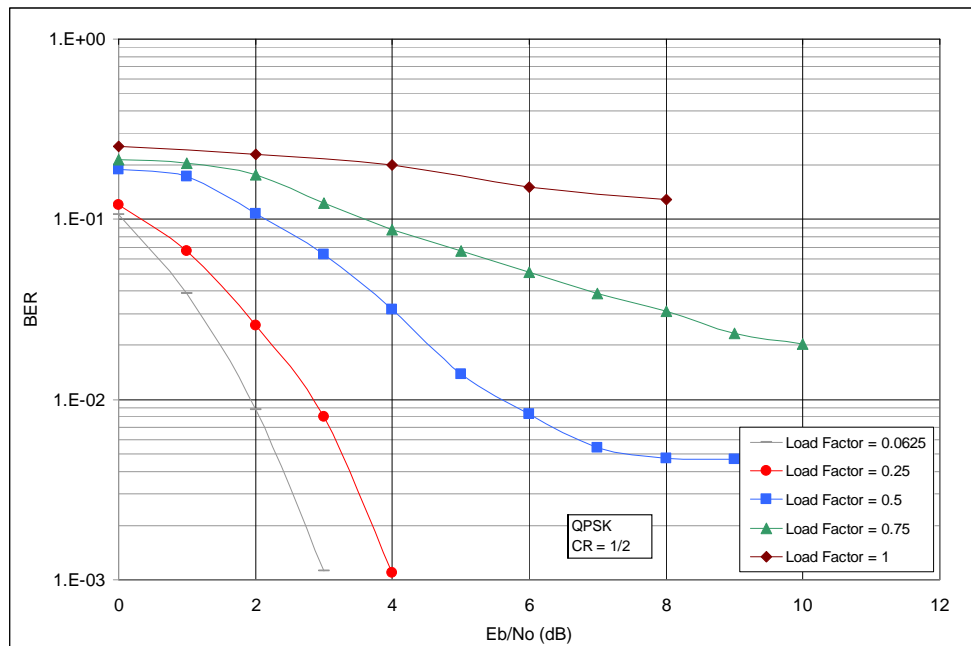
(a)
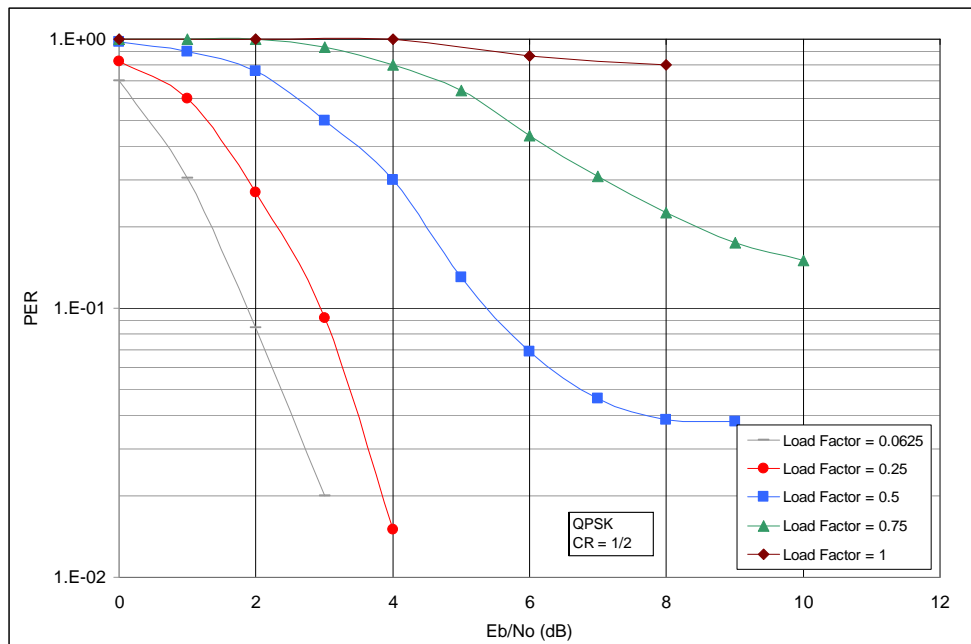
(b)

Figure 4.13   BER and PER Performance of MC-MDMA in multicell environment (*S/I* = 0) with the loading factor *L* as a variable [Rest of parameters as in table (4.1)]

4.5   Conclusions

In this chapter MC-CDMA was described as one way to combine OFDM and CDMA in a joint multiple access scheme. The performance characteristics of MC-CDMA were plotted using computer simulations where both the single-cell and multi-cell environments were considered.

In the single-cell environment, the performance of MC-CDMA was studied with three SUD methods: ORC, MRC and EGC. Although MRC occasionally offers better performance than the rest, EGC can be said to offering the best performance under different conditions and loads.

The study also covered the behaviour of the system with different modulation order and FEC combinations (The main results of the MC-CDMA system's performance are summarised in table 4.2 for the QPSK-modulated system with code rate CR=1/2 in a single cell environment). Results showed that MC-CDMA can maintain a fixed small difference (0.4-0.6dB as in figure (4.8)) between the single and full load performances when the system is aided by channel coding, multiple receive antennas (SIMO) and MMSE MUD. The gain of using multiple antennas with MC-CDMA was also investigated. Although a SIMO system is superior to a MISO system when SNR is low, both systems converge to similar performance at higher SNRs (with the assumption of equal total transmitted power for both systems).

In the multi-cell experiments the performance of MC-CDMA was studied for the worst case of having the receiver at the edge two adjacent cells with S/I =0. The investigation included different modulation orders and coding rates as well as different loading factors in the cells. Results showed that the performance of MC-CDMA degrades gradually with increasing number of users. Moreover, the results

demonstrated that, unlike the observations in the case of MC-DS-CDMA, there is no overlapping between performances of the different coding/modulation combinations when the number of users increases from 1 user to full load, as seen in figure (4.12).

In the following chapter both MC-CDMA and the previously presented MC-DS-CDMA are compared in terms of their strengths and weaknesses and their relative performances are presented.

Table 4.2   Required *Eb/No* for target BER=10^{-4} and target PER=10^{-2} in a MC-CDMA system [Single-cell environment with QPSK and *CR*=1/2]

	BER = 10^{-4}	PER = 10^{-2}
1x1 SISO + 6 iterations	8.5 dB	8.2 dB
1x2 SIMO (Uncoded)	10.3 dB	13.5 dB
1x2 SIMO + 1 iteration	6.5 dB	10 dB

Chapter 5
Frequency & Time Domain Spreading: Comparative Study

C hapters 3 and 4 of this thesis presented MC-DS-CDMA and MC-CDMA as two OFDM-CDMA joint schemes representing time domain spreading and frequency domain spreading, respectively. Both systems were thoroughly described and characterised individually. It was mentioned earlier that a major objective of this thesis is to help in removing the ambiguities regarding the superiority of either MC-CDMA or MC-DS-CDMA over the other. A few publications in the literature have already started this effort and, with their aid, we are going to continue –but not finish- this research track.

The rest of this chapter is set out as follows: The results of our computer simulation based comparative study between MC-CDMA and MC-DS-CDMA are presented and

discussed in the next section. Both MC-DS-CDMA and MC-CDMA are then contrasted highlighting their differences from a system parameterisation perspective. This is followed by a comparison of the advantages and disadvantages of the two schemes. The chapter is finally concluded with a summary of the findings of the comparative study.

5.1   Simulation-Based Comparative Study

5.1.1   System Configuration

The channel model in use is similar to that suggested in [40]. It is an independent identically distributed (IID) 24 path Rayleigh-faded channel with an exponential decay profile of the paths' average power levels. The paths are placed at equal distances of D_{exp} samples. In this chapter's simulation, a fixed delay of 0.3 µsec was used. The guard interval is set so that it is always longer than the delay of the channel.

In the multi-cell environment, the mobile station is assumed to have inter-cell interference from one neighbour cell with an identical total power level received from both the serving and interfering cells, making the signal to interference ratio equal to zero. The signals from different cells are separated by Pseudo Noise (PN) scrambling codes assigned to cells.

The main parameters of the systems under investigation are summarised in table (5.1). When a parameter is used as a variable in any experiment, this will be clearly defined within the experimental description.

Table 5.1   MC-CDMA and MC-DS-CDMA Systems Configuration

	MC-DS-CDMA	MC-CDMA
Bandwidth	100.5 MHz	101.5 MHz
Subcarrier Spacing	500 kHz	131.836 KHz
Guard Interval	0.5 µSec.	1.674 µSec.
Number of Subcarriers (Nc)	200	768
Spreading Code	Walsh-Hadamard	
Scrambling Code	Pseudo random	
Spreading Factor	SF_t=16	SF_f=16
Modulation	QPSK, 16QAM	QPSK, 16QAM
Coding/Decoding	Turbo coding (R =1/3-1/2, K=4, generator polynomials g0=13 and g1=15 (in octal)) Max-Log-MAP decoding	
Interleaving	Bit Interleaving (Block Interleaver)	Bit + Chip Interleaving
User Detection	Single	MUD (MMSE)
CIR	As in figure (3.3)[1]	

5.1.2   Simulation Results and Analysis

The following simulations aim at achieving better understanding of the relative performance of MC-DS-CDMA and MC-CDMA. For the single cell environment, the study investigates the performance of uncoded and coded systems as well as SISO, SIMO and MISO antenna systems. A number of modulation/coding combinations are also investigated in this work. With regards to the multicell environment, the study is concerned with identifying the performance trends of both MC-DS-CDMA and MC-CDMA with different antenna configurations, modulation orders, code rates and load factors.

---

[1] In most wideband channel models it is generally expected to have frequency selective fading rather than fast fading (unless the model is for ultra high speed mobility and high frequencies). Therefore, in our experiments a frequency selective fading channel is assumed across the frequency domain, while slow fading is assumed at the time domain

5.1.2.1 Single-cell environment

5.1.2.1.1 SISO (Single Input Single Output Antennas)

Figure (5.1) presents the BER and PER performance of fully loaded and uncoded MC-CDMA and MC-DS-CMDA systems in a single cell environment with single transmit and receive antennas. MC-CDMA outperforms MC-DS-CDMA by about 4 dB at BER=10^{-2}. Furthermore, MC-DS-CDMA does not exceed the 10^{-3} BER within our range of investigation ($E_b / N_0 \leq 20$ dB). The inferiority of MC-DS-CDMA's performance is due to its lack of diversity. Each symbol in MC-DS-CDMA is placed over one subcarrier. Therefore, when strong fading of any subcarrier leads to wrong decisions about the transmitted information, those decisions cannot be corrected with the lack of other aiding tools such as FEC. On the other hand, the MC-CDMA symbol is spread over a number of subcarriers. By using MUD, the MAI can be reduced while still gaining from the frequency diversity across the length of the spreading sequence. Hence, the effect of severe fading of some subcarriers can be averaged and the MC-CDMA symbol can have a better chance of surviving subcarrier loss even in an uncoded regime.

The performance of coded MC-DS-CDMA and MC-CDMA are depicted in figure (5.2). The results demonstrate that, except for the case of 1 decoding iteration, BER performance gain of MC-DS-CDMA is about 1dB compared to MC-CDMA. An explanation to this is the fact that MC-DS-CDMA does not suffer from MAI. MC-CDMA has the advantage of frequency diversity. However, in the worst case load (i.e. with full load) MAI degrades the performance of MC-CDMA. These differences become minimal, though, in the PER performance results.
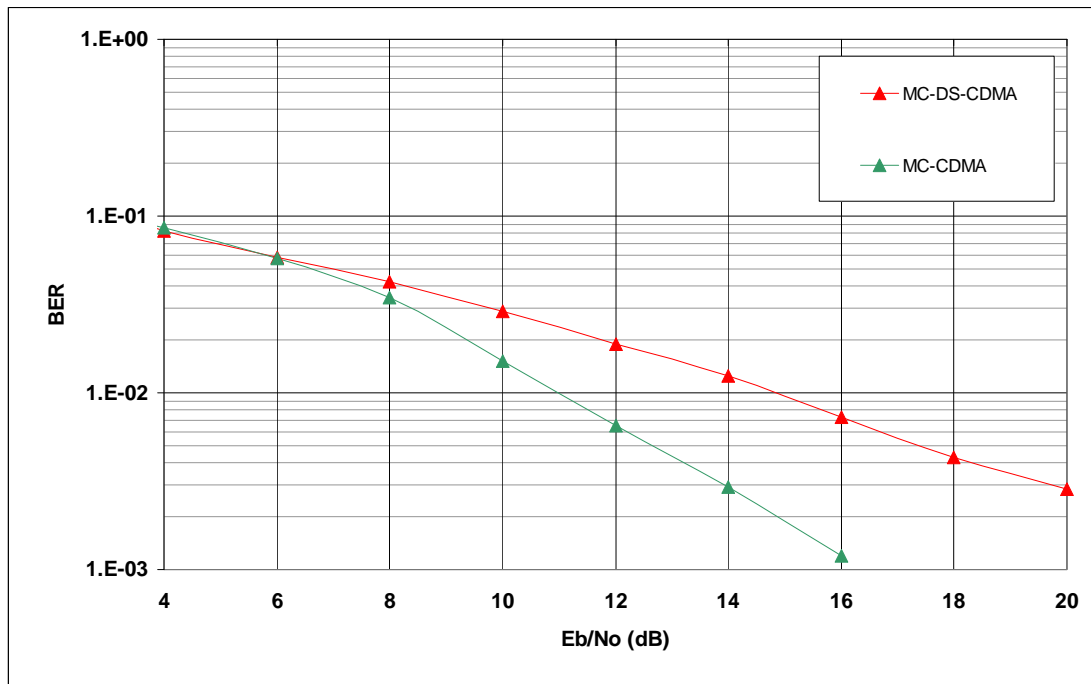
(a)
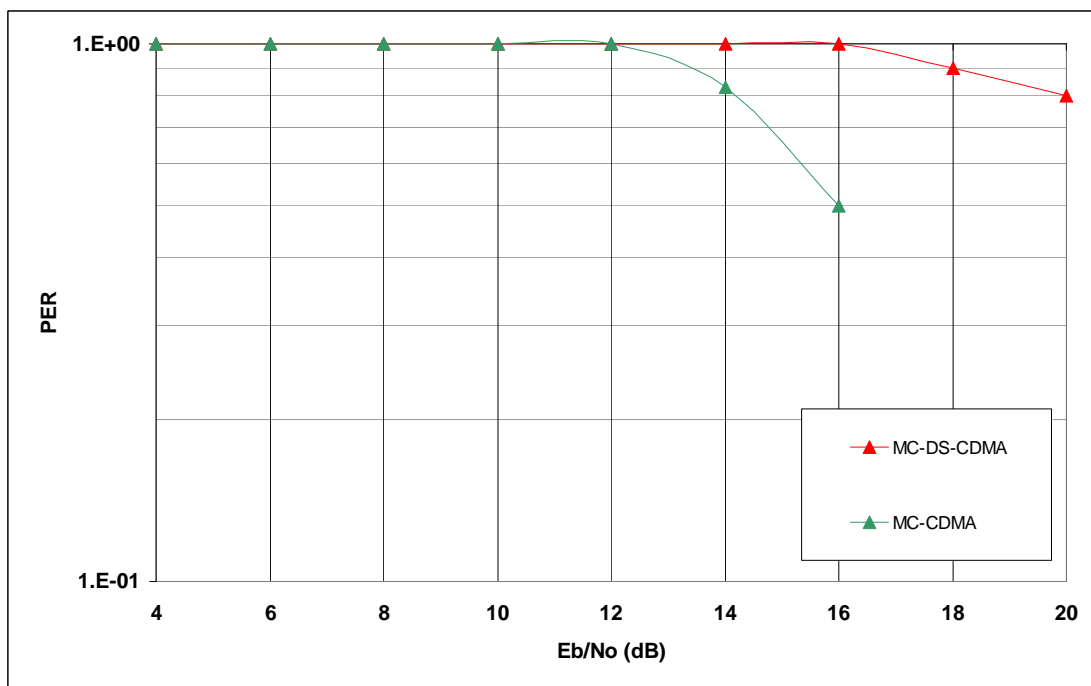
(b)

Figure 5.1   BER and PER Performance of Uncoded MC-CDMA and MC-DS-CMA with Single Transmit and Receive Antennas (SISO) [QPSK with *CR*=1/2. Rest of parameters as in table (5.1)]

(a)

(b)

Figure 5.2   BER and PER Performance of Coded MC-CDMA and MC-DS-CMA with Single Transmit and Receive Antennas (SISO) [Decoding iterations = 1,2 and 6. QPSK with *CR*=1/2.. Rest of parameters as in table (5.1)]

5.1.2.1.2 SIMO (Single-Input Multiple-Output)

Figure (5.3) provides the performance results of uncoded and coded MC-CDMA and MC-DS-CMDA with one transmit and two receive antennas. It can be seen from the graphs that uncoded MC-CDMA outperforms MC-DS-CDMA by 4dB at BER=10^{-3} with the deployment of two receive antennas. This is because the combination of signals received at two antennas gives MC-CDMA a better chance to reduce MAI and exploit the additional antenna diversity. By contrast, although the BER performance of SIMO-assisted uncoded MC-DS-CDMA shows some improvement compared to the single antennas case, the lack of error correction facilities prevents the recovery of some faded symbols.

For coded system performance, MC-DS-CDMA makes the largest improvement compared with the uncoded system performance. Although MC-CDMA performs better than MC-DS-CDMA in the low SNR region with a single decoding iteration, the two system performances change over in the high SNR region as MC-CDMA becomes limited by MAI. With 6 decoding iterations both systems show similar performance (with a 0.5dB gain for MC-DS-CDMA's BER performance).

(a)
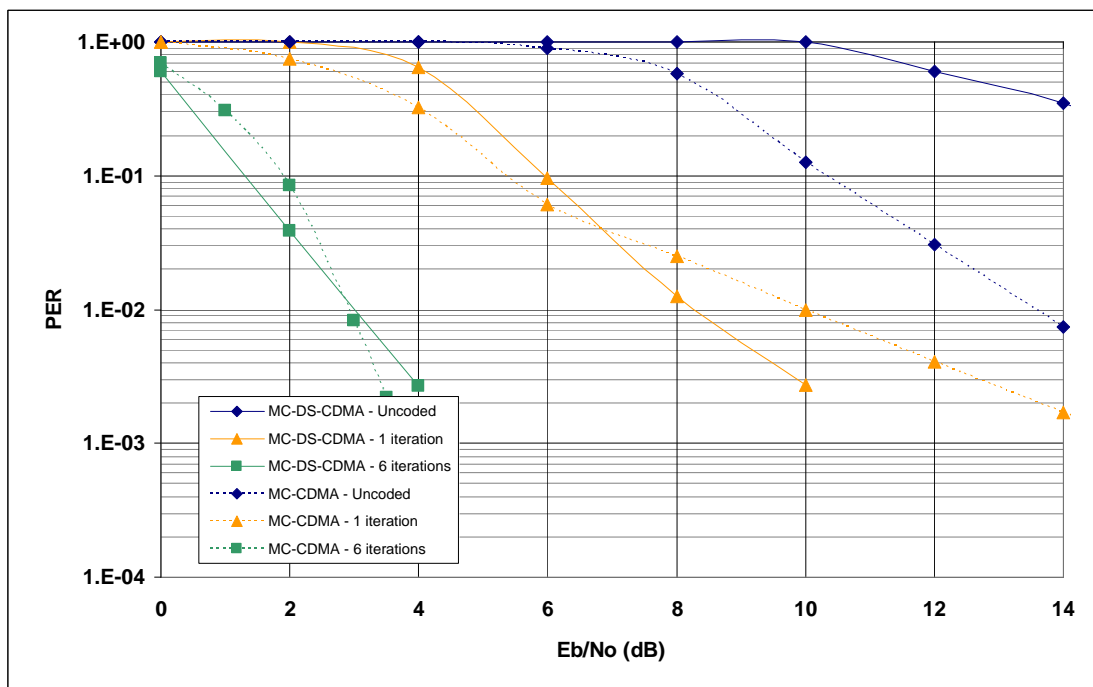
(b)

Figure 5.3   BER and PER Performance of Uncoded and Coded MC-CDMA and MC-DS-CMA with One Transmit and Two Receive Antennas (SIMO) [Deocoding iterations = 1 and 6. QPSK with *CR*=1/2. Rest of parameters as in table (5.1)]

5.1.2.1.3 MISO (Multiple Input Single Output)

Figure (5.4) depicts the performance of coded MC-CDMA and MC-DS-CDMA for two transmit and one receive antennas (MISO). With a single decoding iteration both schemes perform almost similarly. However, MC-DS-CDMA exceeds the BER performance of MC-CDMA by about 2dB when the number of decoding iterations increases to 6. This is interpreted in a similar manner to what was said about the SIMO system performance trends.

5.1.2.1.4 Comparison with different Modulation and Coding schemes

In figure (5.5) the performances of MC-CDMA and MC-DS-CDMA are presented with three different modulation and coding combinations. These combinations are: QPSK with Code Rate $R = 1/3$, QPSK with $R = 1/2$, and 16QAM with $R = 1/2$. Both the single user and full load performances are depicted (These are the same for MC-DS-CDMA). Simulation results show a 0.5dB loss in the performance of MC-CDMA when the load is increased from single user to full load. This is due to the increased MAI introduced by other users.

MC-DS-CDMA generally performs similar to or better than the 1-user MC-CDMA in all combinations. Although MC-CDMA has the advantage of exploiting better the frequency diversity when the load is limited to 1 user, it can be seen in figure (5.3) that when 2 receive antennas and 6 decoding iterations are used (which is the case here) the difference between the performance of the two systems becomes minor as they become closer to the performance lower bound. This explains why MC-CDMA does not gain from its higher diversity.
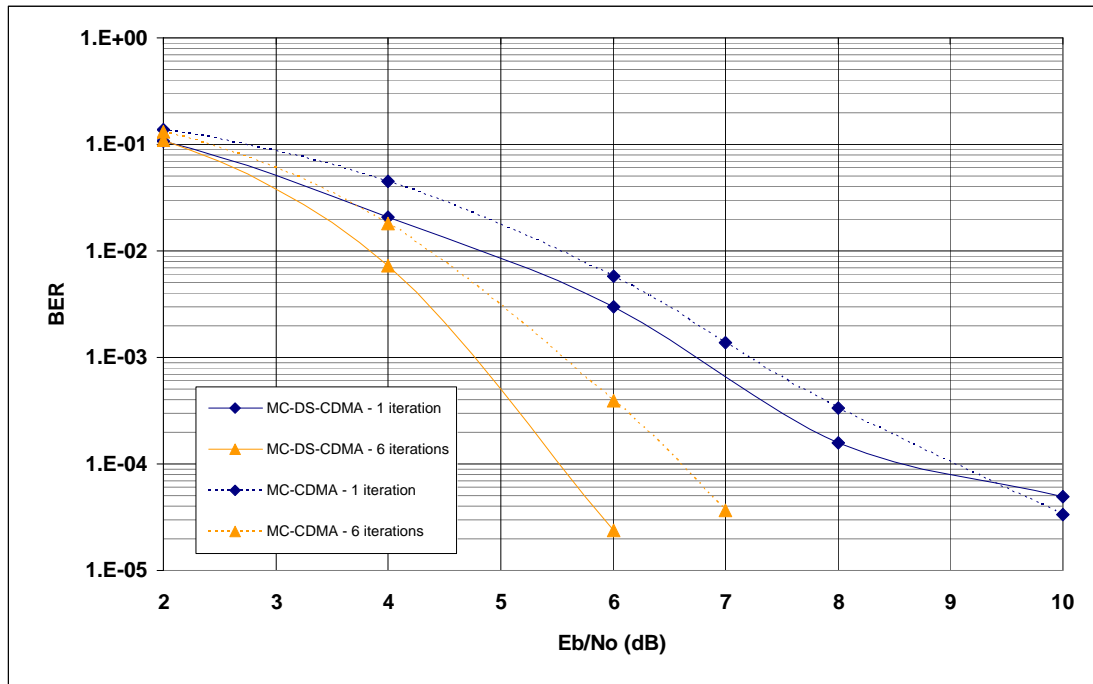
(a)
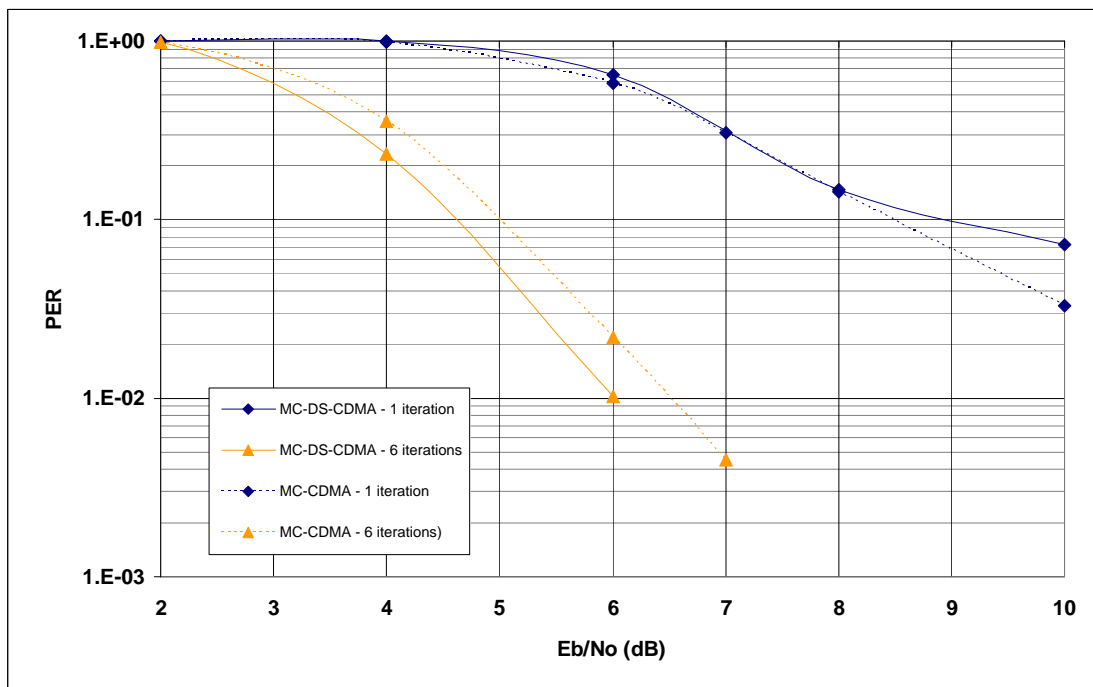
(b)

Figure 5.4   BER and PER Performance of Coded MC-CDMA and MC-DS-CMA with Two Transmit and One Receive Antennas (MISO) [Decoding iterations = 1 and 6. QPSK with *CR*=1/2. Rest of parameters as in table (5.1)]
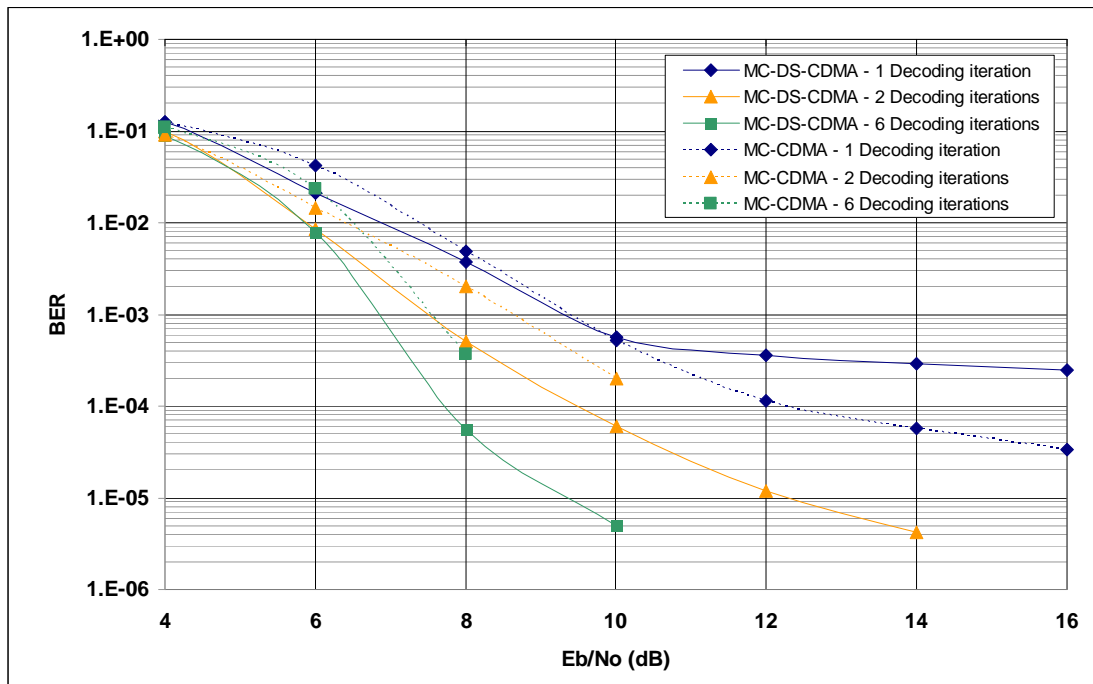
(a)

(b)

Figure 5.5   BER and PER Performance of Coded MC-CDMA and MC-DS-CMA with One Transmit and Two Receive Antennas (SIMO) for the combinations: QPSK with Code Rate =1/3, QPSK with Code Rate =1/2, and 16QAM with Code Rate =1/2 [Decoding iterations = 6. Rest of parameters as in table (5.1)]

5.1.2.2 Multi-cell environment

5.1.2.2.1 SISO Antennas

The performance of coded MC-DS-CDMA and MC-CDMA is depicted in figure (5.6) for the two-cell scenario where the user is at the edge of both cells. Both systems assume the employment of single transmit and receive antennas and are investigated for the single user and full load per cell scenarios. Although this scenario is not realistic (because systems would utilise the macro diversity at the edge of the cell) it helps have an idea about upper bound to the performance of both MC-DS-CDMA and MC-CDMA in a multi-cell environment. QPSK and CTC with $R = 1/2$ were used for the simulations.

It is noticeable from the results that neither MC-DS-CDMA nor MC-CDMA can function when both the serving and interfering cells are fully loaded in the described scenario. This is expected as the inter-cell interference becomes dominant in this case compared to either AWGN or MAI.

Both systems improve significantly when the load is reduced to one user only per cell. MC-DS-CDMA, however, suffers (as in the single cell environment) from the lack of diversity, resulting in an error floor for both the BER and PER performances. MC-CDMA continues to improve its performance with increasing E_b / N_0, because the inter-cell interference looks like an extra AWGN noise which shifts the MC-CDMA's performance graph to the right compared to the single cell scenario.
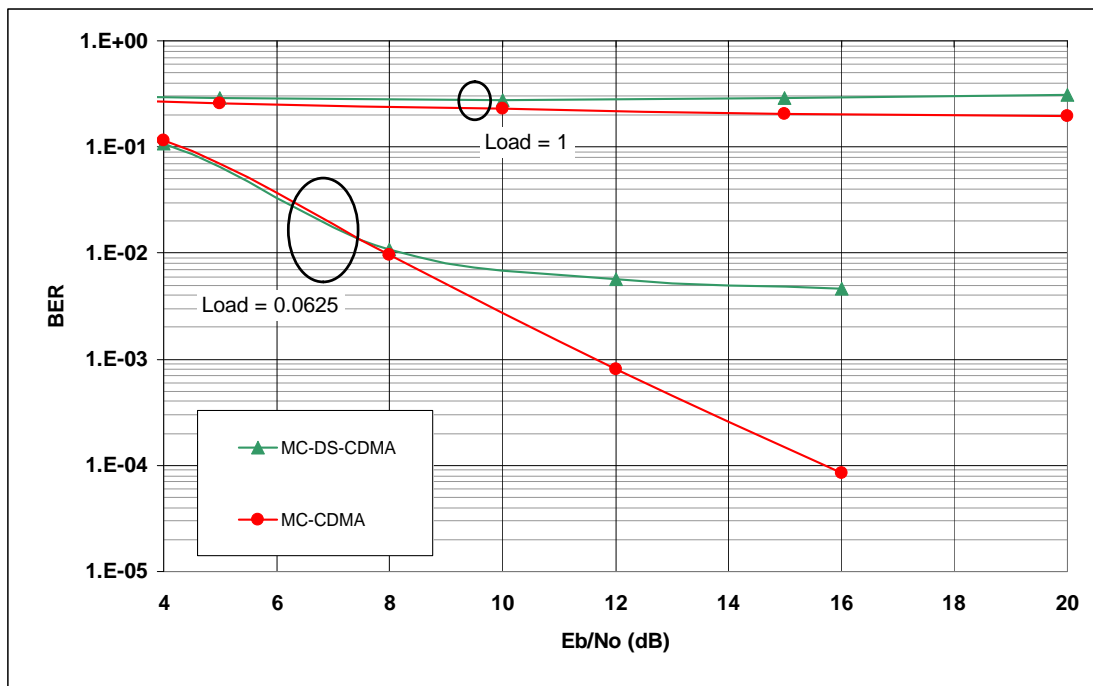
(a)
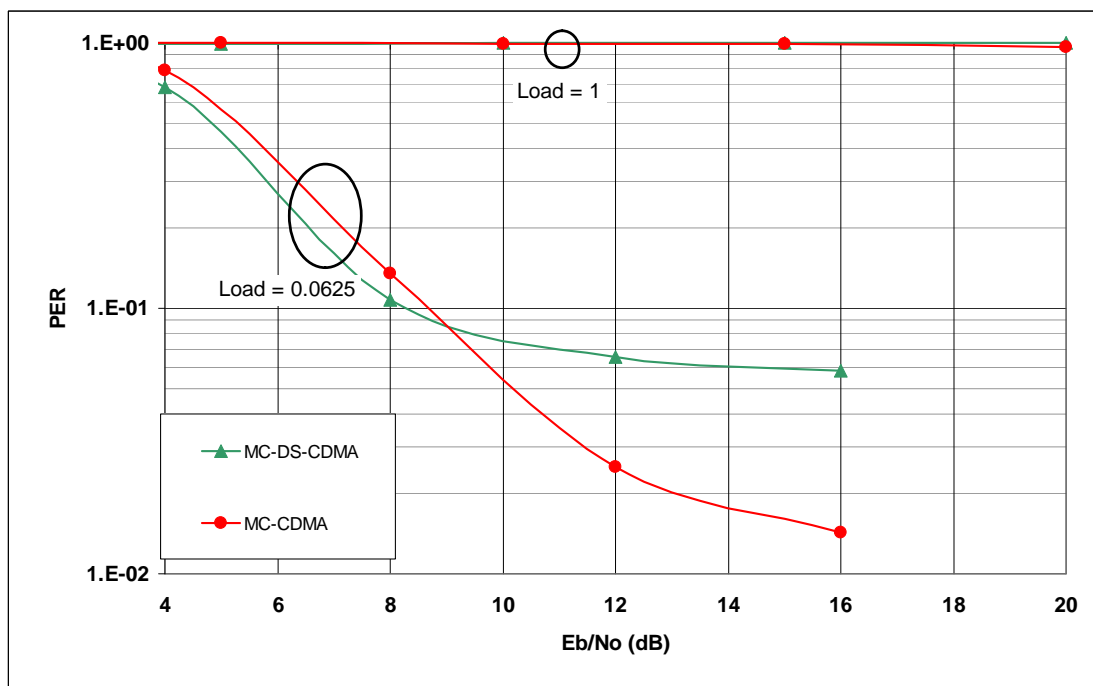
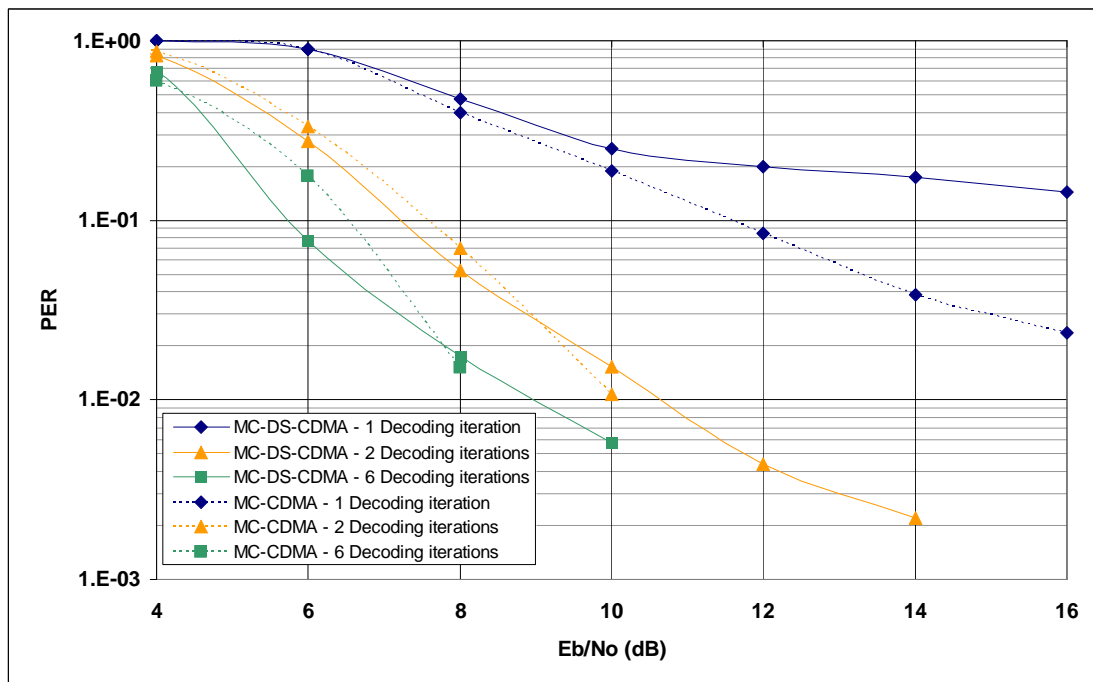
(b)
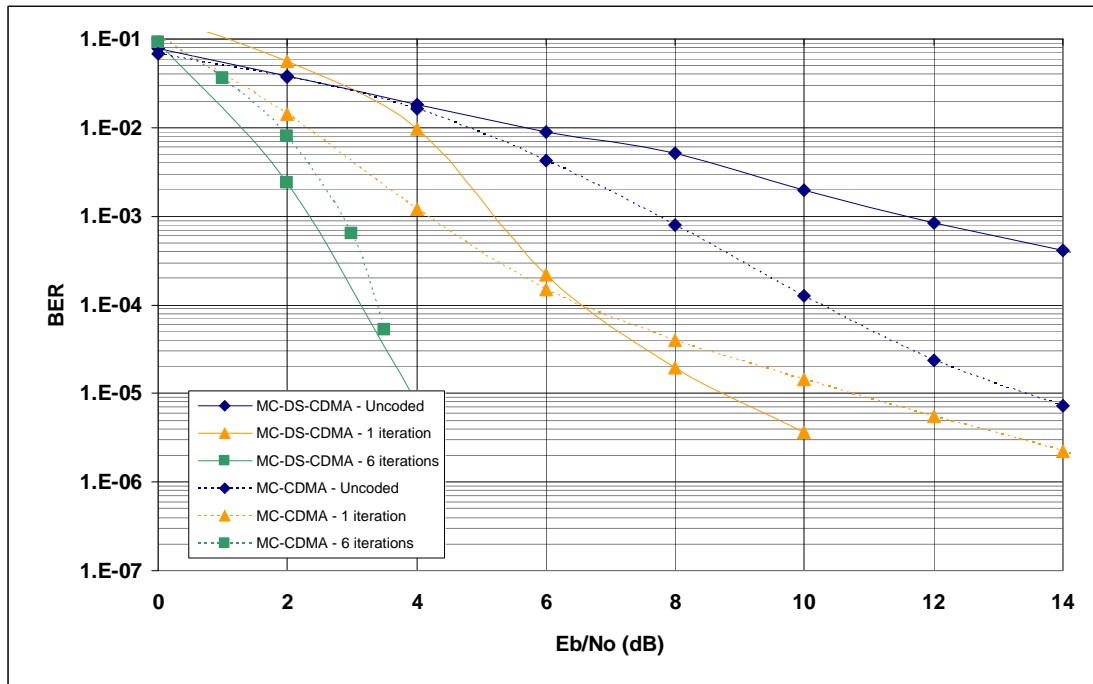
Figure 5.6   BER and PER Performance of Coded MC-CDMA and MC-DS-CMA with Single Transmit and Receive Antennas (SISO) in a Two-Cell environment (*S/I* = 0) [QPSK with *CR*=1/2. Decoding iterations = 6. Rest of parameters as in table (5.1)]

5.1.2.2.2 Multiple Antennas (SIMO and MISO)

The performances of both MC-DS-CDMA and MC-CDMA are depicted in figure (5.7) with a single transmit and two receive antennas configuration. Both systems use QPSK as a mapping scheme with CTC of code rate R =1/2 and 6 decoding iterations. The investigation considers the load factors of 1, 0.5 and 0.0625 (single user).

The results demonstrate that, despite the marginal gains of either MC-DS-CDMA or MC-CDMA in some cases, both schemes generally show the same performance when SIMO antennas and iterative decoding are applied. This agrees with the results observed in single cell simulations presented earlier in this chapter.

Figure (5.8) compares the performances of both MC-DS-CDMA and MC-CDMA with two transmit and one receive antennas. Both systems use the same modulation, coding and load parameters that were used in the previous simulation.

As can be seen from the graphs, both systems show no error correction potential when they are fully loaded. MC-DS-CDMA begins to outperform MC-CDMA when the load is reduced. For the single user case, MC-DS-CDMA has a gain of 2.5dB at BER = 10^{-4}. It suffers however from an earlier error floor compared to MC-CDMA. This is more noticeable from the PER results. The early error floor can be explained as being due to the lack of diversity in MC-DS-CDMA, which makes it more limited by the inter-cell interference.
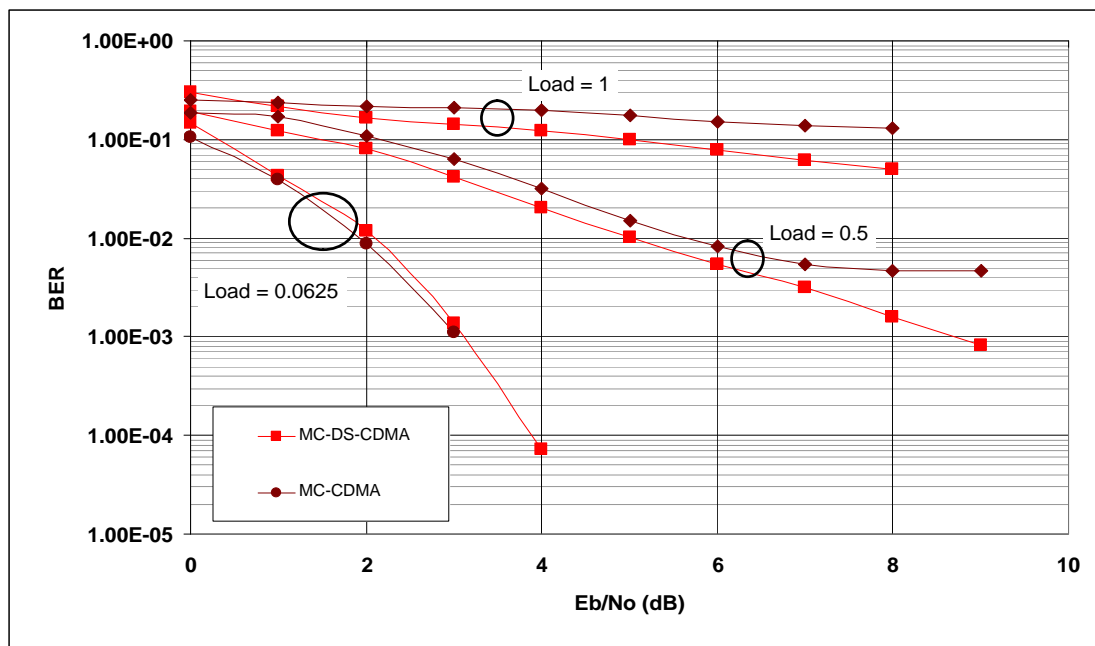
(a)
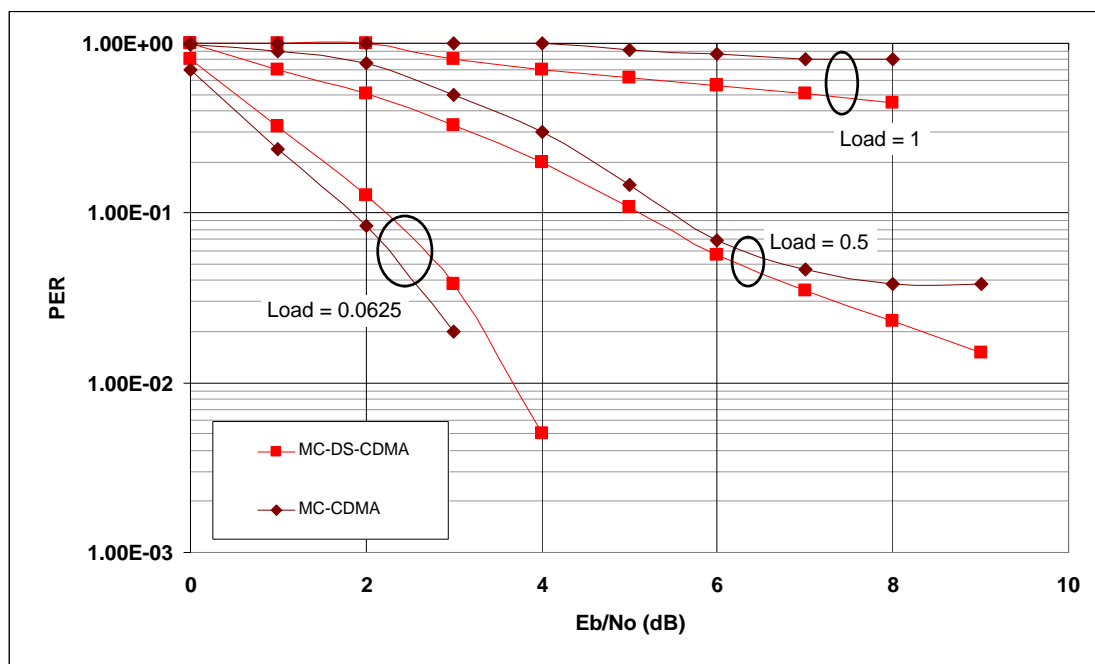
(b)

Figure 5.7   BER and PER Performance of Coded MC-CDMA and MC-DS-CMA with One Transmit and Two Receive Antennas (SIMO) in a Two-Cell environment (*S/I* = 0) [QPSK with *CR*=1/2. Decoding iterations = 6. Rest of parameters as in table (5.1)]
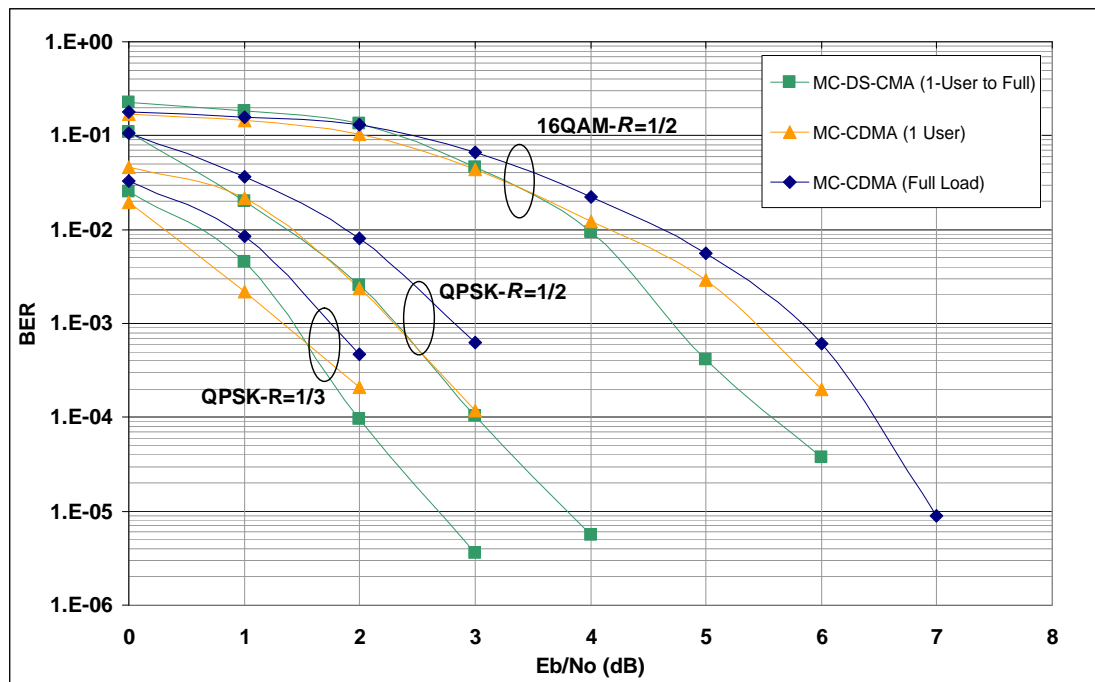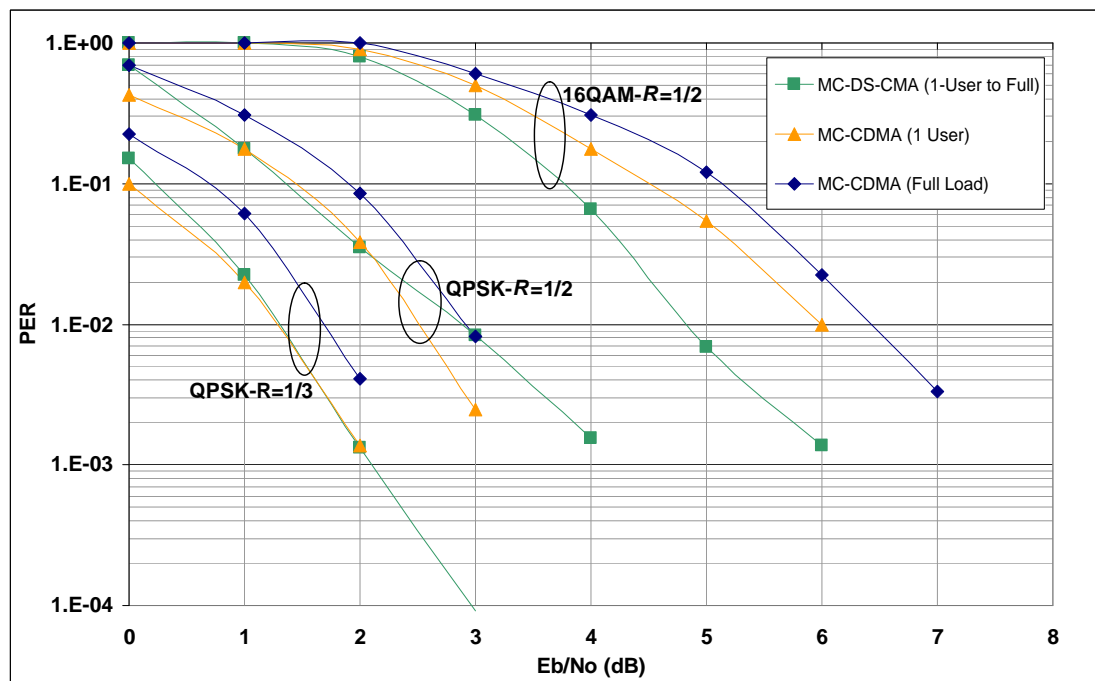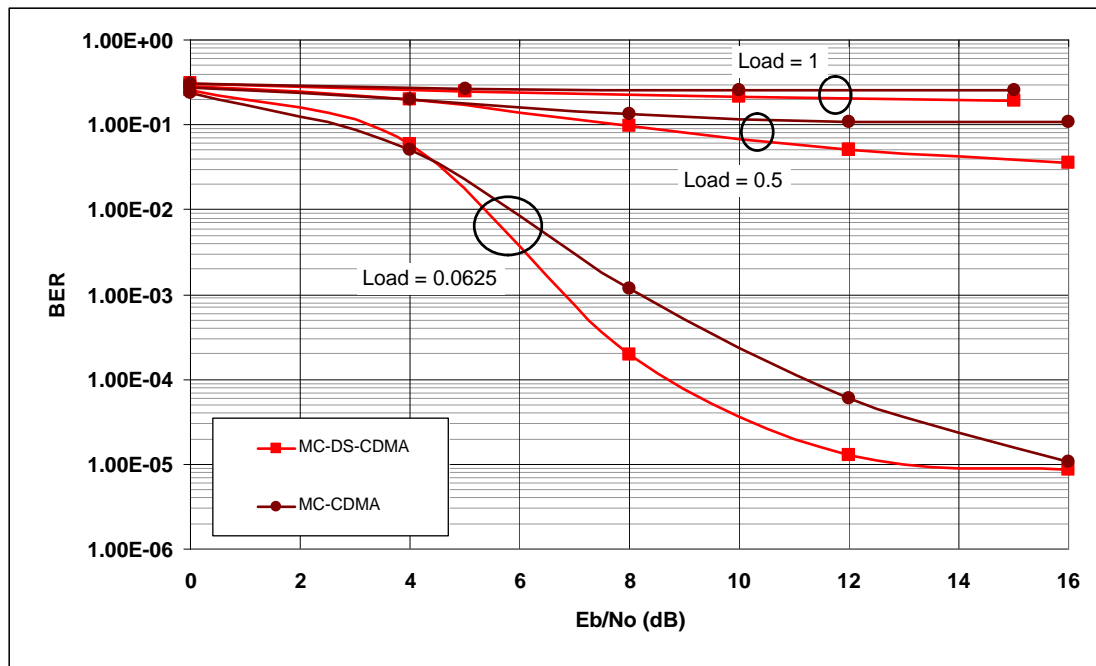
(a)
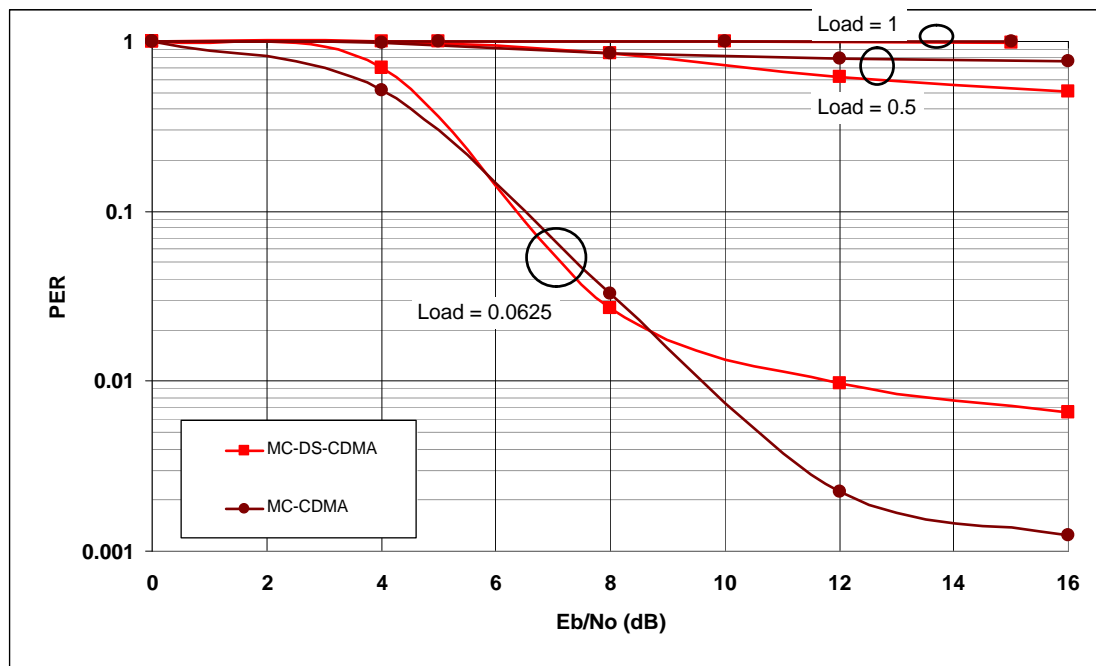
(b)

Figure 5.8   BER and PER Performance of Coded MC-CDMA and MC-DS-CMA with Two Transmit and One Receive Antennas (MISO) in a Two-Cell environment (*S/I* = 0) [QPSK with *CR*=1/2. Decoding iterations = 6. Rest of parameters as in table (5.1)]

117

5.1.2.2.3 Comparison with different Modulation and Coding schemes

Figure (4.9) presents the performances of MC-CDMA and MC-DS-CDMA with the three different modulation and coding combinations of a) QPSK with Code Rate $R = 1/3$, b) QPSK with $R = 1/2$, and c) 16QAM with $R = 1/2$.

In a multi-cell environment, MC-DS-CDMA suffers from inter-cell interference while MC-CDMA suffers from inter-cell interference in addition to MAI (when there is more than one user) due to the breakdown of the orthogonality between codes in the frequency domain, therefore at all times the performance will vary as a result of modifying the load in either systems. It is illustrated in the figure that the performance range between 1-user and full load scenarios increases dramatically with increasing the modulation order.

The single-user MC-CDMA performs slightly better than its equivalent MC-DS-CDMA at low modulation order (i.e. QPSK). In the full load scenario MC-DS-CDMA outperforms MC-CDMA for the same constellations. On the other hand, while both systems perform similarly with full loads for a high modulation order (i.e. 16QAM), MC-CDMA significantly exceeds the performance of MC-DS-CDMA with a sinlge user load for these constellations. The performance of both MC-CDMA and MC-DS-CMA degrade when the number of users increases as this will result in an increasing level of Inter-cell interference (and increasing MAI in the case of MC-CDMA).
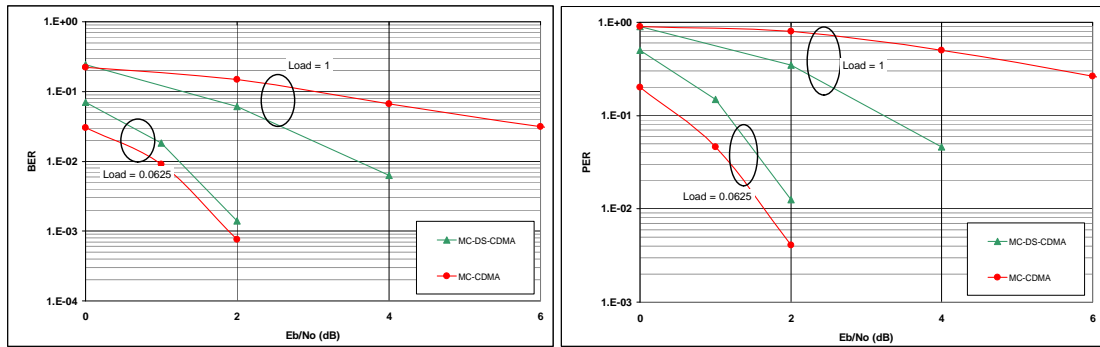
(a) QPSK with Code Rate = 1/3
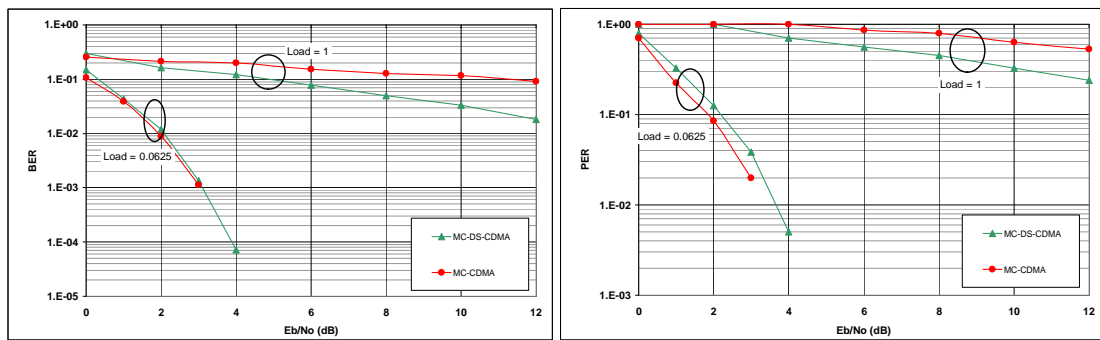
(b) QPSK with Code Rate = 1/2
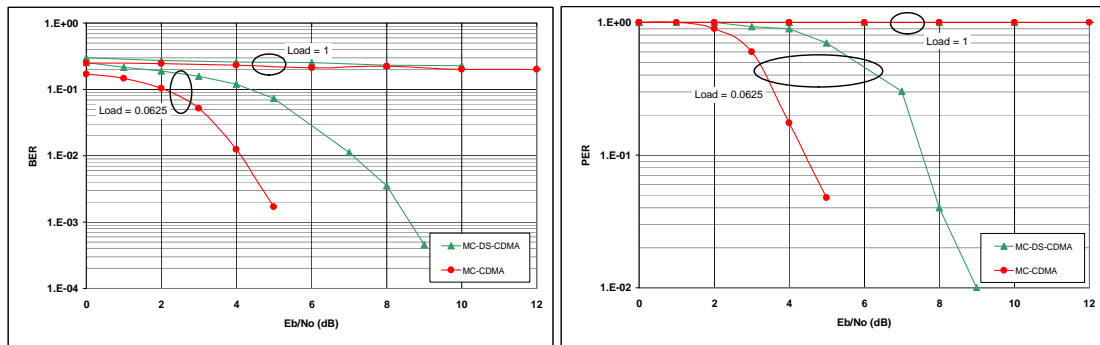
(c) 16QAM with Code Rate = 1/2

Figure 5.9   BER and PER Performance of Coded MC-CDMA and MC-DS-CMA in a Two-Cell environment (*S/I*=0), with One Transmit and Two Receive Antennas (SIMO) for the combinations: QPSK with Code Rate =1/3, QPSK with Code Rate =1/2, and 16QAM with Code Rate =1/2 [Decoding iterations = 6. Rest of parameters as in table (5.1)]

5.2   Systems Parameterisation comparison

Table (5.2) summarises the parameters of MC-DS-CDMA and MC-CDMA. Two approaches were used in the table; the first is when the total bandwidth of the signal is fixed and the second is when the total duration of the spreading code is fixed. It must be mentioned here that the guard interval duration was ignored in the calculation of formulas for the sake of simplifying the information presentation.

When the bandwidth resources are the bottleneck in designing the system (which is usually the case) the designer has theoretically one of four options to tackle the parameterisation of the system with reference to the OFDM signal (assuming OFDM is a special case with processing gain =1 in both the frequency and time domains):

Table 5.2   MC-DS-CDMA and MC-CDMA parameters based on the allocated resources

	Fixed Frequency Resources		Fixed Time Resources	
	MC-DS-CDMA	MC-CDMA	MC-DS-CDMA	MC-CMDA
Symbol Duration ($=T_s$ for OFDM)	T_s	T_s	$\dfrac{T_s}{SF_t}$	T_s
No. of Subcarriers ($=N_c$ for OFDM)	N_c	N_c	$\dfrac{N_c}{SF_t}$	$N_c \bullet SF_f$
Chip Duration ($=T_s$ for OFDM)	T_s	T_s	$\dfrac{T_s}{SF_t}$	T_s
Code Duration ($=T_s$ for OFDM)	$T_s \bullet SF_t$	T_s	T_s	T_s
S/P converted symbols ($=N_c$ for OFDM)	N_c	$\dfrac{N_c}{SF_f}$	$\dfrac{T_s}{SF_t}$	N_c
Total Bandwidth ($=\dfrac{N_c+1}{T_s}$ for OFDM)	$\dfrac{N_c+1}{T_s}$	$\dfrac{N_c+1}{T_s}$	$\left(\dfrac{N_c}{SF_t}+1\right)\bullet\dfrac{SF_t}{T_s}$	$\dfrac{(N_c \bullet SF_f)+1}{T_s}$
Subcarrier Spacing ($=\dfrac{1}{T_s}$ for OFDM)	$\dfrac{1}{T_s}$	$\dfrac{1}{T_s}$	$\dfrac{SF_t}{T_s}$	$\dfrac{1}{T_s}$

a. If frequency spreading is used, fewer symbols per user (SF_f / N_c) can be transmitted in parallel if the number of subcarriers is to remain fixed as in OFDM (i.e. N_c). Chip interleaving can be used to increase the opportunity of independent fading across the chips of a codeword even in low selective fading conditions.

b. Alternatively, the same number of S/P converted symbols (N_c in OFDM) is maintained. This results in a higher number of narrower subcarriers equal to $SF_f \times N_c$ within the same bandwidth. In this case, symbols are stretched in the time domain. By omitting chip interleaving a whole spreading sequence may undergo flat fading if the bandwidth of all subcarriers corresponding to one spreading sequence is within the coherence bandwidth of the channel. Because every symbol is expanded in the time domain it becomes more susceptible to fast fading if the coherence time is smaller than the symbol's duration.

c. With time-domain spreading, one approach is to keep the number of S/P converted symbols the same as that of OFDM i.e. fixing the total number of subcarriers to N_c. Spreading in this case is implemented by duplicating the OFDM symbols a number of times in the time domain equal to the spreading gain SF_t. Unlike MC-CDMA, this method ensures that the spreading sequence experiences flat fading across its length. This is conditional on having the coherence time smaller than $SF_t \times T_s$, where T_s is the OFDM symbol duration (which is equal to the duration of one MC-DS-CDMA chip). In this sense, MC-DS-CDMA is more vulnerable to the Doppler frequency effect, especially when SF_t is large.

d. Another approach is to reduce the number of S/P converted symbols in MC-DS-CDMA, which would result in reducing the total number of subcarriers to maintain the same bandwidth. This yields subcarriers with wider bandwidth and spacing as well as shorter chip duration. If the subcarrier's bandwidth exceeds the coherence bandwidth of the channel OFDM loses the advantage of flat fading per subcarrier.

To get a deeper understanding of MC-CDMA and MC-DS-CDMA, we now consider the opposite case of being bounded by the time domain resources i.e. requiring the spreading duration not to exceed the duration T_s of an OFDM symbol. Again, the problem has four approaches with reference to an OFDM signal:

a. When MC-CDMA is considered i.e. when the chips are distributed along the frequency domain, the number of subcarriers can be increased to SF_f times the original number of subcarriers in OFDM (N_c). This would keep the number of S/P converted symbols the same as OFDM (i.e. equal to N_c). Assuming that the OFDM system is designed to ensure flat fading per subcarrier, there should be no threat of frequency selectivity within the subcarrier width. Nonetheless, the spreading code's chips are less likely in this case to experience flat fading across the whole bandwidth to ensure no enhancement of the MAI interference. If full exploitation of frequency diversity is sought, chip interleaving can be applied to ensure uncorrelated fading across chips of every spreading sequence. This option, however, increases MAI in MC-CDMA.

b. The alternative is to reduce the number of S/P converted symbols to Nc / SF_f.
This way, the same OFDM symbol's bandwidth and duration (i.e. the same
frequency and time resources) are maintained.

c. Applying MC-DS-CDMA within the same time allocated to OFDM means
that the chip duration should go down to T_s / SF_t i.e. SF_t times smaller than
that of an OFDM symbol. Consequently, the subcarrier bandwidth increases
by a factor of SF_t. The result can be thought of as multiple conventional SC-
CDMA signals being transmitted in parallel and overlapping. Such a
configuration enables MC-DS-CDMA to employ a RAKE receiver to resolve
the different delayed paths of the signal if the delay is long enough compared
to the chip duration. However, this also means that every subcarrier will no
longer be flat faded and hence MC-DS-CDMA will have to face the effects of
ISI and ICI.

d. Finally, by reducing the number of S/P converted symbols, the total number of
subcarriers can be reduced resulting in a narrower total bandwidth. If the same
bandwidth originally allocated to the OFDM system is to be maintained, this
gives more room for existing subcarriers to expand in the frequency domain.
This will reduce further the symbol duration of MC-DS-CDMA.

5.3   System features comparison

The following comparison uses as a reference an OFDM system that assumes optimised subcarrier bandwidth to ensure (a) flat fading over individual subcarriers, (b) quasi static fading for the duration of the OFDM symbol and (c) the availability of frequency diversity along the overall bandwidth of the system. Ignoring the guard interval duration, the OFDM system parameters are denoted T_s for the symbol duration, N_c for the number of subcarriers and the number of S/P converted symbols, and $1/T_s$ for the spacing between subcarriers.

5.3.1   Frequency diversity

Results to date have established that MC-CDMA has the advantage of exploiting the frequency diversity embedded in the OFDM format. This means that strong attenuation of one subcarrier does not directly result in the loss of information carried on that subcarrier, because the same data is shared by a number of subcarriers over which a sequence is spread. Interleaving the chips of every sequence across the whole bandwidth available to the signal maximises the opportunity of having uncorrelated fading among these chips i.e. achieving a higher degree of frequency diversity. The exploitation of frequency diversity in MC-CDMA is bound by the availability of frequency selective fading, which is determined by the multipath channel characteristics.

On the contrary, the capability of MC-DS-CDMA to exploit frequency diversity is limited to what is gained through bit interleaving.

5.3.2   Inter-Code Interference

The penalty of MC-CDMA for taking advantage of the frequency diversity is an increased inter-code MAI. When MC-CDMA uses orthogonal spreading sequences, the only chance for these sequences to maintain their orthogonality is by having flat fading across the bandwidth of the subcarriers modulated by those sequences' chips. This scenario is possible only when the delay spread is too short to create frequency selective fading within the bandwidth occupied by the spreading sequence or when the subcarriers are narrow enough to prevent that selectivity. The deployment of MUD or Interference Cancellation becomes a necessity to mitigate MAI and utilise frequency diversity.

In MC-DS-CDMA, MAI enhancement is avoided because the whole spreading sequence is distributed over a single subcarrier as long as the channel is quasi static along the duration of the spreading sequences. This gives MC-DS-CDMA the advantage of simplifying the optimum detection process to single-user detection (when the system is MAI-free).

5.3.3   Frequency Selective Fading

There are three approaches to deal with frequency selective fading in MC-CDMA. One is to avoid it by parameterising the system towards ensuring that all chips of a spreading sequence are attenuated similarly. This is achieved by narrowing the subcarriers' bandwidth and placing the chips corresponding to one spreading sequence on adjacent subcarriers. This setup, however, reduces the chances of MC-CDMA benefiting from frequency diversity within the system.

Another approach is to ensure that MC-CDMA exploits as much frequency diversity as it can through chip interleaving. MAI would be at its peak with this setup. The third and final approach is to keep the system parameters as those of the original unspread OFDM i.e. by fixing the subcarrier bandwidth and not applying chip interleaving. Such a configuration would attain a balance between moderate MAI and frequency diversity gain.

In respect of MC-DS-CDMA, frequency selective fading should not be a problem when subcarrier and symbol sizes are the same as an optimised OFDM system. If the system is reconfigured to mitigate fast fading (by shortening the symbol duration) there is a risk of exposing individual subcarriers to frequency selectivity. This would occur if the subcarrier's bandwidth is wide enough to exceed the coherence bandwidth of the channel. Such a situation compromises the main feature of an OFDM-based system, which is to transform the frequency selective fading over the system's bandwidth to flat fading per subcarrier.

5.3.4 Doppler Frequency Shift

By keeping the MC-CDMA's symbol duration below the coherence time of the channel the system is protected from fast fading effects. MC-CDMA does not require additional resources to what OFDM uses in the time domain when the effect of spreading appears as an expansion of the system's frequency bandwidth or as a reduction of number of S/P converted symbols. The system designer, however, may choose not to sacrifice the extra bandwidth or the number of S/P converted symbols. The solution to this has been discussed earlier and it involves increasing the number of subcarriers to $N_c \times SF_f$ and reducing the subcarriers' width so that the number of

subcarriers can be accommodated within the original OFDM bandwidth. Because the new subcarriers are now much narrower than before and symbols are much longer than the initial T_s duration, MC-CDMA becomes susceptible to fast fading if the symbol is long enough to exceed the coherence time.

MC-DS-CDMA is more likely to experience fast fading across the total length of the spreading sequence, even when the symbol duration is equal to that of MC-CDMA. One method to overcome this is to reduce the number of S/P converted symbols within the same bandwidth. In this case, the resultant symbols are shorter than the original configuration, and should, therefore, be more resistant to channel variations in the time domain.

5.3.5   Pilot signalling

In MC-CDMA pilot signals have to be transmitted independently from data signals. The reason is that it is difficult to retrieve the pilot signal accurately when all spreading codes suffer from MAI, which is the case for MC-CDMA in most situations.

On the other hand, it is possible for MC-DS-CDMA to embed the pilot signal within every transmitted symbol using a dedicated spreading sequence. This allows better and more accurate estimation of the channel state information (CSI) as long as the MC-DS-CDMA's codeword is shorter than the coherence time of the channel. If separate pilot signalling is chosen for MC-DS-CDMA instead, it becomes costly and inefficient to update the CSI frequently if the spreading sequence duration is not short

enough to allow the transmission of sufficient number of symbols before the need to update the CSI.

5.3.6   Inter-Cell Interference

The frequency diversity available to MC-CDMA gives it the capability of recovering the transmitted data relying on the combination of the symbol transmitted on subcarriers with high Signal-to-Noise-and-Interference Ratio (SNIR). When the inter-cell interference becomes larger than MAI, both MUD or IC methods become less useful for MC-CDMA.

In contrast, the successful detection of symbols in a multi-cell MC-DS-CDMA scheme depends solely on the SNIR of the subcarrier on which that symbol is sent. Therefore when SNIR is too low, the content of that subcarrier is lost. Recovery of this lost information depends on the effectiveness of bit interleaving and channel decoding.

5.4 Conclusions

At the end of the third and final chapter dealing with the characterisation and comparison between frequency and time domain spreading (represented by MC-CDMA and MC-DS-CDMA), we can conclude this part of the research with the following key observations:

- In a single cell environment, the results of the study suggest that MC-CDMA would perform better than MC-DS-CDMA when the system is not assisted by multiple antennas or channel coding. The reason for this was given to be the lack of diversity in MC-DS-CDMA compared to the frequency diversity available in MC-CDMA.

- For the coded schemes, the study has shown that for a number of decoding iterations higher than 1, MC-DS-CDMA performs better than MC-CDMA, with a gain of about 0.7dB at BER=10^{-3}. This advantage of MC-DS-CDMA disappears in the PER performance as appeared in figure (5.2).

- The results indicate that when both systems are aided by more than one receive antennas, uncoded MC-CDMA outperforms MC-DS-CDMA because of its frequency diversity advantage. For coded systems, however, the performance of MC-DS-CDMA comes closer to MC-CDMA and even exceeds it in the high SNR region. When the decoding process is iterated both systems offer similar performance (with a small gain for MC-DS-CDMA).

- Our results for three different modulation/coding combinations with SIMO antennas and turbo coding revealed that MC-DS-CDMA generally

performs similar to or better than the 1-user MC-CDMA in all combinations, despite the frequency diversity available only to MC-CDMA

- With regards to the multi-cell environment performances, The investigation results indicate that in the absence of multiple antennas both MC-CDMA and MC-DS-CDMA cannot overcome the dominant inter-cell interference when the cells are fully loaded. Furthermore, with lighter loads MC-CDMA performs better as it has better chances to exploit frequency diversity when the MAI is limited, while MC-DS-CMA converges to an early error floor due to its sensitivity to inter-cell interference and lack of diversity.

- When two receive antennas are used, the results suggested that MC-DS-CDMA would outperform MC-CDMA at loading factors higher than 0.5. The given explanation was that while MC-DS-CDMA has sufficient diversity and error correction capabilities, MC-CDMA continues to suffer from MAI which would be difficult to mitigate with the existence of high level of inter-cell interference. However, the differences between the two systems are minor in this scenario as observed in figure (5.7).

- Three modulation/coding combinations were studied in a multi-cell environment with two receive antennas and iterative channel decoding. Results demonstrated that in general MC-CDMA performs better with light loads (i.e. when the MAI is at a low level). However, by increasing the number of users MAI becomes more severe in MC-CDMA and consequently MC-DS-CDMA begins to offer better performance. Figure (5.9) also showed that MC-DS-CDMA is more sensitive to high modulation orders in a multi-cell environment. A loss of 3.5dB is observed

for the performance of 16QAM MC-DS-CDMA compared to MC-CDMA at BER=10^{-3}.

The main results of both the MC-CDMA and MC-DS-CDMA systems' performances are summarized in table 5.3 for the QPSK-modulated systems with code rate *CR*=1/2 in a single cell environment

Table 5.3   Required *Eb/No* for target BER=10^{-4} and target PER=10^{-2} in MC-CDMA and MC-DS-CDMA systems [Single-cell environment with QPSK and *CR*=1/2]

	MC-CDMA		MC-DS-CDMA	
	BER=10^{-4}	PER=10^{-2}	BER=10^{-4}	PER=10^{-2}
1x1 SISO + 1 iteration	12.3 dB	Not available	∞	∞
1x1 SISO + 6 iterations	8.5 dB	8.2 dB	7.8 dB	9.0 dB
1x2 SIMO + 1 iteration	6.5 dB	10.0 dB	6.5 dB	8.3
1x2 SIMO + 6 iterations	3.3 dB	3.0 dB	3.0 dB	2.9 dB
2x1 MISO + 1 iteration	9.0 dB	Not available	8.5 dB	Not available
2x1 MISO + 6 iterations	6.6 dB	6.5 dB	5.5 dB	6.0 dB

The theoretical comparison and discussion in this chapter highlighted different approaches of understanding and designing MC-CDMA and MC-DS-CDMA. The study has gone some way towards enhancing our understanding of both systems and helps to remove some of the uncertainties regarding the performances of these systems and how they compare with each other. Nevertheless, further research is needed to confirm the general findings of this theoretical discussion.

Taken together, our results suggest two distinctive trends for the performance of MC-DS-CMDA and MC-CDMA in a single cell environment. In the absence of assisting facilities such as multiple antennas and channel coding, the lack of diversity makes MC-DS-CDMA more susceptible to error on deeply faded subcarriers, while MC-CDMA can exploit frequency diversity to offer better performance. On the other hand, the use of multiple antennas and iterative decoding enhances the performance of

MC-DS-CDMA and makes it equal to or better than the 1-user performance of MC-CDMA. In respect to the multi-cell environment, MC-DS-CDMA is more sensitive to inter-cell interference in SISO system. The employment of multiple receive antennas brings closer the performance of both systems. MC-DS-CDMA becomes vulnerable with high order modulations such as 16QAM.

This concludes our comparative study of two multiple access strategies based on Multicarrier modulation combined with different forms of CDMA. In the next chapter we investigate a novel MUD algorithm for one of the previously studied schemes; which is MC-CDMA.

Chapter 6
Chase-Assisted Near-ML MUD for MC-CDMA

A s observed in chapters 3 and 5 of this thesis, a main disadvantage of MC-CDMA is that to achieve acceptable performance in the presence of high MAI the use of MUD becomes a necessity. MUD, however, it is generally a complex process. In particular, the complexity of the optimum ML detector is prohibitive, and it increases exponentially with the number of users.

Different proposals have been made in the literature for suboptimal algorithms which approximate the ML process with less complexity [3,55-56]. These were briefly reviewed in Chapter 2. Among those algorithms is the Chase algorithm [3], which was originally proposed for the ML decoding of linear block codes. A natural next step would be to use the Chase algorithm in the design of a simplified near-ML MUD algorithm for MC-CDMA.

The rest of the chapter is organised as follows. The main features of the Chase algorithm are discussed in the next section. The new MUD detection scheme is then introduced and described. Later in the chapter characterisation results are shown and discussed for both the uncoded and coded MC-CDMA. Finally, the chapter is concluded in Section 6.4.

6.1   The Problem and Motivation

The main idea of the Chase Algorithm as introduced in [3] was to simplify the Maximum Likelihood (ML) search among all possible codewords to a search amongst the most probable alternatives based on some metric. This was first suggested to replace the optimal yet prohibitively complex ML decoding process of block codes. This is explained in depth in Chapter 7

The Chase Algorithm has two major advantages: Simplicity and Flexibility.

- Simplicity: The Chase algorithm replaces the search along the whole lookup table (or code), where every codeword is considered, with a search among a new much smaller lookup table where only the least reliable positions of a code are replaced with their alternatives. This dramatically reduces the complexity of the decoder while still offering a near-ML performance. For example, for a code of base m and length n, the length of the lookup table is reduced from m^n codes for the ML decoder to m^p for the Chase decoder, where $p \ll n$ is the number of least-reliable symbols to be varied. In [3] it was shown that even the latter can be reduced further.

- ▪ Flexibility: unlike the conventional ML decoder or other less complicated decoders, the Chase decoder has different parameters which can be varied and will result in changing the system's complexity. One parameter is the number of least reliable symbols p which can be considered to create the lookup table. This can range from one to the total length of the code in use, n, (the optimal ML filter case). Another parameter is the number of variations for each of the p symbols. For a binary scheme this is limited to the 1, but for a non-binary scheme there may be several alternative symbols to consider. As mentioned earlier, the Chase algorithm offers some flexibility on how to utilise the p symbols and their alternatives to create the lookup table that will be searched for the best matching codeword. The maximum length of lookup table in a Chase decoder is m^p, but this can be reduced with slight degradation in the system's performance. The Chase algorithm is capable of generating and receiving soft values as an output and input; therefore, when the Chase decoder is integrated within a wider decoding scheme the number of decoding iterations depends only on how well the system is required to perform in terms of both error correction and processing time delay.

Motivated by the advantages above, the Chase algorithm is reintroduced with a new application, Multiuser Detection (MUD) for MC-CDMA signals where frequency selective fading among subcarriers with high-delay-spread channels creates Multiple-Access Interference (MAI) among the different spreading codes in use.

The issue here is closely similar to the problem of block code decoding. An optimal MUD will consider all the possible variations of symbols that were spread by each of the spreading codes, regenerate the spread signals, add them together and compare

every combination with the received signal to find the one of minimum distance from the received signal.

Again, the ML detector is extremely complex and even for short spreading codes its implementation is unrealistic. On the other hand, this process can be significantly simplified by creating error patterns using only the least reliable symbols at the output of the detector after an initial estimation using a matched filter as a SUD. Each of these patterns is then used to reconstruct the transmitted codeword corrupted by the channel and the results are compared with the received signal. A decision (soft or hard) is made based on the codeword that is closest to the received signal. In an uncoded system, this output of the detector can be taken as a final hard decision to the demapper. If the signal is encoded, a soft output from the detector based on the reliability metric of the initial SUD detector can be fed to a soft channel decoder.

In the following section the proposed Chase MUD is described in detail.

6.2   Chase-assisted simplified MUD

As mentioned earlier, the proposed Chase-assisted detector is supposed to simplify the complex MUD of a MC-CDMA signal. Without loss of generality, the number of subcarriers in MC-CDMA is assumed to be equal to the spreading factor SF. Thus the received MC-CDMA signal R is given by (6.1):

$$R = X\,H + W\ ,\qquad\qquad (6.1)$$

where X is an SF-length vector representing the symbols spread in the frequency domain, and is given by (6.2)

$$X = \begin{bmatrix} X\,[1] & X\,[2] & \cdots & \cdots & X\,[SF] \end{bmatrix},\qquad\qquad (6.2)$$

where $X\,[k]$ is the result of summing the k-th chip of the spreading sequences corresponding to all active users. This is given by (6.3) as:

$$X\,[k] = \sum_{n=1}^{C_{mux}} C_n\,[k]\,b_n \qquad k = 1,2,\ldots,SF\ ,\qquad\qquad (6.3)$$

where b_n is the data symbol corresponding to user n, $C_n\,[k]$ is the k-th chip of the spreading sequence assigned to user n, and C_{mux} is the total number of user.

H is the diagonal channel matrix and is given by:

$$H = \begin{bmatrix} h(1) & 0 & \cdots & \cdots & 0 \\ 0 & h(2) & 0 & & \vdots \\ \vdots & & \ddots & & \vdots \\ \vdots & & & \ddots & \vdots \\ 0 & \cdots & \cdots & \cdots & h(SF) \end{bmatrix},\qquad\qquad (6.4)$$

where $h(k)$ is the frequency domain channel response at subcarrier k. N is an SF-length Additive White Gaussian Noise (AWGN) vector with zero mean and double-sided power spectral density of $N_0/2$.

A matched filter is then used as a SUD to get an initial estimate of the symbol spread by each spreading code. The output of the matched filter for user n's transmitted symbol can be written as:

$$Y_n = \sum_{k=1}^{SF} (C_n[k]b_n|h(k)|+w_k)\cdot C_n[k],\qquad(6.5)$$

where Y_n, h_k, w_k are the initial estimation of the transmitted symbol b_n of user n, the channel response at subcarrier k and the AWGN noise at subcarrier k, respectively.

For a BPSK signal, Y_n is a soft value representing a +1 if positive and a -1 if negative. The closer the value of $Y_{n,l}$ to zero, the less reliable it is. The next step is to find the p positions with least reliable values of Y_n. The value of p can range from 1 to the total number of bits transmitted, and its selection is based on a tradeoff between the performance and the complexity of the detector. Once the least-reliable positions are found, a number of error patterns X_j', where $j=0,1,\ldots,(2^p-1)$, are created where one or more of the p positions are flipped. For instance, assuming 4 users and $p=2$, if the hard decision estimate X_0' is equal to [1 1 -1 1] and the second and third users' symbols are the least reliable (i.e. $n=2$ and $n=3$), there will be 2^2=4 error patterns which are defined by (6.6)

$$
\begin{array}{cccccc}
n & = & 1 & 2 & 3 & 4
\end{array}
$$

$$
\begin{bmatrix} X_0' \\ X_1' \\ X_2' \\ X_3' \end{bmatrix} = \begin{bmatrix} 1 & 1 & -1 & 1 \\ 1 & -1 & -1 & 1 \\ 1 & 1 & 1 & 1 \\ 1 & -1 & 1 & 1 \end{bmatrix}, \tag{6.6}
$$

where each row X_j' represents the application of one error pattern to the initial estimation. The first row is the hard decision based on the initial estimation Y , and the two least-reliable positions are at columns 2 and 3.

To reconstruct the transmitted signal, the symbols in each column in (6.6) are spread by the corresponding n -th spreading sequence C_n. This is followed by the summation of the spread symbols of all users (i.e. summation along the rows). This gives a different reconstructed symbol for each error pattern. The resultant vector can be written as:

$$
S = \begin{bmatrix} S_0 \\ S_1 \\ \vdots \\ S_{(2^p-1)} \end{bmatrix}, \tag{6.7}
$$

where each sequence S_j is given by (6.8) for $j = 0,1,\cdots,2^p - 1$

$$
S_j = \begin{bmatrix} s_j[1] & s_j[2] & \cdots & s_j[SF] \end{bmatrix}. \tag{6.8}
$$

Each $s_j[k]$ represents the summation of the k –th chip of all spread symbols belonging to error pattern X_j' , and is given by (6.9):

$$
s_j[k] = \sum_{n=1}^{C_{max}} C_n[k]X_j'[n] \qquad j = 0,1,...,2^p - 1, \tag{6.9}
$$

where $X_j'[n]$ is the symbol in error pattern X_j' that belongs to user n.

A new metric M is then defined based on the Euclidean distance between the received signal R and each component in S. M can be formulated as:

$$
M = \begin{bmatrix} M_0 \\ M_1 \\ \vdots \\ M_{(2^p-1)} \end{bmatrix},
\tag{6.10}
$$

where M_j is the Euclidean distance between R and S_j, and is given by:

$$
M_j = \sum_{k=1}^{SF} \left| S_j \left| h(k) \right| - R_k \right|^2 \qquad , j = 0,1,\cdots,2^p - 1,
\tag{6.11}
$$

where R_k is the received signal at subcarrier k.

The error pattern X_j' that belongs to the minimum metric M_j is taken as the hard decision at the output of the detector. If a soft decision output needs to be passed to the channel decoder then each symbol in X_j' is multiplied by the absolute value of its corresponding initial estimate $|Y|$ as a metric of reliability per symbol.

The output can then be taken to a demapper, bit deinterleaver and channel decoder. If an iterative turbo decoder is used the scheme has the potential to be improved further by returning the soft output of the decoder as an input to the Chase-MUD for another iteration. The latter configuration is not part of our investigation.

The above process is summarized in the block diagram of Figure (6.1).
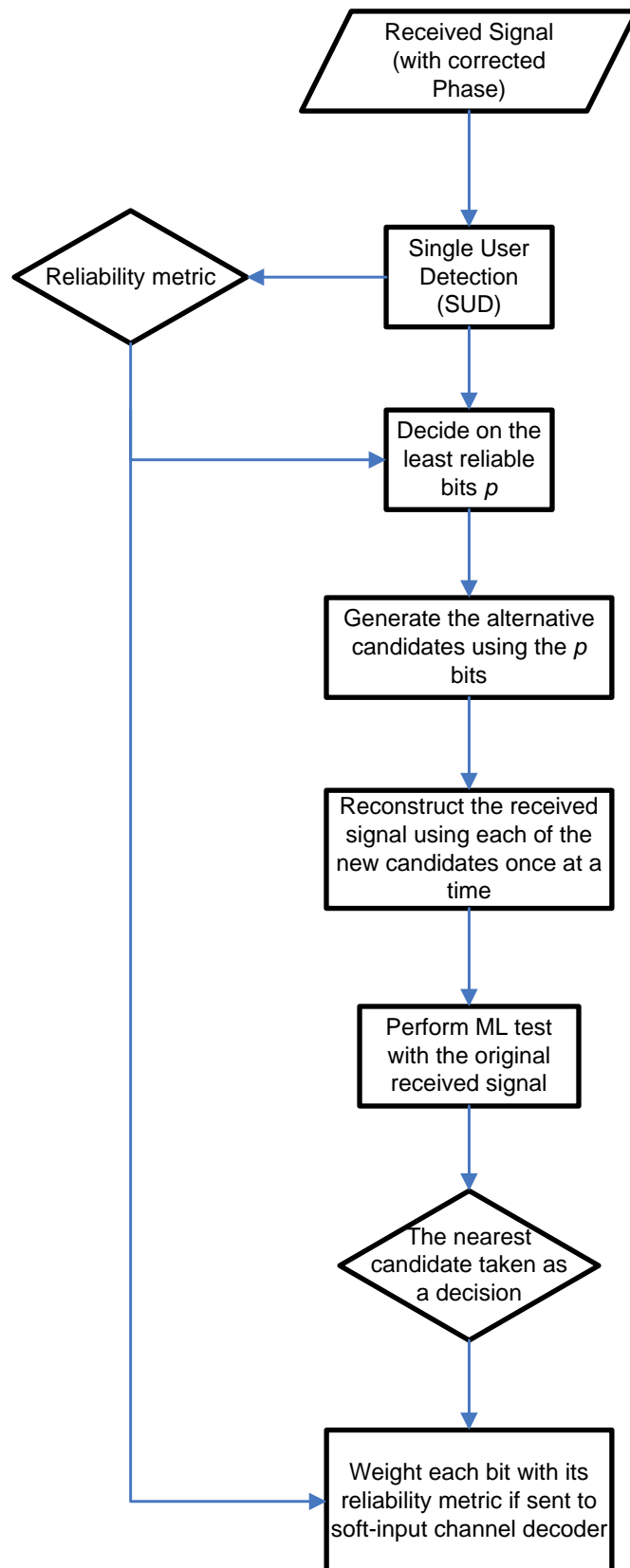
Figure 6.1   The Chase-based MUD Process Flow

6.3   Performance Results and analysis

In this section the results of a characterisation experiment based on computer simulations are depicted and discussed. The simulation used an OFDM channel with 16 subcarriers each modulated by a different symbol in the case of an OFDM signal. In the case of MC-CDMA each subcarrier is modulated by 16 overlapping chips belonging to 16 Walsh-Hadamard spreading sequences. In a similar manner to what was done in subsection 4.4.1.1 of this thesis, the correlation between the channel tabs in the multipath channel is a function of the ratio $R_t = T_{rms}/T_s$ between the delay spread of the channel T_{rms} and the OFDM symbol duration T_s. This allows investigating several aspects of the system's performance with varying channel parameters. Because of the frequency-selective fading nature of the channel MAI is created among spreading codes. That is why MUD is needed to eliminate as much of that interference as possible. The more selective the fading across subcarriers the more MAI can be expected. As for OFDM, symbols transmitted over different subcarriers are orthogonal to each other. Hence there should be no need for a MUD and its performance will be used as a benchmark to evaluate the performance of the proposed Chase-assisted MUD. Whenever channel encoding is applied both systems use convolutional channel encoding with a soft Viterbi decoder at the receiver. Moreover, to make fair comparison between MC-CDMA and OFDM, the spreading sequences in MC-CDMA are assumed to belong all to one user and therefore the despread symbols of all sequences are encoded and decoded as one packet. The parameters of the simulation are summarized in table (6.1).

Table 6.1   Chase-Assisted MUD simulation parameters

	MC-CDMA	OFDM
Spreading Factor SF	8, 16, 32	1
Number of subcarriers	SF	SF (of MC-CDMA)
Mapping Scheme	QPSK	
Load	Full load	
Channel	Rayleigh Fading Channel (Correlation based on $R_t = T_{rms}/T_s$)	
Coding	Binary Convolutional Code (131, 171) Code Rate=1/2	
Channel model	Based on relative values of the delay spread and the symbol duration	

6.3.1   Uncoded System performance

Figure (6.2) shows the BER and PER performance of the proposed Chase-based MUD algorithm for MC-CDMA without channel coding. The algorithm is applied using $p = 1$ and $p = 4$. The ratio R_t varies between $R_t = 1$ (low correlation among subcarriers' fading tabs and high MAI) and $R_t = 0.01$ (High correlation among subcarriers and low MAI). The spreading factor is assumed to be $SF = 16$. The results are compared with the performance of an OFDM system that has the same dimensions.

It can be noticed from the figures that the Chase-algorithm-based MUD improves the performance of MC-CDMA significantly and that MC-CDMA is now capable of surpassing the performance of OFDM up to some value of E_b/N_0. This is because uncoded OFDM does not have any error correction capability while MUD-aided MC-CDMA can have some of its received errors corrected by the Chase Algorithm. The gain of MC-CDMA is around 5dB at BER=10^{-2}.
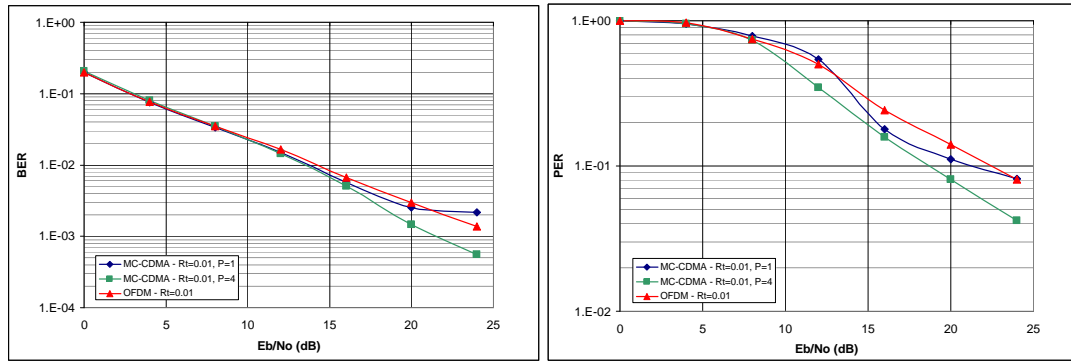
(a)
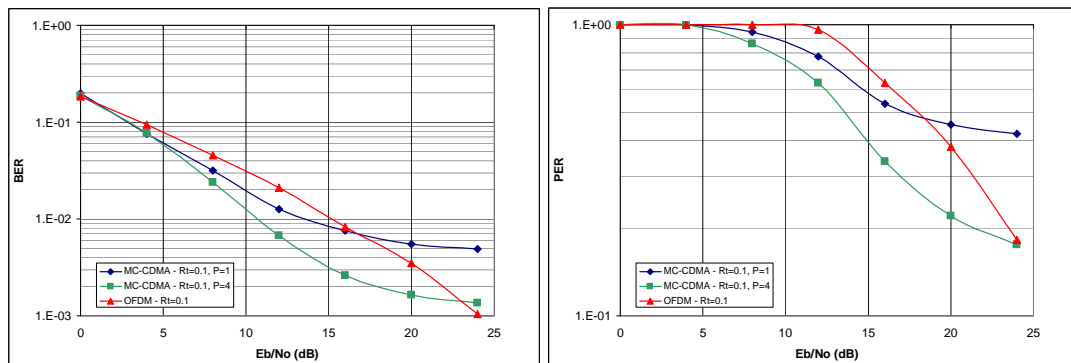
(b)
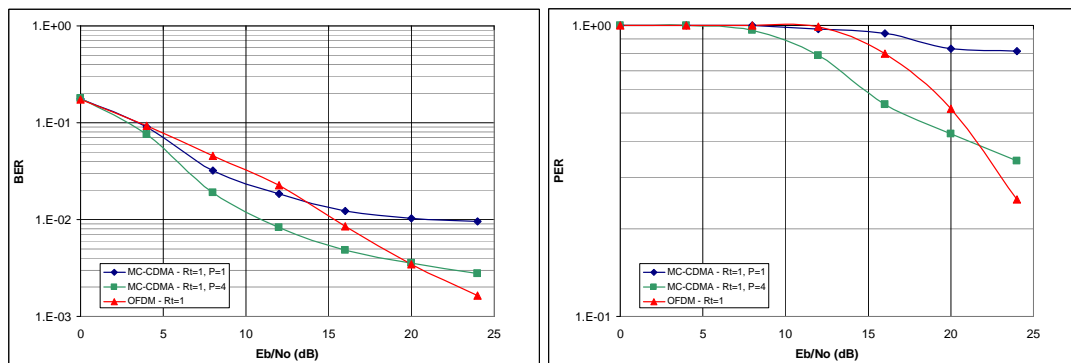
(c)

Figure 6.2   BER and PER performance of MC-CDMA with Chase-Aided MUD, with
$p = 1$ **and** $p = 4$ **, and a)** $R_t = 0.01$ **, b)** $R_t = 0.1$ **and c)** $R_t = 1$ **[Rest of parameters as in table (6.1)]**

144

The results also demonstrate that although high-selective fading channels (e.g. $R_t = 1$) allow MC-CDMA to exploit its frequency-diversity with the aid of MUD (which appears as improvements of MC-CDMA over OFDM at low SNR values), it is clear that the higher the frequency selectivity the earlier the BER and PER approach an error floor.

Furthermore, because MC-CDMA with low frequency selectivity tends to approach the performance of OFDM, it is logical to see MC-CDMA with $p = 4$ and $R_t = 0.01$ outperforming OFDM. An interpretation to this behaviour would be that as MAI is less often issue for MC-CDMA in highly-correlated fading, it still benefits from self error correction through the Chase-based MUD, while OFDM doesn't.

6.3.2   Coded System Performance

The BER and PER performances of coded MC-CDMA with the proposed Chase-based MUD algorithm are depicted in figures (6.3), (6.4) and (6.5) for spreading factors $SF_f = 8$, 16 and 32, respectively. This performance was obtained for a system similar to the one described above for the uncoded simulation except that it uses a convolutional channel encoder at the transmitter and a soft Viterbi decoder at the receiver. The results are also compared with the performance of non-MUD-assisted MC-CDMA.
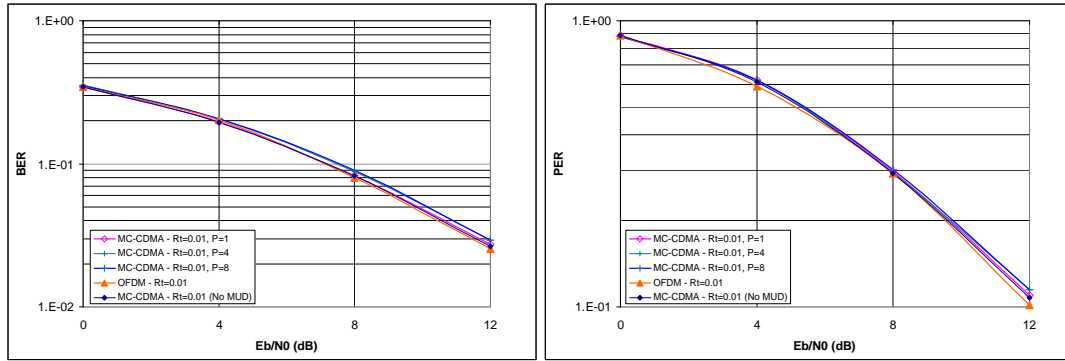
(a)
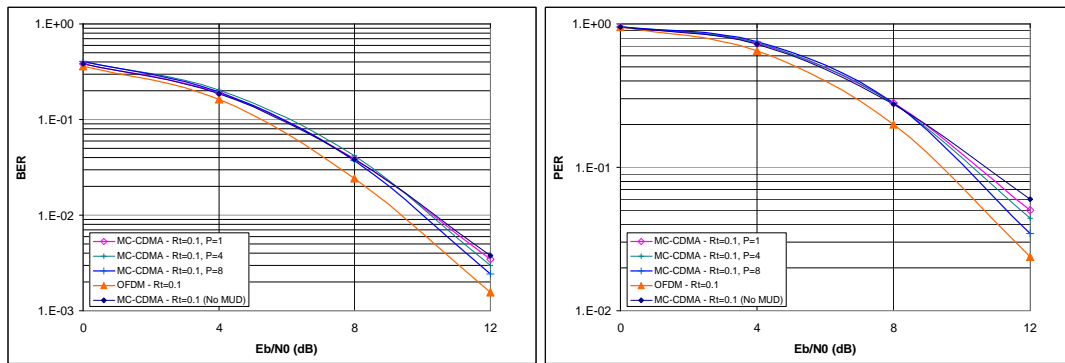
(b)
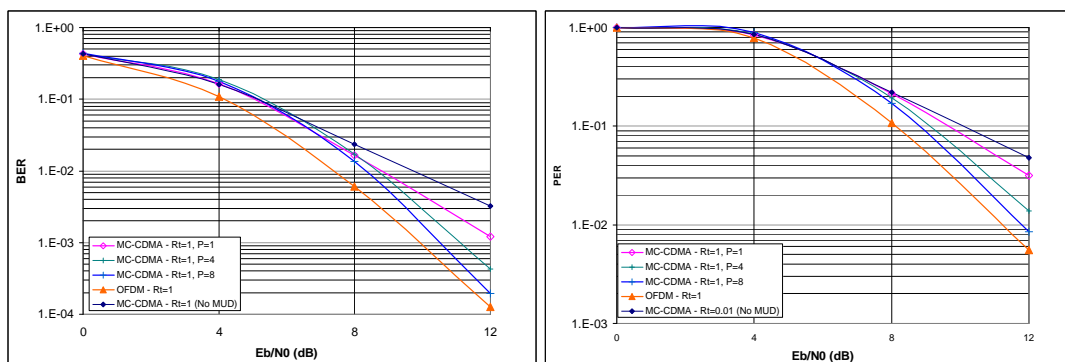
(c)

Figure 6.3   BER and PER performance of coded MC-CDMA with Chase-Aided MUD, with $[SF_f = 8]$, $[p = 1, 4$ and $8]$, and $[$ a$)$ $R_t = 0.01$, b$)$ $R_t = 0.1$ and c$)$ $R_t = 1]$ [Rest of parameters as in table (6.1)]

(a)

(b)

(c)
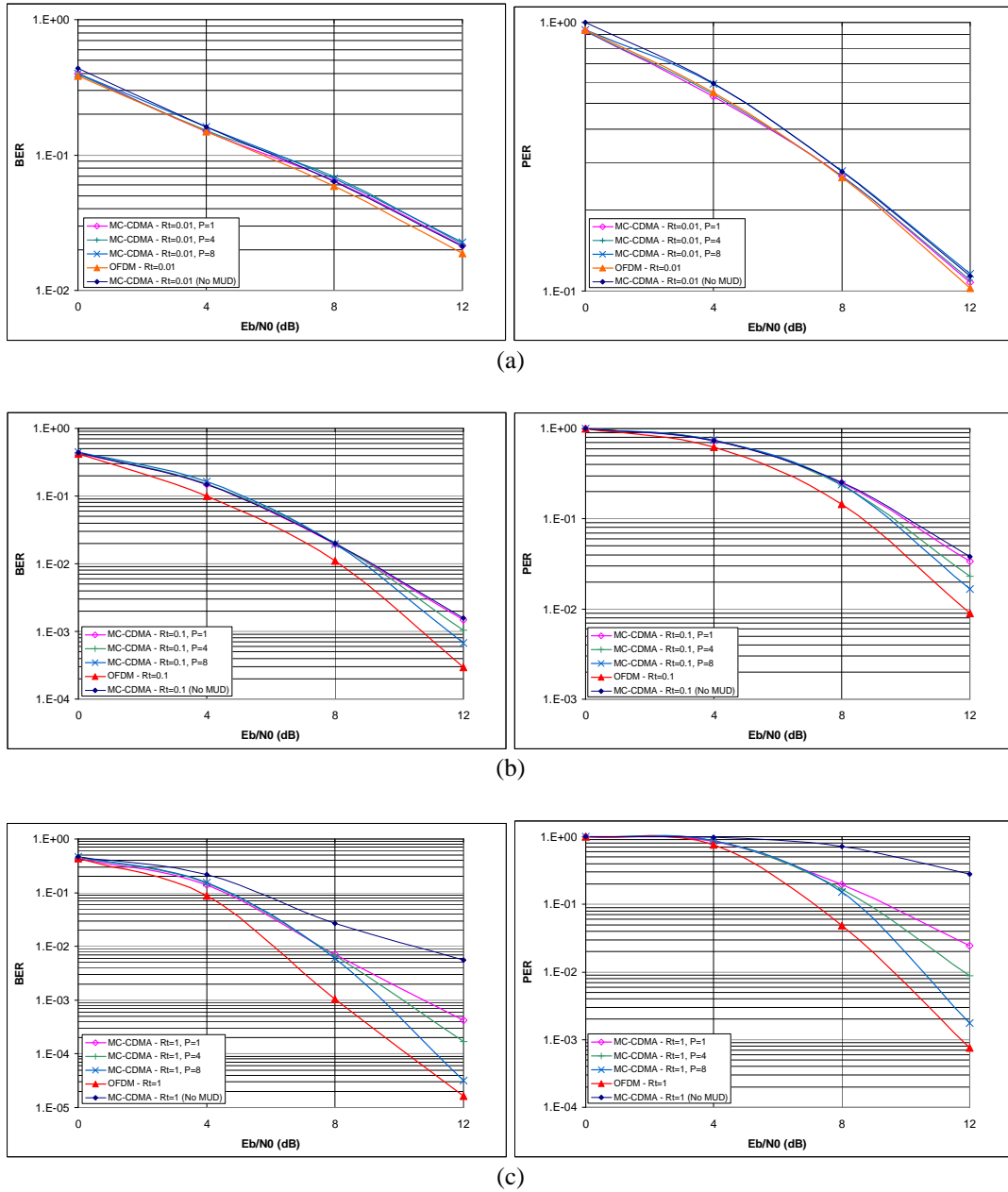
Figure 6.4   BER and PER performance of coded MC-CDMA with Chase-Aided MUD, with $[SF_f = 16]$, $[p = 1, 4 \text{ and } 8]$, **and** $[$ **a)** $R_t = 0.01$, **b)** $R_t = 0.1$ **and c)** $R_t = 1]$ **[Rest of parameters as in table (6.1)]**

(a)

(b)

(c)
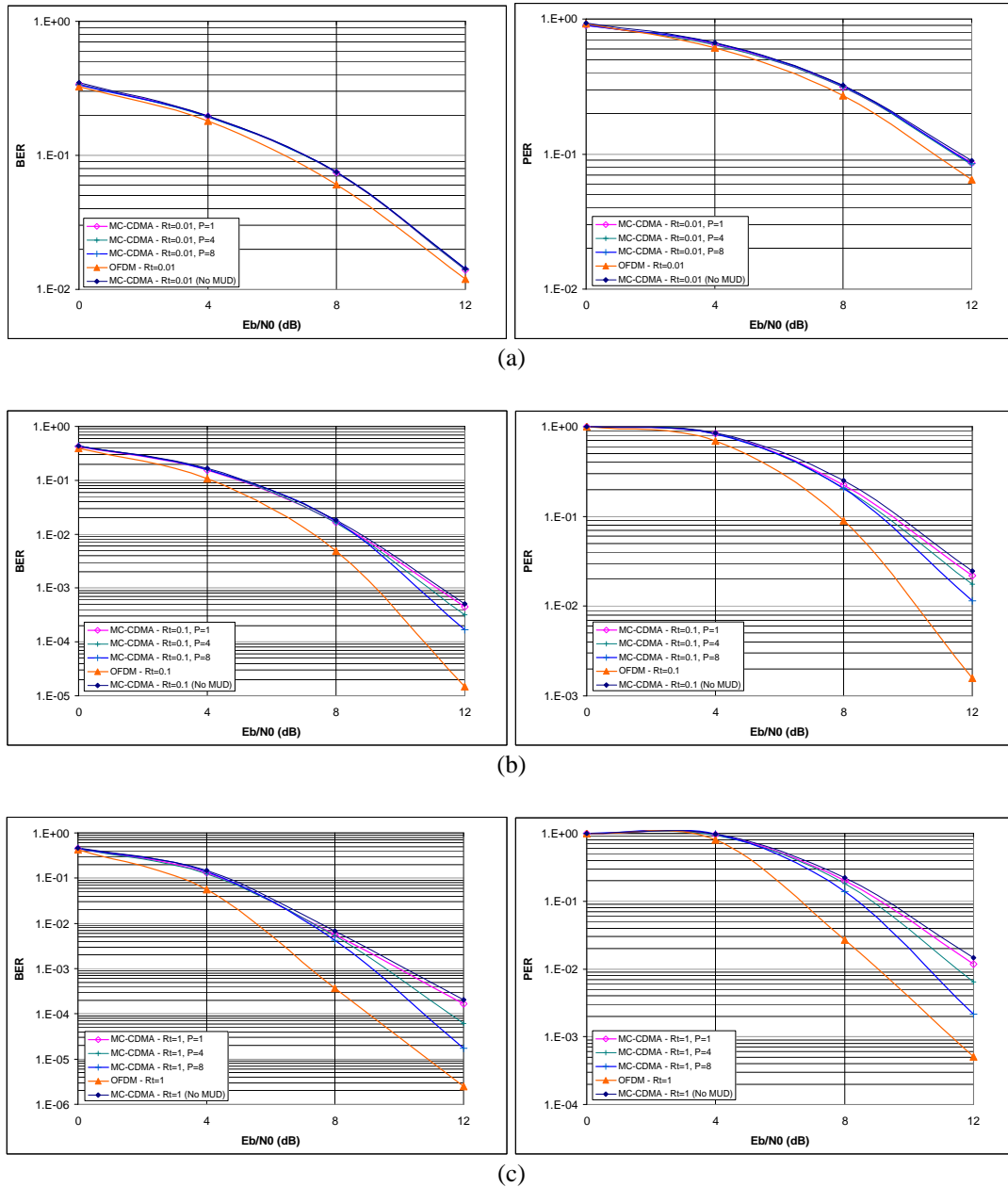
Figure 6.5   BER and PER performance of coded MC-CDMA with Chase-Aided MUD, with
$[SF_f = 32]$**, [** $p = 1, 4$ **and** 8 **], and [a)** $R_t = 0.01$**, b)** $R_t = 0.1$ **and c)** $R_t = 1$ **] [Rest of**
parameters as in table (6.1)]

It can be seen from the graphs that MC-CDMA loses all the gain from the Chase-based MUD in highly-correlated channels ($R_t = 0.01$). This is mainly due to the fact that with the lack of frequency selectivity there are incidents where the fading is severely low across the whole bandwidth resulting in the loss of most transmitted symbols, unlike the situation of high frequency selectivity where there will usually be both amplified and nullified symbols, giving the decoder the chance to recover the lost symbols using the surviving ones. The same behaviour is followed by OFDM at low frequency selectivity. Furthermore, because of the high correlation, the MAI is limited in this case and no difference is observed between the performances of the MUD and non-MUD systems.

In a highly frequency-selective channel (i.e. $R_t = 1$) the Chase-based MUD offers a significant improvement to the performance of MC-CDMA. A gain ranging from 1dB to 4dB (depending on the spreading factor) can be observed in comparison with the performance of MC-CDMA with no MUD. Moreover, the gap between MC-CDMA and OFDM decreases to 0.4dB at BER=10^{-4} and 0.5dB at PER=10^{-2} with $SF = 8$ and $p = 8$ (i.e. the optimal ML case for $SF = 8$).

Additionally, the results in figures (6.4) and (6.5) confirm that achieving a near-OFDM performance is not limited to the optimal ML case. With $SF_f = 16$ and $p = 8$, the performance of MUD-assisted MC-CDMA is just 0.7dB worse than OFDM at BER=10^{-5} and PER=10^{-3}.

6.4   Conclusions

The observations from the performance results of MC-CDMA in chapters 3 and 5 of this thesis confirm that MAI remains an issue for MC-CDMA. Although the use of optimal ML-MUD to reduce the effects of MAI is theoretically possible, its implementation is prohibitively complex and costly. In this chapter we proposed a novel MUD algorithm for MC-CDMA. The new algorithm is a near-ML detector based on the Chase Algorithm. The proposed algorithm dramatically reduces the MUD processing complexity compared to conventional MUD methods.

Furthermore, the algorithm was shown to offer significant improvement to the performance of channel coded MC-CDMA. A gain of 1dB to 4dB over the non-MUD performance was achieved depending on the spreading factor and the size of error patterns. The algorithm was also proven to be capable of coming as close as 0.4dB to the performance of OFDM in convolutionally-encoded schemes. With regards to the uncoded schemes, although Chase-based MUD allows MC-CDMA to performs better than OFDM in the low SNR region, its performance is generally weak as it converges to an error floor due to MAI. We should bear in mind that these results are for the fully loaded MC-CDMA (i.e. the worst case scenario), and that by reducing the number of users the performance of MC-CDMA is expected to improve further. The amount of this improvement remains an open topic for future research.

In the next chapter, the Chase algorithm is taken back to its original proposed application of decoding block codes. The use of the Chase algorithm in the decoding non-binary BTCs is investigated with application to Multicarrier systems.

Chapter 7
Non-Binary Chase Based BTC for OFDM Systems

I n the previous chapter, the Chase algorithm was utilised to simplify the MUD of MC-CDMA. It was stated earlier in section 2.4 of Chapter 2 that the Chase algorithm was originally proposed to decode linear block codes [3]. The recent interest in the Chase algorithm was driven by its use as the core part of the Block Turbo Code (BTC) decoder [2].

Turbo codes have been extensively studied and employed since they were reintroduced by Berrou in 1996 [91] following the developments by Bahl in 1974 [92]. These codes extract extrinsic information in the decoding process; this

information is then used in subsequent decoding iterations to improve the reliability of the soft decision metric. Different methods have been proposed in the literature to apply the concept to both convolutional and block codes, leading to the terms Convolutional Turbo Codes (CTC) and BTC, respectively.

Among the BTC codes, the one that is probably of most interest is the one introduced by Pyndiah [2]. Pyndiah's work is based on a simplified Chase algorithm [3] applied to product codes. They were shown to reach a capacity efficiency as high as 98% in Gaussian channels using high code rates. However, the original algorithm proposed by Pyndiah has been continuously applied to both binary and non-binary codes (e.g. Reed Solomon Codes) ignoring the fact that non-binary codes do not originate from binary components. The development of a new algorithm that used symbols rather than bits would free the system from the binary components constraint and offer simplification to the decoding process by processing symbols instead of bits.

The rest of this chapter is organised as follows: in the following section the concept of the block turbo code is briefly described. The binary Chase-algorithm-based BTC decoder is then presented followed by our novel contribution of the non-binary Chase-based BTC decoding algorithm. Later in the chapter the performance of BTC is compared with CTC via computer simulations before the new non-binary BTC decoding algorithm is compared with Pyndiah's binary approach. This part of our investigation is concluded in the last section of this chapter.

7.1   Block Turbo Coding (BTC)

A linear block code is defined with the parameters (n, k, δ), where n is the codeword length, k the number of information symbols, and δ its minimal hamming distance.

A product code φ is formed using two linear block codes $\varphi^1(n_1, k_1, \delta_1)$ and $\varphi^2(n_2, k_2, \delta_2)$. The information symbols are arranged in a $(k_2 \times k_1)$ array. The k_2 rows are coded using φ^1 and the resulting n_1 columns are coded each using φ^2 [63]. The parameters of the resulting product code φ are given by $n = n_1 \times n_2$, $k = k_1 \times k_2$ and $r = r_1 \times r_2$, where r_i is the code rate of code φ^i and is equal to $r_i = \dfrac{k_i}{n_i}$.
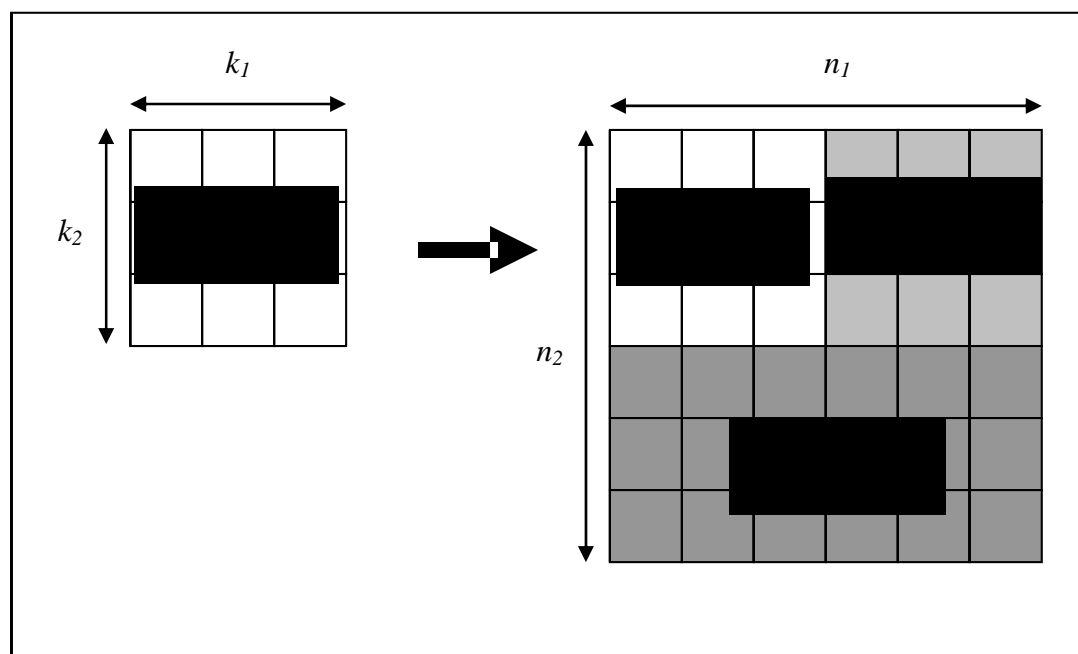
Figure 7.1   The construction of a Product Code

In the case of a binary code, each element of the new code φ is a binary symbol (0 or 1) representing either an information or redundancy bit. On the other hand, any element in a non-binary block code (and its resultant product code) would belong to some non-binary field. For example, in the case of a Reed Solomon (RS) code, every

element belongs to a Galois Field GF($q = 2^m$). Nevertheless, it is understood that every element of a Galois field can be represented by a positive integer which in turn can be written in terms if its equivalent binary components (e.g. 5 = 0 1 0 1). This equivalence does not apply any more to non-binary codes where there would be no relation between the binary field and their own non-binary fields.

7.2   Bit-Level Iterative Decoding of Non-Binary BTC codes using the Chase Algorithm

We stated earlier that n refers to the total length of the product code resulting from the multiplication of the row and column code lengths, n_1 and n_2. However, because the section describes one decoding iteration (which can be either a code or row decoding iteration), $n = 2^m$-1 is used to represent either n_1 or n_2 for the sake of simplicity. m is also chosen to be the order of the mapping constellation (e.g. $m = 4$ for 16QAM modulation).

With binary presentation, a transmitted non-binary codeword E (i.e. one row or column of the product code) is a binary vector of length $n * m$, and can be written as:

$$E = \begin{bmatrix} e_{11} & e_{12} & \cdots & e_{1m} & e_{21} & \cdots & e_{nm} \end{bmatrix}, \tag{7.1}$$

where e_{ij} is the j-th bit in the binary presentation of the i-th non-binary symbol in the code E.

The received word R can be expressed as in (7.2),

$$R = \begin{bmatrix} r_{11} & r_{12} & \cdots & r_{1m} & r_{21} & \cdots & r_{nm} \end{bmatrix}. \tag{7.2}$$

Upon receiving the signal, the Log-Likelihood Ratio (LLR) of each bit in R is calculated using the general expression in (7.5) :

$$LLR\left(e_{ij}\right) = \ln\left(\frac{\Pr\{e_{ij} = +1/r_{ij}\}}{\Pr\{e_{ij} = -1/r_{ij}\}}\right) \qquad i = 1,2,...n \text{ and } j = 1,2,...m. \qquad (7.5)$$

The Expansion of (7.5) depends on the constellation scheme in use.

Having calculated the LLR values, a hard decision Y^{0} of the transmitted signal is found using the sign of the LLR values for each received bit:

$$Y^{o} = \begin{bmatrix} y_{11} & y_{12} & \cdots & y_{1m} & y_{21} & \cdots & y_{nm} \end{bmatrix} \qquad (7.6)$$

and
$$y_{ij} = \begin{cases} +1 & \text{if } LLR(e_{ij}) \geq 0 \\ -1 & \text{if } LLR(e_{ij}) < 0 \end{cases}. \qquad (7.7)$$

The optimum decoding method for the linear code is the maximum likelihood (ML) rule defined in (7.8),

$$D = C^{l} \text{ if } \Pr(E = C^{l}|R) > \Pr(E = C^{g}|R) \; \forall l \neq g , \qquad (7.8)$$

where C^{l} is the lth codeword of code ϕ used for the encoding of either the rows or the columns of the product code (i.e. φ^{1} or φ^{2}), and is expressed as in (7.9)

$$C^{l} = \begin{bmatrix} c_{11}^{l} & c_{12}^{l} & \cdots & c_{1m}^{l} & c_{21}^{l} & \cdots & c_{nm}^{l} \end{bmatrix}. \qquad (7.9)$$

The decision D can be written in a similar manner as:

$$D = \begin{bmatrix} d_{11} & d_{12} & \cdots & d_{1m} & d_{21} & \cdots & d_{nm} \end{bmatrix}. \qquad (7.10)$$

Equation (7.8) can be rewritten using the Euclidean distance metric between R and the codeword members of code ϕ. That is:

$$D = C^l \text{ if } \left|R - C^l\right|^2 < \left|R - C^g\right|^2 \quad \forall l \neq g, \tag{7.11}$$

where the Euclidean distance between R and a codeword C^l can be found by (7.12),

$$\left|R - C^i\right|^2 = \sum_{i=1}^{n}\sum_{j=1}^{m}(r_{ij} - c_{ij}^i)^2. \tag{7.12}$$

In a ML decoder, the search for the nearest code among all the q^k possible code words in φ introduces prohibitive complexity to the system implementation. Driven by the aim of reducing the complexity of the ML decoder, the Chase algorithm was introduced [3] as a flexible decoding technique that takes advantage of the low complexity of algebraic decoders and the optimal performance of the ML decoder. The idea behind it is to extend the correction capability of the conventional algebraic decoder by increasing the viewing range of the decoder using the following steps:

- Decode the hard decision on R (i.e. Y^0) using algebraic decoder to get the initial codeword estimate C^0.

- Find the p least reliable binary symbols in R and mask them (flip their values from +1 to -1 and vice versa) to obtain $2^p - 1$ new words denoted by Y^l, $l = 1,2,...2^p - 1$.

- Decode each of Y^l to get a new codeword candidate C^l (instead of having only one using the conventional decoder). The new subset C contains 2^p candidate codewords including the initial estimate C^0. Notice that some codewords may be repeated in the set.

- The Euclidean distance metric is then used to find the nearest code word in C to the received word R. This will also be called $C^{\min(b)}$ as it represents the codeword with minimum distance to R among all codes in C, where b is described later.

The next step is to extract the extrinsic information to update the soft input for the following decoding iteration, which is the heart of the turbo concept. To achieve this, first the reliability of each decoded bit is calculated using the LLR of each element of D based on R, defined by:

$$LLR_{ij} = \ln \frac{\Pr\{e_{ij} = +1/R\}}{\Pr\{e_{ij} = -1/R\}}, \qquad (7.13)$$

which was shown in [62] to simplify after expansion, normalisation and approximation to:

$$r'_{ij} = \frac{\sigma^2}{2} LLR_{ij} = r_{jf} + w_{ij}, \qquad (7.14)$$

where w_{ij} is the extrinsic information needed to update the soft input going into the BTC decoder in the next decoding iteration.

The value r'_{ij} has been given in [62] as:

$$r'_{ij} = \frac{M^{\min(-b)} - M^{\min(b)}}{4} \cdot c_{ij}^{\min(b)}, \qquad (7.15)$$

where for each symbol (bit) in the codeword $C^{\min(b)}$, $M^{\min(b)}$ represents the Euclidean distance between R and $C^{\min(b)}$, and $M^{\min(-b)}$ represents the Euclidean distance

between R and the codeword $C^{\min(-b)}$, which is the next closest codeword in subset

C with the bit value in position ij opposite to that in codeword $C^{\min(b)}$. $c_{ij}^{\min(b)}$ is the

binary element of the codeword $C^{\min(b)}$ at position ij. If $C^{\min(-b)}$ cannot be found in

C, then r'_{ij} is defined as:

$$r'_{ij} = \beta \cdot c_{ij}^{\min(b)}, \tag{7.16}$$

where β is a weighting factor that can either be set as an increasing constant or

approximated as the following LLR [90]:

$$\beta \approx \ln\left(\frac{\Pr\{d_{ij} = e_{ij}\}}{\Pr\{d_{ij} \neq e_{ij}\}}\right). \tag{7.17}$$

After getting r'_{ij}, w_{ij} is calculated for each binary element in the codeword using

(7.14). From there, elements of R can be updated using the equation:

$$r_{ij}(2) = r_{ij} + \alpha(2) \cdot w_{ij}(2), \tag{7.18}$$

where the number 2 refers to the second decoding iteration, and α is another

weighting factor that is meant to reduce the dependency on w_{ij} at early stages of the

decoding process when its values are not reliable enough to make decisions.

The algorithm described above and summarised in figure (7.2) is the common method

of decoding BTCs, both binary and non-binary .In respect of the non-binary codes, the

algorithm represents the non-binary code by a set of binary components, which is not

consistent with the non-binary structure of those codes. Our hypothesis is that by

creating an algorithm which treats the components of a non-binary code as non-binary

symbols, an improvement of performance is expected. Besides, the described algorithm requires mapping to be Grey coded. By working at the symbol level instead of the bit level this constraint is removed and the system will be free to use any mapping constellation. This is especially useful for QAM constellations which cannot be Grey mapped and other arbitrary constellations which enhance power efficiency and PAPR effects.

In the next section we introduce a novel algorithm to decode non-binary product codes iteratively with all the signal processing applied to non-binary symbols instead of binary bits. This algorithm is independent from the binary representation of symbols as well as their locations on the mapping constellation.
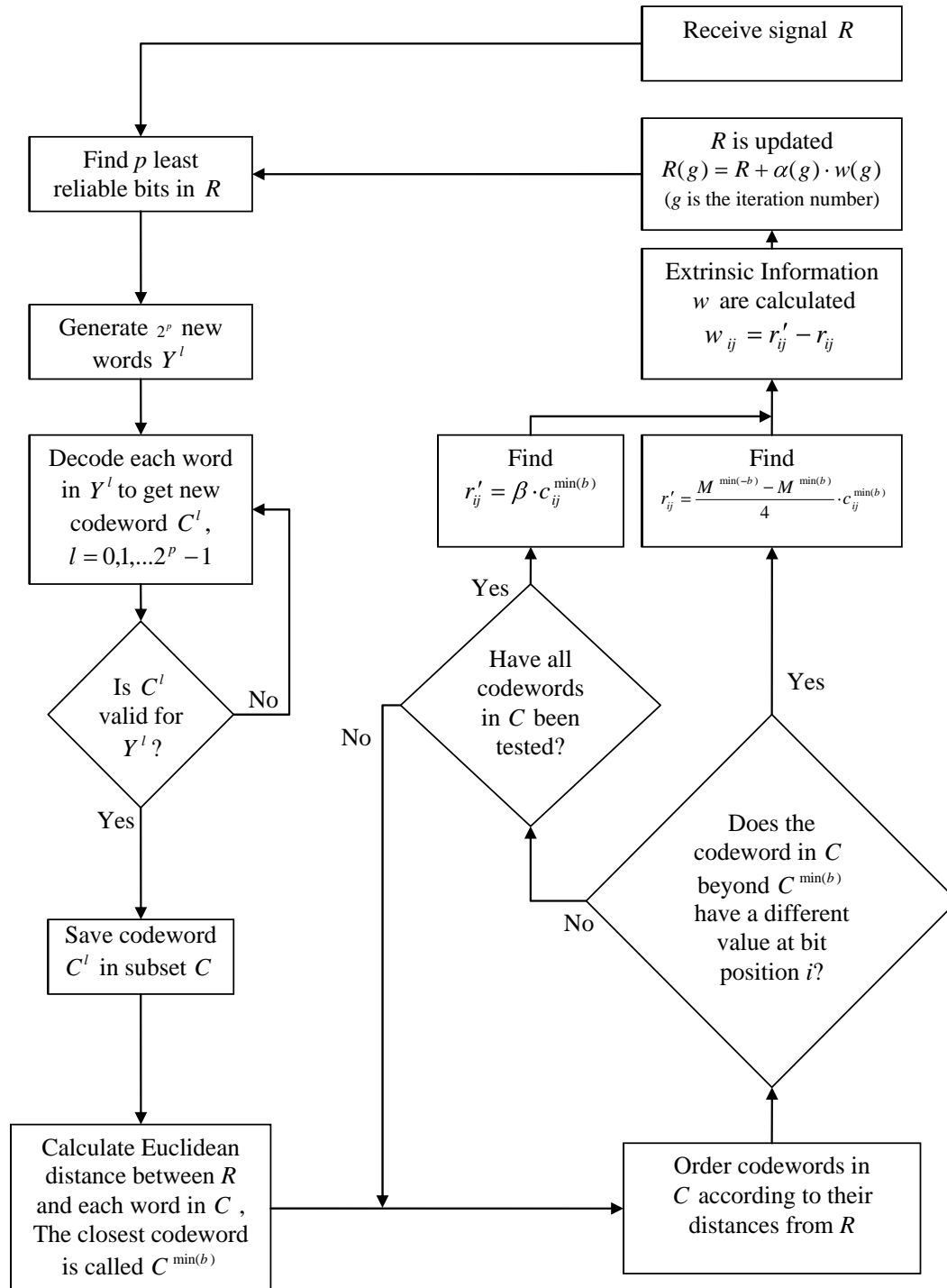
Figure 7.2   The Binary Chase-based BTC Decoding Process

7.3   Symbol-Level Chase Algorithm for Non-Binary BTC Codes

In this new algorithm, the transmitter and receiver do not use any binary representation of the code. The investigation has been limited such that the length n of the row (or column) codeword corresponds to the number of points in the modulation constellation. For example, with a 16QAM constellation a value of $n = 16$ is used.

In the study a RS code is used for the non-binary code. The output of the RS encoder (i.e. one row or column of the product code) is denoted by:

$$E = \begin{bmatrix} e_1 & e_2 & \cdots & \cdots & e_n \end{bmatrix}, \tag{7.19}$$

where e_i is an element of the codeword that belongs to the non-binary finite field. At the receiver, R can be represented as in (7.20):

$$R = \begin{bmatrix} r_1 & r_2 & \cdots & \cdots & r_n \end{bmatrix}. \tag{7.20}$$

The first data recovery step is to demap R using the ML algorithm in (7.21) to obtain a hard decision Y^o based on R.

$$y_i^0 = s_k \quad if \ \left| r_i - s_k \right|^2 < \left| r_i - s_l \right|^2 \quad \forall i, k, l \in [1, n], i \neq k. \tag{7.21}$$

In (7.21) s_k is the k-th symbol of the mapping constellation.

The Euclidean distance metric $M_{ik} = \left| r_i - s_k \right|^2$ is saved for all $i = 1, 2, \ldots, n$ and $k = 1, 2, \ldots, n$ (i.e. for all constellation points and for each symbol in R), resulting in the matrix M described by (7.22):

$$M = \begin{bmatrix} M_{11} & M_{12} & \cdots & \cdots & M_{1n} \\ M_{21} & \ddots & & & \vdots \\ \vdots & & \ddots & & \vdots \\ \vdots & & & \ddots & \vdots \\ M_{n1} & \cdots & \cdots & \cdots & M_{nn} \end{bmatrix}, \qquad (7.22)$$

where M_{ik} is the Euclidean distance between the received symbol r_i and the

constellation point s_k. The constellation point corresponding to the hard decision y_i^o

for r_i will have the minimal corresponding value in the i-th row of M.

Having calculated the hard decision Y_0 and the Euclidean distance for all available

constellation points, the algorithm searches for the least reliable symbol within each

received codeword. The procedure can differ according to the mapping scheme in use

and the nature of the channel applied. For example, for a QAM constellation in an

AWGN channel it was shown in [91] that a reliability metric can be derived from the

maximum among the Euclidean distances in both dimensions, the real and imaginary,

between the hard decision and the received signal r_i for any given symbol. This is

expressed in (7.23) where q_i is the reliability of the i-th:

$$q_i = \max\left(\mathrm{Re}\left|r_i - y_i^0\right|^2, \mathrm{Im}\left|r_i - y_i^0\right|^2\right) \quad i = 1, 2, \ldots n. \qquad (7.23)$$

A large q_i means a low confidence for symbol y_i^0. Recalling the original Chase

algorithm, the process of expanding the decoding to a subset of words besides Y^0 can

be summarized, with symbol-processing borne in mind, as follows:

Decode the hard decision Y^0 to get the codeword C^0.

Find the p least reliable symbols (i.e. those with largest values of q_i).

For each of the p symbols find the next closest constellation point (i.e. the point that has the second lowest value in the i-th row of M). An error pattern is then created by replacing the low-reliability symbol by the next closest symbol. More error patterns can be generated by considering more competing symbols to replace each of the p least reliable symbols, one at a time. However, this would be at the cost of increasing the system's complexity and processing delay. If f alternatives are considered for each of the p symbols, $f^p - 1$ new error patterns are generated and each can be denoted Y^l, where $l = 1, 2, \ldots f^p - 1$.

Each word Y^l is decoded to get a subset C with f^p candidate codewords instead of having a single codeword C^0. The Euclidean distance metric is then used to find the nearest codeword in C to the received word R. A decision D is made and is also called $C^{\min(s)}$.

The next step in the original Chase algorithm for binary codewords was to measure the reliability of each bit in the decoded word $C^{\min(b)}$ based on the Euclidean distance between the codeword and the next closest codeword $C^{\min(-b)}$ in the subset C with the bit value at position ij inverted from that in $C^{\min(b)}$ for all $i = 1, 2, \ldots n$ and $j = 1, 2, \ldots m$. In the new algorithm we would instead be looking for the codeword in the subset C in which the symbol at position i differ from that in $C^{\min(s)}$ (notice that there are n-1 possible values). The codeword that satisfies the latter condition is denoted $C^{\min(\neq s)}$.
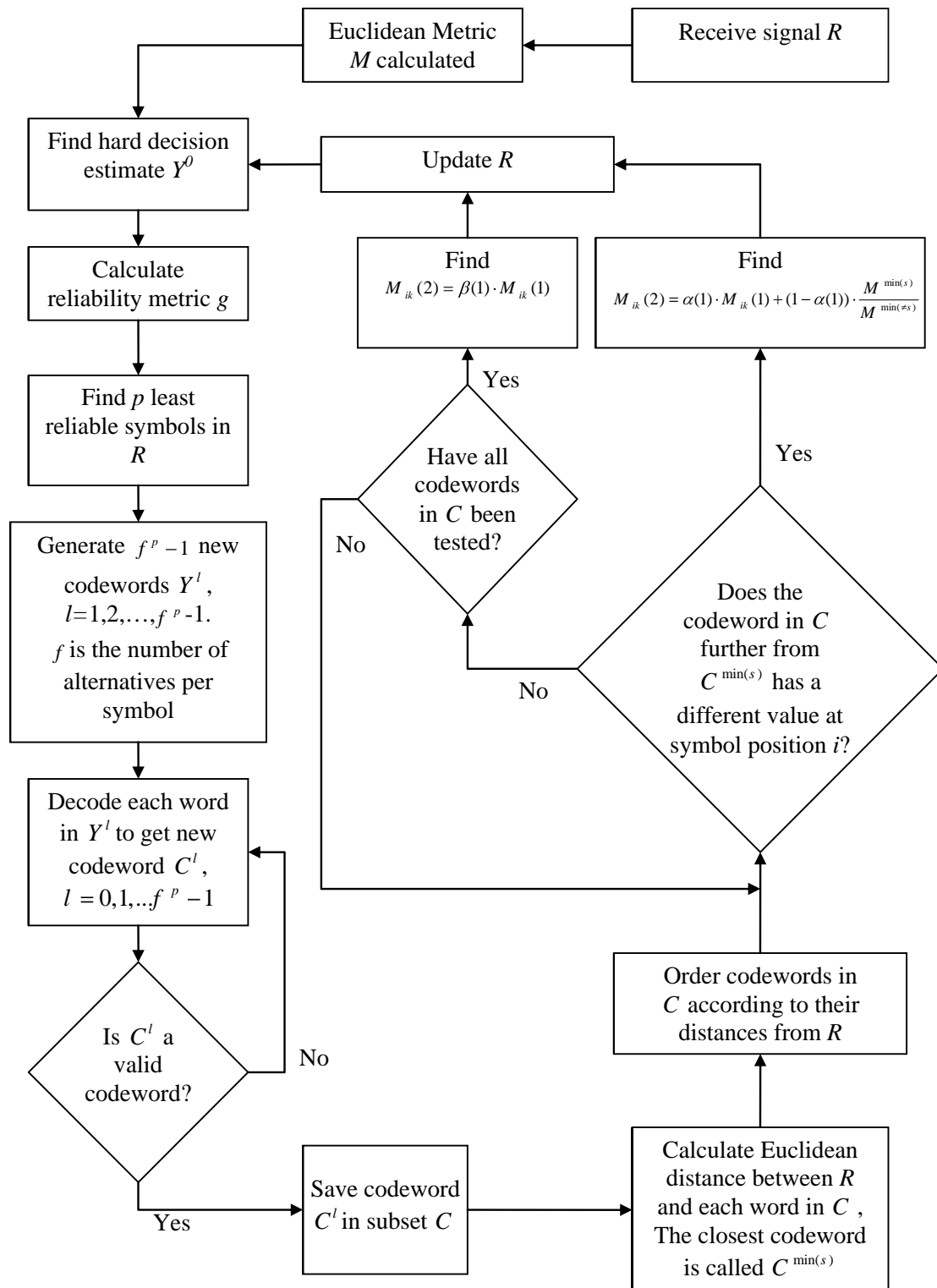
Figure 7.3   The Non-Binary Chase-based BTC Decoding Process

The reliability metric M_{ik} corresponding to the i-th symbol of $C^{\min(s)}$ is then updated using:

$$M_{ij}(2) = \alpha(1) \cdot M_{ij}(2) + (1 - \alpha(1)) \cdot \frac{M^{\min(s)}}{M^{\min(\neq s)}},\qquad(7.24)$$

where for each symbol in the codeword $C^{\min(s)}$, $M^{\min(s)}$ represents the Euclidean distance between R and $C^{\min(s)}$ (i.e. D), and $M^{\min(\neq s)}$ represents the Euclidean distance between R and the codeword $C^{\min(\neq s)}$, which is the next closest code word in subset C with a value at position i different from that in codeword $C^{\min(s)}$. α is a weighting factor that is meant to reduce the dependency at early decoding iterations.

If $C^{\min(\neq s)}$ cannot be found, M_{ik} is updated by:

$$M_{ik}(2) = \beta(1) \cdot M_{ik}(1),\qquad(7.25)$$

where β is a weighting factor similar to the one described in section 7.2. The updating of the M matrix implies updating the values of R as well. A second iteration begins by updating the hard decision Y^0 and the values of q_i based on the new R.

7.4   Simulation Results and Analysis

7.4.1   Block Turbo Codes versus Convolutional Turbo Codes

The performance of the bit-level Chase BTC is studied and compared with that of a comparable Convolutional Turbo Code (CTC). The simulation platform is based on an OFDM system with an AWGN channel and Rayleigh fading. Independent channel

fading is assumed among OFDM subcarriers and the guard interval is assumed to be longer than the delay spread of the channel resulting in full elimination of ISI and ICI.

The BTC code in use is based on a Reed Solomon Code with parameters (15,11,2) resulting in the Product code $(15,11,2)^2$ with code rate $r = (11)^2 / (15)^2 \cong 0.54$. On the other hand the Convolutional Turbo Code is a punctured code with $r = 0.5$. 4 decoding iterations are used for both the BTC and CTC. Each iteration of the BTC decoding involves a row and column iteration. The Simulation parameters are summarized in table (7.1).

Table 7.1   CTC vs. BTC simulation parameters

	CTC	BTC
Code parameters	g0=13 and g1=15 Max-Log-MAP	RS $(15,11,2)^2$
Code Rate	0.5	0.54
Mapping Scheme	Gray-Coded 16QAM	
No. of Iterations	4 iterations	4 iterations (4 column + 4 row)
Block Length	900 coded bits	
Channel	AWGN (Figure 4) Rayleigh Fading Channel (Figure 5)	

Figure (7.4) presents the BER and PER performances of both CTC and BTC in an AWGN channel. The graphs demonstrate that CTC outperforms BTC by about 2.5dB. CTC converges to an error floor around BER=10^{-6} and PER=10^{-4} while the BTC does not show any sign of converging to an error floor within the investigated E_b / N_0 range.
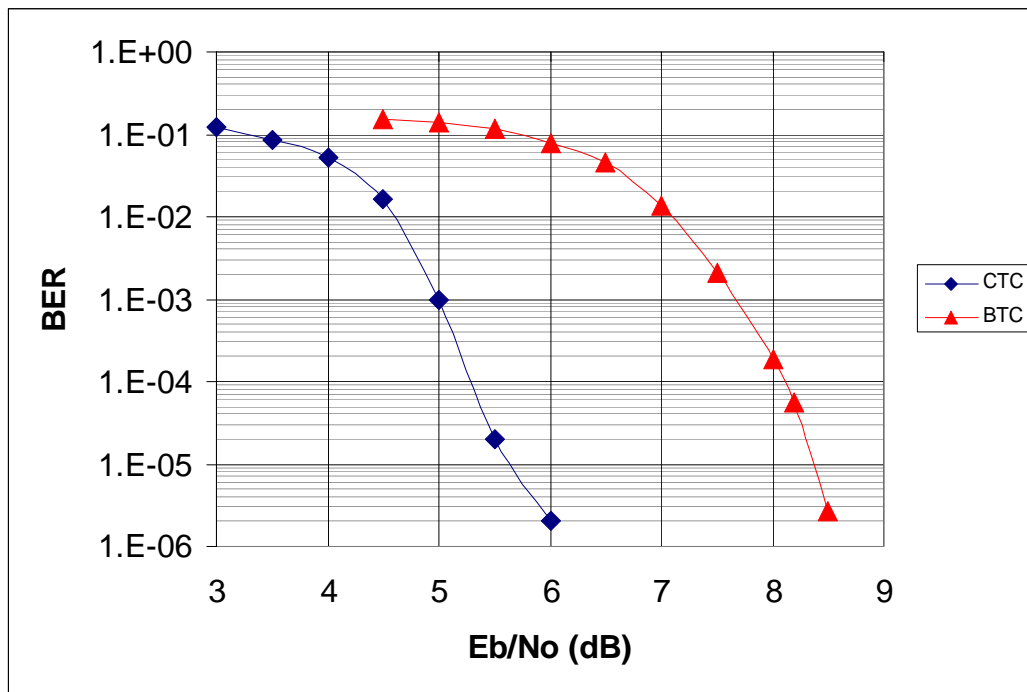
(a)
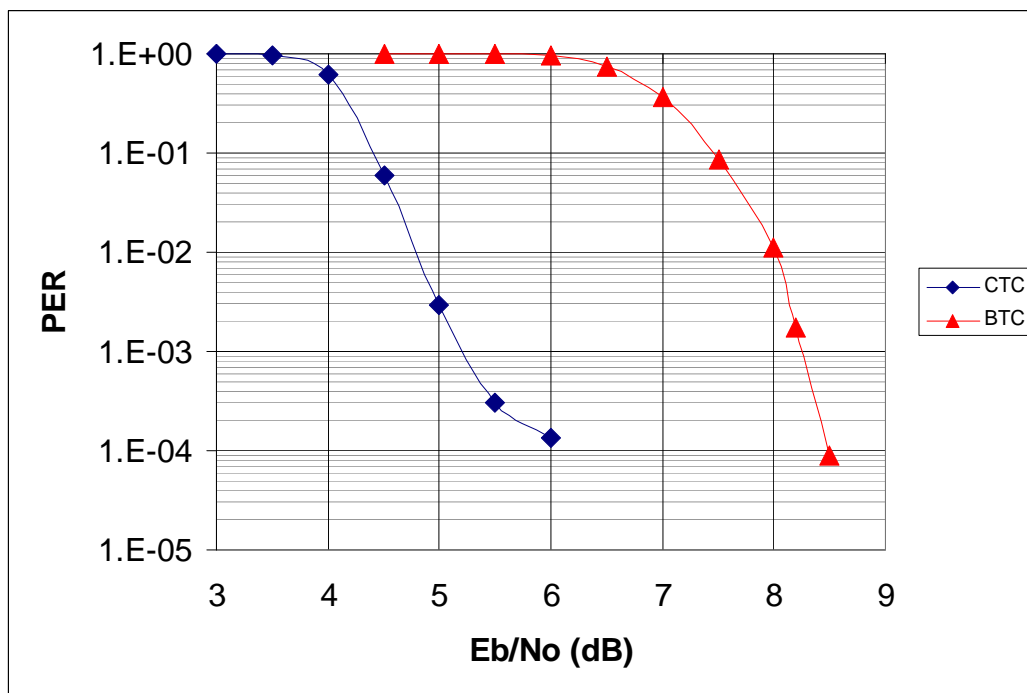
(b)

Figure 7.4   BER & PER performances of BTC and CTC in an AWGN Channel with 16QAM and 4 decoding iterations [Parameters as in table 7.1]
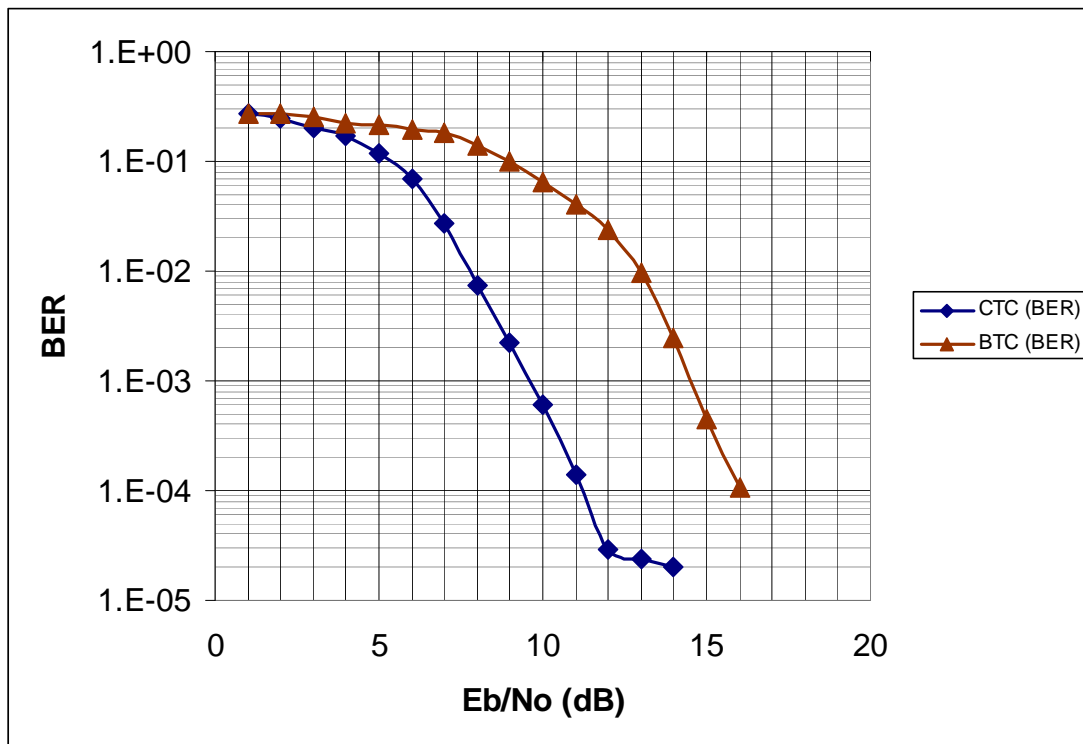
(a)
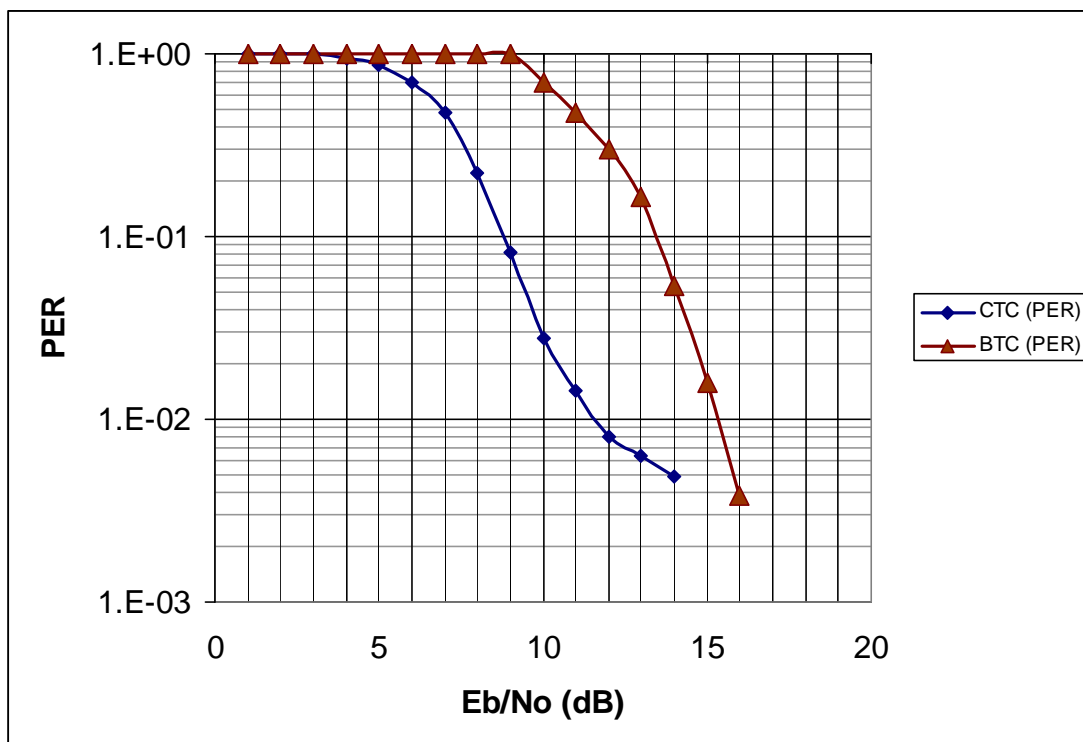
(b)

Figure 7.5   BER & PER performances of BTC and CTC in a Rayleigh Fading Channel with 16QAM and 4 decoding iterations [Parameters as in table 7.1]

The results for a Rayleigh fading channel are depicted for the two systems in figure (7.5). It can be seen that CTC performs significantly better than BTC at low signal-to-noise ratio values. However, CTC still incurs from an error floor for values of $E_b / N_0 > 12$dB. On the other hand, BTC remains reducible with increasing E_b / N_0, until it gets to an intersection point after which BTC outperforms CTC. This performance trend suggests that BTC can be a strong candidate for applications where high signal-to-noise ratios are expected and where the system is required to boost its performance to its maximum capability.

7.4.2   Binary Chase Algorithm vs. Non-binary Chase Algorithm for BTC

The previous results in section (7.4.1) motivate a study of the BTC with non-binary codes and high constellation orders. The original Chase algorithm is now compared with the modified Chase algorithm for non-Binary codes. To set a benchmark both systems' performance is studied with a Grey-coded 8PSK modulation scheme. Because 8PSK is a Grey coded constellation, the condition of the binary Chase algorithm is still met. However 8PSK is more sensitive to bit changes compared to other Grey coded constellations. Therefore, the studying of 8PSK helps expose the weaknesses of the binary Chase decoding algorithm when it is applied to non-binary codeds. A RS (7,4) code is used for the comparison and an AWGN channel is applied on the signal. The parameters of the computer simulation are summarised in table (7.2).

Table 7.2   BTC system parameters (8PSK)

	BTC
Code parameters	RS $(7,4)^2$
Code Rate	0.33
Mapping Scheme	Gray-Coded 8PSK
No. of Iterations	2 and 4 iterations
Channel	AWGN

Figure (7.6) shows the BER and PER performance of both algorithms. The Non-Binary Chase algorithm shows slightly better performance compared to the original binary Chase algorithm. In an 8PSK constellation, one bit change will result in a shift from constellation point to a neighbour point. However when more than one bit changes, the shift becomes large and not directly related to the number of bit changes. On the other hand, the symbol-level Chase decoding algorithm treats the non-binary symbols as they are ensuring that the decoding process will only involve symbols that are close to the received symbol in the constellation. This explains the better performance of the symbol-level decoding algorithm.

One step further would be to give the original Chase algorithm the advantage of using a stronger Grey-coded QAM modulation such as 16QAM, in which bit changes result in smalls shifts in the constellation compared to 8PSK. For this case a RS $(15,11)^2$ code is used with a 16QAM modulation to fit the code length. The simulation parameters are summarised in table (7.3), and the performance of both algorithms is depicted in figure (7.7) for BER and PER measures.

Table 7.3   BTC system parameters (16QAM)

	BTC
Code parameters	RS $(15,11)^2$
Code Rate	0.54
Mapping Scheme	Gray-Coded 16QAM
No. of Iterations	4 iterations
Channel	AWGN

The Non-binary Chase algorithm continues to show better performance than the binary case but the SNR gain is less than in 8PSK. This confirms our expectations with regards to 16QAM being beneficial to the conventional bit-level Chase algorithm.
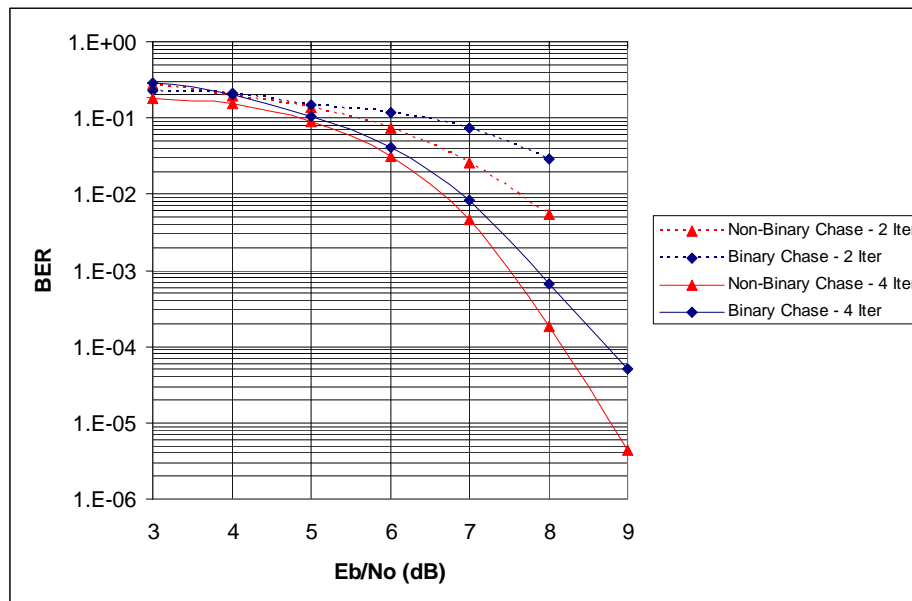
(a)
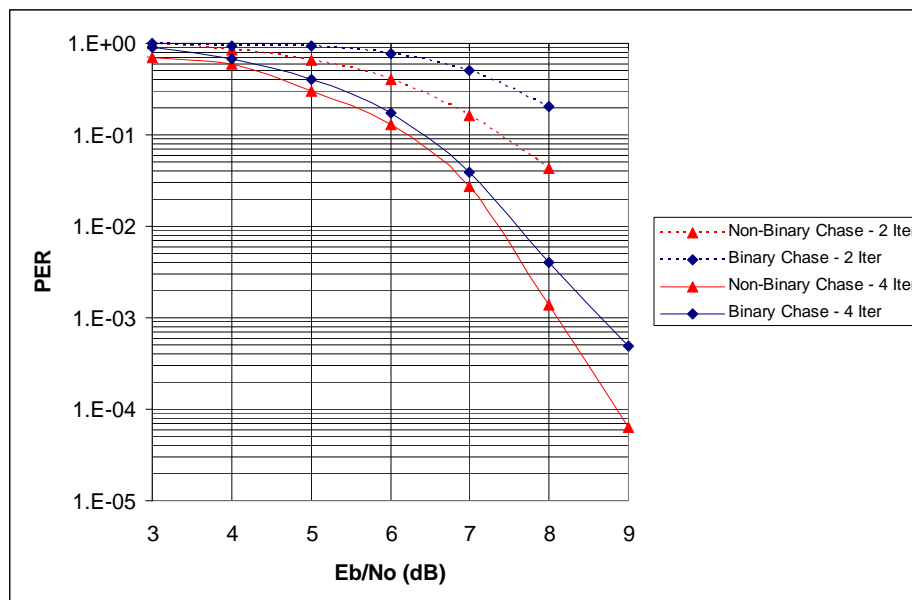
(b)

Figure 7.6   BER & PER performances of Binary-Chase and Non-binary Chase based BTC in an AWGN Channel with 8PSK and 2 and 4 decoding iterations [Parameters as in table 7.2]

171
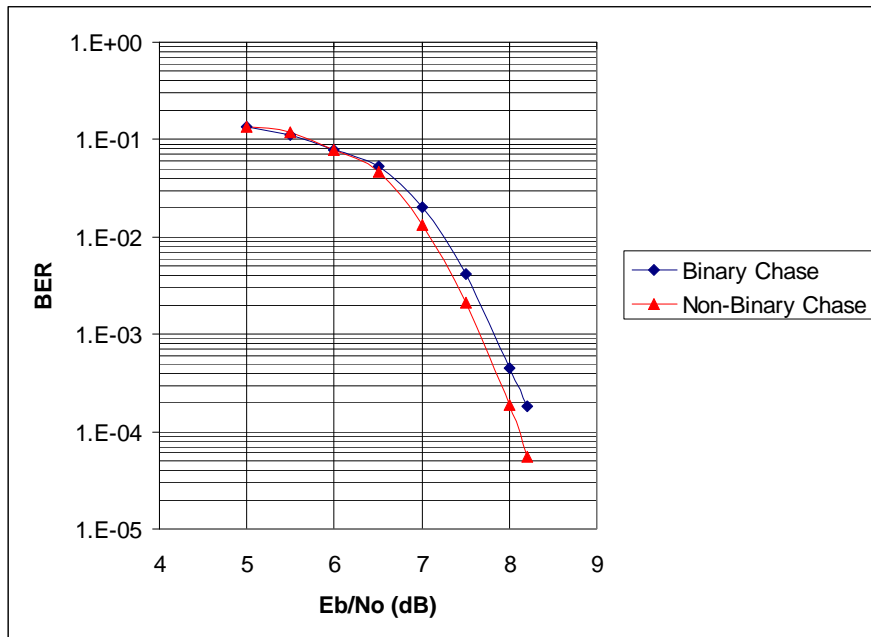
(a)
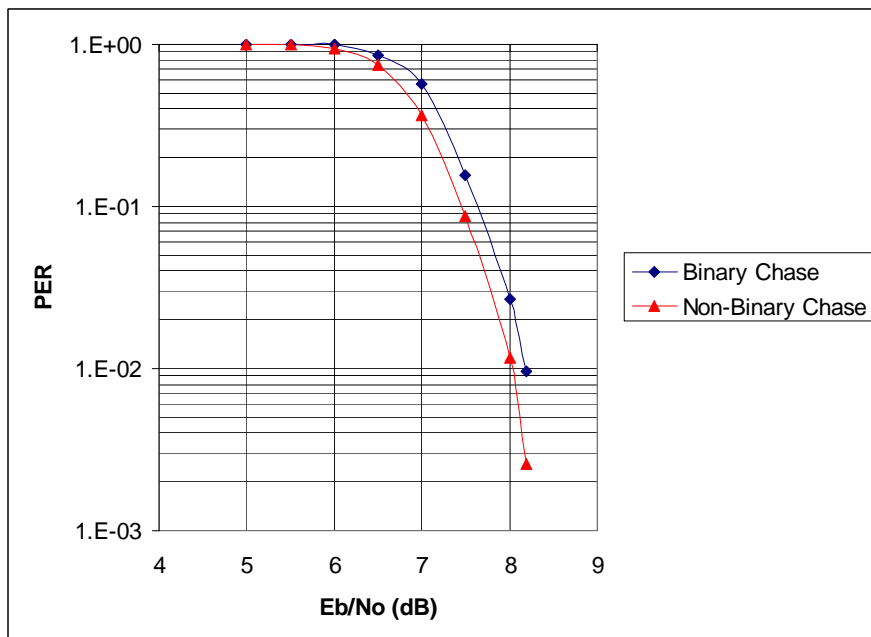
(b)

Figure 7.7   BER & PER performances of Binary-Chase and Non-binary Chase based BTC in an AWGN Channel with Gray-coded 16QAM and 4 decoding iterations [Parameters as in table 7.3]

The systems were evaluated without Grey coding, which corresponds to a full non-binary mapping of the constellations. In this experiment the same RS (15,11) code is used with a randomly distributed 16QAM constellation instead of the Grey coded QAM. The random distribution remains fixed for the whole length of the packet. Simulation configurations are listed in table (7.4). The AWGN channel results are depicted in figure (7.8) for BER and PER performances.

Table 7.4   BTC system parameters (Non-Grey 16QAM)

	BTC
Code parameters	RS $(15,11)^2$
Code Rate	0.54
Mapping Scheme	Randomly distributed 16QAM
No. of Iterations	4 iterations
Channel	AWGN

Once the Grey coding is removed the performance of the original Chase algorithm deteriorates badly while the performance of the modified algorithm is hardly affected by the distribution of the constellation points. In Grey mapping, the Euclidean distance and bit changes are correlated up to some degree (i.e. a single bit change should correspond to a small Euclidean distance shift while many bit changes should correspond to large shifts). Without Grey mapping, the Euclidean distances and the bit changes are no longer tightly correlated. The bit-level Chase algorithm becomes of no use in this case. On the other hand, as the proposed symbol-level Chase algorithm does not require Grey coding, it maintains the same performance regardless of the mapping constellation.

(a)
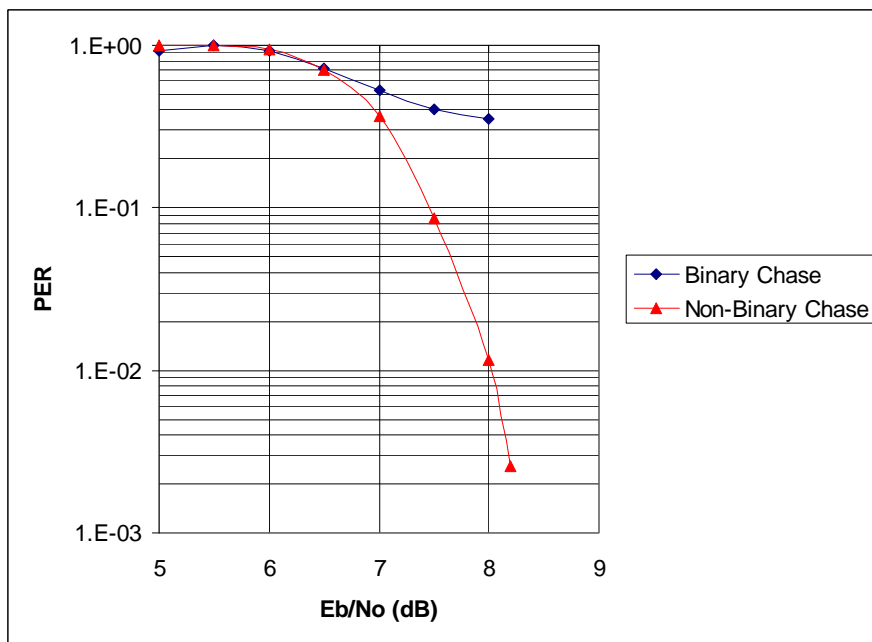
(b)

Figure 7.8   BER & PER performances of Binary-Chase and Non-binary Chase based BTC in an AWGN Channel with randomly distributed 16QAM and 4 decoding iterations [Parameters as in table 7.4]

174

7.5   Conclusions

In this chapter we presented and studied BTC as a candidate for the channel coding in high data rate applications of an OFDM system. Although BTC does not perform as good as CTC in low ranges of E_b / N_0, it has the advan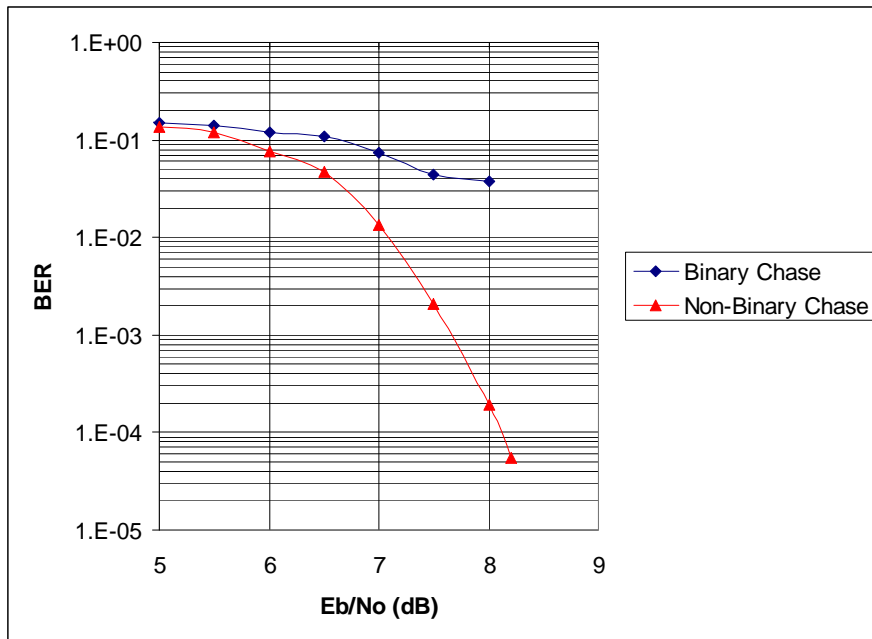tage of not suffering from an error floor for both the BER and ER performances. This allows continuous improvement of the BTC aided system at high signal levels.

Additionally, a novel non-binary Chase-based BTC decoding algorithm was proposed that treats the elements of non-binary codes as symbols not bit, which is more consistent with the nature of non-binary codes. Moreover the proposed algorithm removes the requirement for a binary Grey mapping originally required by the conventional BTC decoding algorithm. We showed through the computer simulation results that the new algorithm slightly outperforms the conventional algorithm when those constraints are respected. When the Grey coding conditions is breached the new algorithm is not affected while the performance of the original algorithm deteriorates.

Whilst the proposed algorithm takes the BTC decoding algorithms a step forward, there remain a number of unresolved issues which should be subject to future investigation and research. For instance, the new algorithm is limited to code lengths equal to the number of mapping constellation points. This limitation can be overcome via additional research on constellations in which one point can take different values of the non-binary code symbols.

This is the last part of the conducted research in this thesis. The next chapter concludes the thesis, points out some limitations and suggests suitable topics for future research.

Chapter 8
Conclusions and Future Work

The research carried out in this thesis aimed to investigate different multiple access, MUD and channel coding methods based on multicarrier modulation which have been proposed in the literature as a potential candidate for the air interface of the fourth generation of wireless communication systems. Two multiple access schemes, MC-DS-CDMA (representing time domain spreading) and MC-CDMA (representing frequency domain spreading), were studied individually and then compared in terms of their performances with different configurations. A simplified Chase-based Near-ML MUD method was developed for MC-CDMA. Finally, a new symbol-level Chase-based algorithm was presented for the decoding of BTC with application to OFDM.

This chapter presents the main conclusions of the work, points out some limitations, and suggests suitable topics for future work.

8.1   Conclusions

In Chapter 3 we were concerned with the performance trends of MC-DS-CDMA. Our results suggested that MC-DS-CDMA generally lacks enough diversity that would help to recover the information transmitted on severely faded subcarriers. When the issue of diversity is resolved with the assistance of multiple receive antennas, the system's performance is boosted by over 8dBs for the uncoded system. The introduction of channel coding offers a further 6dB improvement for the non-iterative channel decoder with the potential of additional enhancement when the decoding is iterated (5dB improvement with 6 decoding iterations). The performance of MC-DS-CDMA with multiple transmit antennas is always inferior to that for multiple receive antennas for the same total transmitted power, with the gap between the two performances becoming wider with more decoding iterations. Moreover, MC-DS-CDMA maintains the same performance in a single cell environment whether it is heavily or lightly loaded in an ideal regime where ISI and ICI do not exist.

As for the multi-cell environment, the performance of MC-DS-CDMA degrades gradually with the increase of inter-cell interference. MC-DS-CDMA is also capable of achieving BER$=10^{-3}$ and PER$=10^{-2}$ at the edge of two fully loaded cells with low modulation orders and code rates. Besides, there exist areas of overlapping performances between different modulation and coding combinations. For instance, a lightly loaded 16QAM system can perform better than a fully loaded QPSK system for the same code rate. This highlights the possibility of achieving a similar or higher efficiency by switching to higher modulation orders beyond certain loading factors.

The performance of MC-CDMA was the body of investigation derived in Chapter 4. Three SUD strategies, EGC, ORC and MRC, were compared for MC-CDMA in a

single cell environment. The results showed significant changes in the differences between the three strategies when the correlation between the subcarriers' fading is set as a variable. When the channel taps are highly correlated the performances of all three methods are relatively close and generally weak. On the other hand, when there is little or no correlation between subcarriers the performances of EGC, MRC and ORC become more sensitive to the loading factor of the system, and the span between the single user and full load performances becomes much larger compared with the high correlation case. Regardless of the channel correlation, EGC always performs better than the other two combining techniques when the system is fully loaded (a gain of more than 10dB was observed for EGC over the other two methods in a highly frequency selective channel). In the single user case, MRC offers the best performance for MC-CDMA with marginal differences from EGC (0.2dB gain for MRC at BER=10^{-3}). Therefore, these results suggest that EGC is the best choice amongst the three strategies if good performance is expected no matter what the system's load is.

The investigation in Chapter 4 also found that in a single cell environment MC-CDMA can maintain a fixed small difference (0.5-0.7dB from our results) between the single and full load performances when the system is aided by channel coding, multiple receive antennas (SIMO) and MMSE MUD. Although a SIMO system is superior to a MISO system when SNR is low, both systems converge to similar performance at higher SNRs. A number of results that cover the performance trends of MC-CDMA with turbo coding and multiple antennas were also presented in the chapter.

In a multi-cell environment, the performance of MC-CDMA degrades gradually with the increase of inter-cell interference. The results demonstrated that, unlike the observations in the case of MC-DS-CDMA, there is no overlapping between the performances of different coding/modulation combinations. For example, a single user 16QAM system with code rate $R = 1/2$ is better than a fully loaded QPSK with $R = 1/3$. Furthermore, irreducible error floors start appearing in the performance of MC-CDMA beyond a load factor $L = 0.5$ (half load) due to high MAI and inter-cell interference.

The performance of both MC-DS-CDMA and MC-CDMA were compared in Chapter 5. In a configuration where neither system is supported by error correction tools or multiple antennas, MC-CDMA outperforms MC-DS-CDMA. This superiority of MC-CDMA becomes less consistent when one or more of those aiding features are introduced to both systems. In other words, the SNR splits into at least two regions; one where MC-CDMA performs better and the other where MC-DS-CDMA performs better. The latter becomes more obvious when the system is strengthened by more error correction and diversity enhancement. For example, when both systems use turbo coding with 6 iterations and SIMO antennas, MC-DS-CDMA performance becomes similar to the single user (i.e. best case) performance of MC-CDMA.

Our results for the multi-cell environment were similar in their trends with the findings from the single cell performances. With the existence of two performance extremes for MC-DS-CDMA in a multi-cell scenario (i.e. single user and full load), new observations were noticed in regards to the relative behaviours of the two systems. When more error coding/modulation combinations are used (e.g. QPSK and $R = 1/3$) MC-CDMA offers the best case MRC performance at light loads. It becomes,

however, more affected by MAI and inter-cell interference when the load factors increase for both the serving and interfering cells. On the other hand, when the immunity of the system is sacrificed for the sake of higher bit efficiency (e.g. by using 16QAM and $R = 1/2$), MC-DS-CDMA performs better than MC-CDMA for all load factors. This advantage of MC-DS-CDMA changes from marginal gain with QPSK modulation to about 3dB gain with 16QAM modulation.

We also provided a generic theoretical discussion about MC-DS-CDMA and MC-CDMA that, we believe, should help to better understand the different approaches of applying time and frequency spreading to multicarrier systems.

In Chapter 6 we proposed a novel simplified near-ML MUD algorithm for MC-CDMA based on the Chase algorithm. When compared with the performance of OFDM our algorithm worked better than OFDM in an uncoded system and just 0.4dB worse than OFDM when binary convolutional channel coding is employed. Furthermore, a gain of 1dB to 4dB was achieved over the non-MUD performance depending on the spreading factor and the size of error patterns. The proposed algorithm is not affected by increased MAI when the fading across subcarriers is less correlated. In fact, the less the correlation the better the performance of the new algorithm becomes. This is because of the availability of more frequency diversity to exploit when the subcarriers are less correlated.

Finally, in Chapter 7 we introduced a new algorithm to iteratively decode non-binary BTC at the symbol level unlike the conventional algorithm which requires a codeword to be represented by binary components before being decoded. Our proposed algorithm integrates more appropriately with non-binary BTC and was found to enhance their performance. Moreover, the algorithm makes it possible to employ

arbitrary constellations even if they are not Grey coded. The results in an OFDM system demonstrated that the new algorithm performs better than the original binary Chase algorithm under all conditions even when all constraints of the conventional bit-level algorithm are implemented. A 0.5 dB gain for BER=10^{-4} was achieved in an 8PSK modulated system after 4 decoding iterations. This gain depends on the modulation order and number of decoding iterations. Besides, when any of the constraints limiting the binary-level algorithm is breached (e.g. using non-Grey mapping) our proposed algorithm significantly outperforms the binary decoding algorithm. In fact, the binary algorithm fails to perform with a non-Grey mapping constellation.

8.2   Limitations of the Work and Scope for Further Research:

The major contributions made by this study included the characterisation and comparison of MC-DS-CDMA and MC-CDMA, the exploitation of the Chase algorithm to simplify the MUD of MC-CDMA, and the introduction of the symbol-level processing concept for the decoding of non-binary BTC with application to multicarrier modulation. However, certain simplifications and assumptions have been adopted in the study. This adds to the fact that because of the broad area we have been looking at and the new algorithms we developed, a single study is far beyond the full characterisation of the behaviours of the investigated algorithms and methods in diverse environments and scenarios.

Firstly, in order to achieve a fair generic characterisation of both MC-DS-CDMA and MC-CDMA it was necessary to make the following assumptions and simplifications:

- Perfect knowledge of the channel state information was assumed
- Perfect time and frequency synchronisations were assumed.

- The guard interval was taken to be always larger than the delay spread of the channel.

- The effects of PAPR were ignored.

- All users were assumed to be sent signals of equal power regardless of their distances from the base station.

In addition to the assumptions above, the following assumptions were adopted in regard to the multi-cell performance:

- No mobility was considered, and therefore the effect of fast fading was not looked at.

- Uniform user distribution in adjacent cells was assumed.

- No sectorisation was considered and the user at the edge of the cell was assumed to receive equal power signals from both the serving and interfering cells.

- No macro diversity at cell boundaries was considered.

In this context, we have to say that our study's focus was mainly on the single cell behaviour of the two investigated systems, and our aim from devoting part of our study to multi-cell investigation was to have a "flavour" of the relative performance trends of both systems in such environments rather than having a deep understanding of their behaviours in those environments. The association of those factors ignored or assumed perfect by us is required to be investigated in future studies before we can have strong appreciable understanding of the behaviour of both MC-DS-CDMA and MC-CDMA compared with each other. Besides, the dimensions of both MC systems were fixed throughout the study. Investigating MC-DS-CDMA and MC-CDMA with

different dimensions that would aim to exploit certain features of the system or channel would help to better understand their strengths and weaknesses.

Furthermore, our investigation was limited to convolutional turbo codes and one type of block interleavers. It would be interesting in future research to include other channel coding and interleaving methods. Our simulation also used one channel model throughout the study. It is worth evaluating the effect of different channel models on the performance of MC-DS-CDMA and MC-CDMA.

With regards to multiple antennas, the investigation was limited to the use of two antennas in either the transmitter or the receiver (but not both). Further investigation is required in the future to characterise the performance of both MC-DS-CDMA and MC-CDMA when they are aided by a real MIMO system, in which two or more antennas are used in both the transmitter and receiver.

Secondly, we mentioned in Chapter 6 that the soft input/output of the Chase-based MUD makes it possible to be investigated in future research as part of a broader joint iterative process in which both the MUD and channel decoder pass extrinsic information to each other in order to achieve better performance. Moreover, it would be interesting for future research to compare the performance of the proposed algorithm with other MUD strategies for MC-CDMA. Also, our investigation was limited to QPSK modulation and hence higher modulation orders can be investigated in the future.

Finally, the proposed symbol-level non-binary BTC decoder in Chapter 7 is limited, in its current design, to codeword lengths equal to the number of the constellation points. What is now needed is further research on BTC that would allow non-binary

symbols to be represented by smaller modulation orders. Moreover, the current reliability metric calculation method does not directly apply to multipath channels. Further development of the algorithm is required to allow the use of the algorithm with non-binary BTC codes transmitted through such channels. Our investigation considered relatively short RS codes as a representative of non-binary codes. The inclusion of longer RS codes as well as other types of non-binary block codes is highly recommended before general conclusions can be made about the symbol-level decoding of non-binary BTC. Our investigation with regards to non-Grey mapping was limited to a one-shot randomly ordered 16QAM constellation. It would be interesting for future research to investigate the performance of the symbol-level decoding algorithm with other non-Grey constellations such as 32QAM and other more power efficient constellations. Also, there is always room for further optimisation of the calculation and updating strategies of the soft values processed within the proposed algorithm.

Bibliography

[1]   A. g. F. Bauer, S. Mayrargue, J. Rodriguez, S. Zazo, M. Neos, R. Aguiar, F. Kienle, D. Pace, M. Hamon, and M. Sakamoto, "Synthesis Report of worldwide research on 4G systems," MATRICE IST-2001-32620, 2001.

[2]   R. M. Pyndiah, "Near-optimum decoding of product codes: Block turbo codes," *IEEE Transactions on Communications*, vol. 46, pp. 1003-1010, 1998.

[3]   D. Chase, "Class of algorithms for decoding block codes with channel measurement information," *IEEE Transactions on Information Theory*, vol. 18, pp. 170-182, 1972.

[4]   S. Verdu, *"Multiuser detection / Sergio Verdu"*. Cambridge University Press, 1998.

[5]   "IEEE Standard for Local and metropolitan area networks Part 16: Air Interface for Fixed and Mobile Broadband Wireless Access Systems Amendment 2: Physical and Medium Access Control Layers for Combined Fixed and Mobile Operation in Licensed Bands and Corrigendum 1," *IEEE Std 802.16e-2005 and IEEE Std 802.16-2004/Cor 1-2005 (Amendment and Corrigendum to IEEE Std 802.16-2004)*, pp. 0_1-822, 2006.

[6]   B. I. Wookbong Lee, Ronny (Yong-Ho) Kim, "Requirements for 802.16m," IEEE C802.16m-07/007, 2007.

[7]   3GPP "LTE Physical Layer - General Description (Release 8)," 3GPP TS 36.201 V1.0.0 (2007-03), 2007.

[8]   3GPP, Long Term Evolution of the 3GPP radio technology. http://www.3gpp.org/Highlights/LTE/LTE.htm, 2005 (accessed 27 September 2007).

[9]   IEEE802.20 Working Group, "System Requirements for IEEE 802.20 Mobile Broadband Wireless Access Systems - Version 14," IEEE 802.20-PD-06, 2004.

[10]   R. v. Nee, *OFDM for wireless multimedia communications / Richard van Nee, Ramjee Prasad*. Boston ; London :: Artech House, 2000.

[11]   J. H. Stott, "Explaining some of the magic of COFDM," presented at *20th International Television Symposium*, Switzerland, 1997.

[12]   S. Weinstein and P. Ebert, "Data Transmission by Frequency-Division Multiplexing Using the Discrete Fourier Transform," *IEEE Transactions on Communications*, vol. 19, pp. 628-634, 1971.

[13]   W. Y. Zou and W. Yiyan, "COFDM: an overview," *IEEE Transactions on Broadcasting*, vol. 41, pp. 1-8, 1995.

[14]   S. Hara, *Multicarrier techniques for 4G mobile communications / Shinsuke Hara, Ramjee Prasad*. Boston, MA :: Artech House, 2003.

[15]   R. Caldwell and A. Anpalagan, "Meeting mobile's demands with multicarrier systems," *IEEE Potentials*, vol. 24, pp. 27-31, 2005.

[16]   N. Maeda, H. Atarashi, and M. Sawahashi, "Performance comparison of channel interleaving methods in frequency domain for VSF-OFCDM broadband wireless access in forward link," *IEICE Transactions on Communications,* vol. E86B, pp. 300-313, 2003.

[17]   G. Caire, G. Taricco, and E. Biglieri, "Bit-interleaved coded modulation," *IEEE Transactions on Information Theory*, vol. 44, pp. 927-946, 1998.

[18] K. Tayoon, K. Jaeweon, J. G. Andrews, and T. S. Rappaport, "Multi-code multicarrier CDMA: performance analysis," *2004 IEEE International Conference on Communications*, vol. 2, pp. 973-977, 20-24 June 2004

[19] Z. Wu and C. R. Nassar, "FD-MC-CDMA: A Frequency-Based Multiple Access Architecture for High Performance Wireless Communication," *IEEE Transactions on Vehicular Technology*, vol. 54, pp. 1392-1399, 2005.

[20] S. H. Tsai, Y. P. Lin, and C. C. J. Kuo, "MAI-Free MC-CDMA Systems Based on Hadamard-Walsh Codes," *IEEE Transactions on Signal Processing*, vol. 54, pp. 3166-3179, 2006.

[21] J. M. Auffray and J. F. Helard, "Performance of multicarrier CDMA technique combined with space-time block coding over Rayleigh channel," *2002 IEEE Seventh International Symposium on Spread Spectrum Techniques and Applications*, vol. 2, pp. 348-352, 2-5 Sept. 2002

[22] T. He, N. Arumugam, and G. H. Krishna, Performance of space-time coded MC-CDMA over time and frequency selective fading channel," *2002 4th International Workshop on Mobile and Wireless Communications Network*, pp. 419-423, 2002

[23] D. Juinn-Horng, W. Jwo-Yuh, and L. Ta-Sung, " "Space-path spreading for high rate MIMO MC-CDMA systems with transmit diversity," *Global Telecommunications Conference, 2003. GLOBECOM '03. IEEE*, vol. 6, pp. 3397-3401, 1-5 Dec. 2003

[24] IST, "MATRICE - MC-CDMA Transmission Techniques for Integrated Broadband Cellular Systems," 2001.

[25] IST, "4MORE Project," 2002.

[26] L. Hanzo, L.-L. Yang, E.-L. Kuan and K. Yen, *Single- and Multi-Carrier DS-CDMA: Multi-User Detection, Space–Time Spreading, Synchronisation, Standards and Networking,* IEEE Press–Wiley, New York, 2003.

[27]   E. A. Sourour and M. Nakagawa, "Performance of orthogonal multicarrier CDMA in a multipath fading channel," *IEEE Transactions on Communications*, vol. 44, pp. 356-367, 1996.

[28]   S. Hara and R. Prasad, "Overview of multicarrier CDMA," *Communications Magazine, IEEE*, vol. 35, pp. 126-133, 1997.

[29]   Y. Lie-Liang and L. Hanzo, "Performance of generalized multicarrier DS-CDMA over Nakagami-m fading channels,"*, IEEE Transactions on Communications*, vol. 50, pp. 956-966, 2002.

[30]   H. Steendam and M. E. Moeneclaey, "The sensitivity of downlink MC-DS-CDMA to carrier frequency offsets," *Communications Letters, IEEE*, vol. 5, pp. 215-217, 2001.

[31]   H. Steendam and M. Moeneclaey, "The effect of carrier phase jitter on MC-DS-CDMA," *IEEE International Conference on Communications*, vol. 6, pp.1881-1884, 2001

[32]   C. Lingyun, X. Youyun, Z. Haibin, L. Hanwen, and S. Wentao, "Performance of SFH/MC DS-CDMA system using transmit diversity with space-time block coding," *2004 IEEE 60th Vehicular Technology Conference, 2004. VTC2004-Fall*, vol. 7, pp. 4988-4990, 26-29 Sept. 2004

[33]   L. Jianjun, F. Pingyi, and C. Zhigang, "Space time spreading in forward links of the multicarrier DS CDMA system," *ICII 2001 - Beijing. 2001 International Conferences on Info-tech and Info-net*, vol. 2, pp.285-290, 2001

[34]   B. Hu, L.-L. Yang, and L. Hanzo, "Performance of the Smart Antenna Aided Generalized Multicarrier DS-CDMA Downlink Using Both Time-Domain Spreading and Steered Space-Time Spreading," *2005 6th IEE International Conference on 3G and Beyond*, pp.1-5, 7-9 Nov. 2005

[35]   M. Dillinger, "TRUST (Transparent Re-configurable UbiquitouS Terminal)," IST, 2000.

[36]   H. Matsutani and M. Nakagawa, "Multi-carrier DS-CDMA using frequency spread coding," *1999 IEEE International Conference on Personal Wireless Communication*, pp.244-248, 1999

[37]   L-L. Yang and L. Hanzo, Lie-Liang Yang; Hanzo, L., "Performance of broadband multicarrier DS-CDMA using space-time spreading-assisted transmit diversity," *IEEE Transactions on Wireless Communications*, vol.4, no.3, pp. 885-894, May 2005

[38]   H. Bin, L-L. Yang, and L. Hanzo, "Differential space-time modulation schemes for smart antenna aided generalized multicarrier DS-CDMA systems," *Wireless Communications and Networking Conference, 2006. WCNC 2006. IEEE* , vol.3, pp.1650-1654, 2006.

[39]   X. Chong, H. Bin, L-L. Yang, and L. Hanzo, "Multi-Functional Antenna Array Assisted MC DS-CDMA Using Downlink Preprocessing Based on Singular Value Decomposition," *IEEE 65th Vehicular Technology Conference, 2007. VTC2007-Spring.* pp.1936-1940, 22-25 April 2007

[40]   H. Atarashi, N. Maeda, S. Abeta, and M. Sawahashi, "Broadband packet wireless access based on VSF-OFCDM and MC/DS-CDMA," *The 13th IEEE International Symposium on Personal, Indoor and Mobile Radio Communications, 2002.* vol.3, pp. 992-997, 15-18 Sept. 2002

[41]   A. M. K. Miyoshi, and M. Uesugi, "A study on time domain spreading for OFCDM," IEICE, Technical Report RCS2001-179, Nov. 2001 2001.

[42]   T. N. A. Sumaso, K. Nitagara, M. Uesugi, and O. Kato, "An OFDM-CDMA system using combination of time and frequency domain spreading," IEICE, Technical Report Apr. 2000.

[43]   N. Maeda, H. Atarashi, S. Abeta, and M. Sawahashi, "Throughput comparison between VSF-OFCDM and OFDM considering effect of sectorization in forward link broadband packet wireless access," *2002 IEEE 56th Vehicular Technology Conference, 2002. VTC 2002-Fall,* vol.1 , pp. 47-51, 2002

[44] Y. Q. Zhou, J. Wang, and M. Sawahashi, "Turbo-Coded OFCDM Systems for 4G Mobile Communications," *2005 6th IEE International Conference on 3G and Beyond,* pp.1-5, 7-9 Nov. 2005

[45] Y. Zhou, J. Wang, and T.-S. Ng, "A Novel Code Assignment Scheme for Broadband OFCDM Systems," *TENCON 2006. 2006 IEEE Region 10 Conference ,* pp.1-4, 14-17 Nov. 2006

[46] R. Caldwell and A. Anpalagan, "Performance Analysis of Subcarrier Allocation in Two Dimensionally Spread OFCDM Systems," *2006 IEEE 64th Vehicular Technology Conference, 2006. VTC-2006 Fall*, pp.1-5, Sept. 2006

[47] L. Khalid and A. Anpalagan, "Threshold-Based Adaptive Modulation with Adaptive Subcarrier Allocation in OFCDM-Based 4G Wireless Systems," *2006 IEEE 64th Vehicular Technology Conference, 2006. VTC-2006 Fall*, pp.1-6, Sept. 2006

[48] R. Prasad and S. Hara, "An overview of multi-carrier CDMA," *IEEE 4th International Symposium on Spread Spectrum Techniques and Applications Proceedings, 1996,* vol.1, pp.107-114, 22-25 Sep 1996

[49] L. Mingqi, P. Qicong, and L. Yubai, "Performance evaluation of MC-DS-CDMA systems in multipath fading channels," *IEEE 2002 International Conference on Communications, Circuits and Systems and West Sino Expositions,* vol.1, pp. 308-312, 29 June-1 July 2002

[50] L-L. Yang and L. Hanzo, "Multicarrier DS-CDMA: a multiple access scheme for ubiquitous broadband wireless communications," *Communications Magazine, IEEE*, vol. 41, pp. 116-124, 2003.

[51] R. S. El-Khamy, S. E. Shaaban, I. A. Ghaleb, and H. N. Kheirallah, "The enhanced performance of combined multicarrier and CDMA techniques in multipath fading channels," *Proceedings of the Twenty-First National Radio Science Conference, 2004. NRSC 2004*, pp. C34-1-10, 16-18 March 2004

[52] N. Hathi, I. Darwazeh, and J. O'Reilly, "Peak-to-average power ratio performance comparison of different spreading code allocation strategies for MC-CDMA and MC-DS-CDMA," *Electronics Letters*, vol. 38, pp. 1219-1220, 2002.

[53] N. Hathi, M. Rodrigues, I. Darwazeh, and J. O'Reilly, "Performance assessment of MC-CDMA and MC-DS-CDMA in the presence of high power amplifier non-linearities," *IEEE 55th Vehicular Technology Conference, 2002. VTC Spring 2002*, vol.3, pp. 1467-1471, 2002

[54] H. Steendam and M. Moeneclaey, "Comparison of the sensitivities of MC-CDMA and MC-DS-CDMA to carrier frequency offset," *Symposium on Communications and Vehicular Technology, 2000. SCVT-200*, pp.166-173, 2000

[55] T. Sheng-Fu, L. Yi-Lin, and L. Yumin, "Relative threshold tree pruning multi-user detection with user ordering and user partitioning for MC-CDMA," *2004 IEEE Wireless Communications and Networking Conference, 2004. WCNC*, vol.1, pp. 48-53, 21-25 March 2004

[56] L. Rugini, P. Banelli, and G. B. Giannakis, "Local ML detection for multicarrier DS-CDMA downlink systems with grouped linear precoding," *IEEE Transactions on Wireless Communications,* vol. 5, pp. 306-311, 2006.

[57] N. Tendolkar and C. Hartmann, "Generalization of chase algorithms for soft decision decoding of binary linear codes," *IEEE Transactions on Information Theory*, vol. 30, pp. 714-721, 1984.

[58] J. E. M. Nilsson, "Difference between two soft-decision decoding algorithms," *Electronics Letters*, vol. 30, pp. 1665-1666, 1994.

[59] T. Kaneko, T. Nishijima, H. Inazumi, and S. Hirasawa, "An efficient maximum-likelihood-decoding algorithm for linear block codes with algebraic decoder," *IEEE Transactions on Information Theory,* vol. 40, pp. 320-327, 1994.

[60]   C. Tao and C. Tellambura, "Generalized feedback detection for MIMO systems," *Global Telecommunications Conference, 2005. GLOBECOM '05. IEEE*, vol.5, pp. 5, 28 Nov.-2 Dec. 2005

[61]   D. J. Love, S. Hosur, A. Batra, and R. W. Heath, Jr., "Chase decoding for space-time codes," *2004 IEEE 60th Vehicular Technology Conference, 2004. VTC2004-Fall*, vol.3, pp. 1663-1667, 26-29 Sept. 2004

[62]   R. Pyndiah, A. Picart, and A. Glavieux, "Performance of block turbo coded 16-QAM and 64-QAM modulations," *IEEE Global Telecommunications Conference, 1995. GLOBECOM '95*, vol.2, pp.1039-1043, 14-16 Nov 1995

[63]   O. Aitsab and R. Pyndiah, "Performance of Reed-Solomon block turbo code," *IEEE Global Telecommunications Conference, 1996. GLOBECOM '96*, vol.1, pp.121-125, 18-22 Nov 1996

[64]   R. Zhou, A. Picart, R. Pyndiah, and A. Goalic, "Potential applications of low complexity non-binary high code rate block turbo codes," *IEEE Military Communications Conference, 2004. MILCOM 2004*, vol.3, pp. 1694-1699, 31 Oct.-3 Nov. 2004

[65]   A. Picart and R. Pyndiah, "Adapted iterative decoding of product codes," *IEEE Global Telecommunications Conference, 1999. GLOBECOM '99*, vol.5, pp. 2357-2362, 1999

[66]   K. Cavalec-Amis and R. Pyndiah, "Block turbo codes for space-time systems," *IEEE Global Telecommunications Conference, 2000. GLOBECOM '00*, vol.2, pp.1021-1025, 2000

[67]   A. Stefanov and T. M. Duman, "Turbo coded modulation for wireless communications with antenna diversity," *IEEE VTS 50th Vehicular Technology Conference, 1999. VTC 1999 - Fall*, vol.3, pp.1565-1569, 1999

[68]   T. H. Liew, L. L. Yang, and L. Hanzo, "Iterative decoding of redundant residue number system codes," *2000 IEEE 51st Vehicular Technology Conference Proceedings, 2000. VTC 2000-Spring Tokyo*, vol.1, pp.576-580, 2000

[69]   S. Hirst and B. Honary, "Application of efficient Chase algorithm in decoding of generalized low-density parity-check codes," *Communications Letters, IEEE*, vol. 6, pp. 385-387, 2002.

[70]   S. A. Hirst, B. Honary, and G. Markarian, "Fast Chase algorithm with an application in turbo decoding," *IEEE Transactions on Communications*, vol. 49, pp. 1693-1699, 2001.

[71]   Y. Nam Yul, K. Young, and L. Pil Joong, "Iterative decoding of product codes composed of extended Hamming codes," *Fifth IEEE Symposium on Computers and Communications, 2000. Proceedings. ISCC 2000*, pp.732-737, 2000

[72]   Y. Chen and K. K. Parhi, "A very low complexity block turbo decoder composed of extended Hamming codes," *IEEE Global Telecommunications Conference, 2001. GLOBECOM '01*, vol.1, pp.171-175, 2001

[73]   C. B. Vicente and J. H. Weber, "Dynamic Chase decoding algorithm," *2003 IEEE Information Theory Workshop, 2003. Proceedings*, pp. 312-315, 31 March-4 April 2003

[74]   G. Arico and J. H. Weber, "Limited-trial Chase decoding," *IEEE Transactions on Information Theory*, vol. 49, pp. 2972-2975, 2003.

[75]   J. H. Weber and M. P. C. Fossorier, "Limited-trial chase-like algorithms achieving bounded-distance decoding," *IEEE Transactions on Information Theory,* vol. 50, pp. 3318-3323, 2004.

[76]   B. Geller, I. Diatta, J. P. Barbot, C. Vanstraceele, and F. Rambeau, "Block Turbo Codes: From Architecture to Application," *IEEE International Symposium on Information Theory, 2006*, pp.1813-1816, July 2006

[77]   T. Yinshu and L. Moonho, "Iterative chase-2 algorithm using threshold for block turbo codes decoding design," *IEEE International Symposium on Microwave, Antenna, Propagation and EMC Technologies for Wireless Communications, 2005. MAPE 2005*, vol.2, pp. 1154-1157, 8-12 Aug. 2005

[78]   L. Xingcheng, Z. Wei, W. Zhongfeng, and P. Cull, "An Efficient Adaptive Decoding for Block Turbo Codes," *International Conference on Wireless Communications, Networking and Mobile Computing, 2006. WiCOM 2006*, pp.1-5, 22-24 Sept. 2006

[79]   A. Mahran and M. Benaissa, "Adaptive Chase algorithm for block turbo codes," *Electronics Letters*, vol. 39, pp. 617-619, 2003.

[80]   A. Mahran and M. Benaissa, "Adaptive application of the Chase algorithm on Reed-Solomon product codes," *5th European Personal Mobile Communications Conference, 2003*, pp. 343-347, 22-25 April 2003

[81]   N. Le, A. R. Soleymani, and Y. R. Shayan, "Distance-based-decoding of block turbo codes," *Communications Letters, IEEE*, vol. 9, pp. 1006-1008, 2005.

[82]   M. Lalam, K. Amis, D. Leroux, D. Feng, and J. Yuan, "An improved iterative decoding algorithm for block turbo codes," *2006 IEEE International Symposium on Information Theory,* pp.2403-2407, July 2006

[83]   C. Argon and S. W. McLaughlin, "A parallel decoder for low latency decoding of turbo product codes," *Communications Letters, IEEE*, vol. 6, pp. 70-72, 2002.

[84]   Z. Xiujun, Z. Ming, Z. Shidong, and W. Jing, "Parallel decoding of turbo product codes for high data rate communication," *The 57th IEEE Semiannual Vehicular Technology Conference, 2003. VTC 2003-Spring*, vol.4, pp. 2372-2375, 22-25 April 2003

[85]   M. Torabi and M. R. Soleymani, "Turbo coded OFDM for wireless local area networks," *Canadian Conference on Electrical and Computer Engineering, 2002. IEEE CCECE 2002*, vol.3, pp. 1363-1367, 2002

[86]   Y. Chen and K. K. Parhi, "On the performance and implementation issues of block turbo code with antenna diversity," *Conference Record of the Thirty-Sixth Asilomar Conference on Signals, Systems and Computers, 2002*, vol.1, pp. 604-608, 3-6 Nov. 2002

[87]   D. Yinggang and C. Kam Tai, "Enhancements of STBC-OFDM systems by concatenating block turbo codes," *Proceedings of the IEEE 6th Circuits and Systems Symposium on Emerging Technologies: Frontiers of Mobile and Wireless Communication, 2004*, vol.2, pp. 655-658, 31 May-2 June 2004

[88]   H. Yejun and Z. Guangxi, "On the performance of TPC-based STBC coded MIMO-OFDM system over IMT2000 channels," *2006 IEEE International Symposium on Circuits and Systems, 2006. ISCAS 2006. Proceedings*, pp. 4, 21-24 May 2006

[89]   H. A. Sadayuki Abeta, Mamoru Sawahashi, Fumiyuki Adachi "Performance of Coherent Multi-Carrier/DS-CDMA and MC-CDMA for Broadband Packet Wireless Access," *IEICE TRANSACTIONS on Communications*, vol. E84-B, pp. 406-414, 2001.

[90]   R. M. Pyndiah, "Near-optimum decoding of product codes: block turbo codes," *IEEE Transactions on Communications,* vol. 46, pp. 1003-1010, 1998.

[91]   G. D. Forney, Jr. and A. Vardy, "Generalized minimum-distance decoding of Euclidean-space codes and lattices," *IEEE Transactions on Information Theory,* vol. 42, pp. 1992-2026, 1996.

[92]   L. Bahl, J. Cocke, F. Jelinek, and J. Raviv, "Optimal decoding of linear codes for minimizing symbol error rate (Corresp.)," *IEEE Transactions on Information Theory,* vol. 20, pp. 284-287, 1974.

[93]   T. Otsu, N. Umeda, and Y. Yamao, "System architecture for mobile communications systems beyond IMT-2000," *IEEE Global Telecommunications Conference, 2001. GLOBECOM '01*, vol.1, pp.538-542, 2001

Publications

[1]   A. Awad and T. O'Farrell, "Performance of Block Turbo Coded OFDM with 16-QAM Modulation in Rayleigh Fading Channel," *London Communications Symposium 2006*, pp. 69-72, 14-15 Sep. 2006.

[2]   A. Awad and T. O'Farrell, "Performance evaluation of OFCDM and MC-DS-CDMA for the forward link in next generation mobile communication systems," *IEEE 16th International Symposium on Personal, Indoor and Mobile Radio Communications, 2005. PIMRC 2005*, vol.3, pp. 1910-1914, 11-14 Sept. 2005

[3]   A. Awad and T. O'Farrell, "Comparative Study of OFCDM and MC-DS-CDMA with MMSE MUD and Iterative Decoding," *London Communications Symposium 2005*, pp. 69-72, 8-9 Sep. 2005.

[4]   A. Awad and T. O'Farrell, "An Investigation of Equalisation Methods for COFDM," *IEEE International Symposium on Broadband Communications (ISBC)*, Dec 2004

[5]   A. Awad and T. O'Farrell, "The Optimal Employment of CSI in COFDM-Based Receivers," *London Communications Symposium 2004*, pp. 41-44, 13-14 Sep. 2004.